The Evolution of Intraspecific Variation, Growth, and Body Size in Early Theropod Dinosaurs

Christopher T. Griffin

Department of Geosciences

Thesis submitted to the faculty of the Virginia Polytechnic Institute and State University
in partial fulfillment of the requirements for the degree of

Master of Science
In
Geosciences

Sterling J. Nesbitt, Chair
Michelle R. Stocker
Lawrence E. Freeman
Matthew W. Colbert

April 26 2016
Blacksburg, VA

Keywords: Ontogeny, variation, dinosaur, theropod, extinction

The Evolution of Intraspecific Variation, Growth, and Body Size in Early Theropod Dinosaurs

Christopher T. Griffin

ABSTRACT

Understanding the changes undergone during the life of an organism is often crucial to properly interpreting the evolutionary history of a group. For extinct organisms, this process can only be directly studied through growth series of fossils representing individuals at different stages of maturity. The growth patterns of the earliest dinosaurs (230–190 million years ago), in particular the morphological changes undergone during the life history of an individual (i.e., ontogeny) is poorly understood.

To tackle this problem, I studied the changes undergone during growth of two early theropod dinosaurs, *Coelophysis bauri* and *Megapnosaurus rhodesiensis*. To reconstruct the growth of these dinosaurs I used ontogenetic sequence analysis (OSA). I found that, unlike living birds, early dinosaurs possessed an extremely high amount of intraspecific variation in growth. This variation had been previously interpreted as sexual difference; however, I found no evidence of this. Because this variation is widespread among early dinosaurs and their relatives, I hypothesize that this is the ancestral condition of dinosaurian growth, and that this was lost along the evolution to birds. These ontogenetic events are conserved through evolution, and I used this to assess the maturity of large Triassic theropods: I suggest that all known large-bodied Triassic theropods were still growing rapidly at death, and that the maximum body size of Triassic theropods was higher than previously supposed. Theropods were large before the end Triassic mass extinction, unlike what has been previously hypothesized.

TABLE OF CONTENTS

LIST OF FIGURES

Chapter 1

Chapter 2

Chapter 3

ATTRIBUTION

Chapter 1 was conceived of and designed by CTG, with input from SJN, and Chapter 3 was conceived of by SJN, with design by CTG. All data collection and analysis was conducted by CTG with advisement from SJN. All figures were made by CTG and all chapters were written by CTG, with advisement from SJN.

Chapter 1

ANOMOLOUSLY HIGH VARIATION IN ONTOGENY IS THE ANCESTRAL DINOSAURIAN GROWTH CONDITION

C. T. Griffin, Virginia Polytechnic Institute and State University. ctgriff@vt.edu

Sterling J. Nesbitt, Virginia Polytechnic Institute and State University.

Formatted for *Nature Communications*

ABSTRACT

The biology of birds is highly unusual with respect to all other living reptiles, especially in their growth, which is extremely fast and possesses unusually low levels of intraspecific variation. To explore this transition between other reptiles and birds, we investigated morphological ontogenetic trends of early theropods and extant avians using ontogenetic sequence analysis (OSA) and non-metric multidimensional scaling (NMDS). Our analyses suggest intraspecific variation in growth is high in early dinosaurs but largely absent in birds, and NMDS analysis suggests this variation is not related to sexual differences. Because this variation is widespread among early-diverging dinosaurs and their closest relatives, anomalously high intraspecific variation—higher even than extant crocodylians—is likely the ancestral dinosaurian growth condition. The strong phylogenetic signal suggests environment is not solely responsible for this developmental variation, but because the Late Triassic environment across Pangaea was volatile, this variation may have contributed to the rise of dinosaurian dominance.

1. INTRODUCTION

In comparison with the biology of other reptiles, birds are highly unusual, with 'hollow' bones and postcranial skeletal pneumaticity, feathers, a unique forelimb digit formula, endothermy, and rapid growth rates. However, these peculiarities of avian biology initially arose in non-avian dinosaurs (e.g., Wagner and Gauthier 1999; Padian et al. 2001; Erickson et al. 2001; Norell and Xu 2005; O'Connor and Claessens 2005; Benson et al. 2011; Eagle et al. 2011), and the transition from more typical 'reptilian' modes of life to those seen in extant birds was a gradual process occurring over tens of millions of

years (e.g., Chiappe 2009; Brusatte et al. 2014). In addition to their extremely rapid rates of growth, avian ontogeny possesses a characteristically low level of morphological variation within a species relative to other reptiles. The majority of individuals in a given avian species undergo the same morphological changes during ontogeny, in the same order, at the same body sizes (Tumarkin-Deratzian et al. 2006; Bailluel et al. 2016), whereas their closest living relatives, crocodylians, possess much higher intraspecific variation in ontogeny (Brochu 1992; 1996; Tumarkin-Deratzian et al. 2007; Bailluel et al. 2016). In order to understand how this transition from non-avian to more typically avian growth patterns occurred within Archosauria, and how this may have contributed to the abundance, diversity, and ecological dominance of dinosaurs (including birds), we turned to the ontogenetic patterns of extinct dinosaurs.

Because this transition took place between the last common ancestor of archosaurs (crocodylians + birds) along the evolution to birds, knowledge of the ontogenetic patterns of the earliest dinosaurs and their closest relatives and how those patterns evolved through time is essential to understanding the evolution of the living avian growth condition. However, most studies of the ontogeny of non-avian dinosaurs have focused on Late Jurassic and Cretaceous dinosaurs (e.g., Carr 1999; Horner et al. 2000; Scannella and Horner 2010; Woodward et al. 2015). Our knowledge of ontogenetic patterns of early-diverging dinosaurs from the Late Triassic and Early Jurassic is relatively poor, in part because of a dearth of growth series for most of these taxa. What data are available suggest that early-diverging dinosaurs and silesaurids (the dinosaurian sister group; Nesbitt 2010; Nesbitt 2011) possess an unusually high degree of intraspecific variation in size of skeletal elements at skeletal maturity, (Raath 1977; 1990;

Colbert 1989; 1990; Benton et al. 2000; Carrano et al. 2002; Tykoski and Rowe 2004; Lee and O'Connor, 2013; Piechowski et al. 2014; Griffin and Nesbitt 2016), age at which growth ceases (Sander and Klein, 2005; Klein and Sander, 2007), the sequences in which developmental events occur during ontogeny (e.g., *sequence polymorphism*, Garn 1966) (Griffin and Nesbitt, 2016), and the presence/absence of ontogenetically variable features (Colbert 1989; 1990; Raath, 1990; Benton et al., 2000; Carrano et al., 2002; Tykoski and Rowe, 2004; Lee and O'Connor, 2013; Piechowski et al. 2014; Griffin and Nesbitt, 2016). This last category of variation has been studied in the most detail in the early-diverging theropods *Coelophysis bauri* and *Megapnosaurus* (= *'Syntarsus', Coelophysis*) *rhodesiensis*, as well as the Late Triassic silesaurid *Silesaurus opolensis* (Piechowski et al. 2014), in which variation of bone scar presence/absence in femora of similar lengths has been thought to form a robust/gracile dichotomy interpreted as sexual dimorphism (Raath, 1990). However, although there is similar variation in the femoral scars of the Middle Triassic silesaurid *Asilisaurus kongwe*, these scars fail to differentiate into a robust/gracile dichotomy with a large sample size of femora and a greater number of bone scars. Instead, that intraspecific variation was interpreted as a combination of sequence polymorphism and femoral length being a poor correlate for skeletal maturity in all but the smallest and largest femora (Griffin and Nesbitt 2016). This interpretation suggests that intraspecific variation in bone scars and other developmental characters in silesaurids and early dinosaurs is not indicative of sexual dimorphism, but instead predicts a highly variable growth strategy that was inherited by the earliest dinosaurs from their most recent common ancestor with silesaurids (Griffin and Nesbitt, 2016).

For an ideal study system to understand the ontogenetic condition in early dinosaurs, and placed within a comparative context the ancestral ontogenetic condition for Dinosauria, we turned to *Coelophysis bauri*, an early theropod for which an excellent growth series is known from single population preserved in the same horizon (Schwartz and Gillette 1994). Additionally, we analyzed another early coelophysoid theropod with a large growth series in which this variation has been reported, *Megapnosaurus rhodesiensis*. We used non-metric multidimensional scaling (NMDS) of femoral characters of *C. bauri* and *Meg. rhodesiensis*, as well as a larger matrix incorporating other skeletal elements of *C. bauri*, to test whether this variation in the presence of bone scars is indicative of sexual dimorphism. We then utilized ontogenetic sequence analysis (= OSA; Colbert and Rowe 2008) to reconstruct all equally parsimonious growth sequences for these characters, as well as quantify sequence polymorphism and the relationship between maturity and size in these taxa. This is the first published study to use OSA to reconstruct ontogenetic patterns in dinosaurs. Finally, to quantify the level of intraspecific variation in the growth of extant birds, we used both NMDS and OSA to analyze ontogenetic trends in two species (*Branta canadensis*, the Canada Goose, and *Meleagris gallopavo*, the Wild Turkey), allowing us to place the ancestral dinosaurian condition into a broader phylogenetic context along the transition to the typical avian growth strategy. In these analyses, we assume that the ontogenetic characters analyzed (postcranial muscle scar absence/presence and suture fusion events) are irreversible. The analyses also assume that individuals proceed from the immature to mature character state for all characters during ontogeny, so that individuals with more muscle scars and

coossified elements have attained a higher degree of skeletally mature than those lacking these features.

2. RESULTS

Ontogenetic Sequence Analysis

Our OSA indicates that both *Coelophysis bauri* and *Megapnosaurus rhodesiensis* possessed a high level of intraspecific variation, both in the relative sequence of ontogenetic characters reaching maturity and in body size at different levels of skeletal maturity (Figs. 1, 2). Analysis of the 27 ontogenetic characters of *C. bauri* predicted in 136 equally parsimonious developmental sequences (Fig. 1; Supplemental Fig. 1), with the modal sequence representing only 12.57% the support weight of all semaphoronts (an organism or morphotype at a specific stage of ontogeny, Hennig 1966). OSA for the ten femoral ontogenetic characters of *Coelophysis bauri* resulted in 82 developmental sequences (Fig. 2A; Supplemental Fig. 2), and for *Megapnosaurus rhodesiensis*, 145 developmental sequences (Fig. 2B; Supplemental Fig. 3) were reconstructed for 13 femoral characters. Femoral length is a qualitatively poor predictor of skeletal maturity in all analyses (Figs. 1-2), although almost all semaphoronts are represented by a range of sizes (Supplemental Figs. 1-3)

In contrast, we found extant birds to possess low levels of intraspecific variation relative to early theropods, consistent with other studies of the relative order of ontogenetic events in avian ontogeny (Tumarkin-Deratzian et al. 2006; Bailluel et al. 2016). The OSA of 36 ontogenetic characters of *Branta canadensis* returned 9 equally parsimonious developmental sequences (Fig. 3A; Supplemental Fig. 4) with a modal

sequence possessing 87.22% of the support weight of all semaphoronts combined. The OSA of 35 ontogenetic characters of *Meleagris gallopavo* returned four developmental sequences (Fig. 3B; Supplemental Fig. 5) with the modal sequence possessing 90% of all combined semaphoront support weights. In these avian taxa the femoral length of individuals at any given level of skeletal maturity is much less variable than the early theropod taxa. In general, smaller individuals of *B. canadensis* and *Mel. gallopavo* are more likely than those of *C. bauri* and *Meg. rhodesiensis* to be less skeletally mature than larger conspecific individuals.

Non-Metric Multidimensional Scaling

To test whether these characters in early theropods were bimodally distributed, and therefore suggestive of sexually dimorphic features, we used non-metric multidimensional scaling (NMDS). NMDS is an ordination method useful for visualizing similarity in a dataset of either continuous or discrete variables, and is therefore an excellent way of testing whether individuals possessing different character states form multiple groups, or if these characters vary continuously within the group. Our NMDS analyses do not indicate a bimodal distribution of femoral character states in either *Coelophysis bauri* or *Megapnosaurus rhodesiensis* (Fig. 4A, B), nor in the larger, full body dataset of *C. bauri* character states in all skeletal elements (Fig. 4C). Instead, the semaphoronts used in these analyses form a single large cluster in three-dimensional space, and do not produce distinct groups of similar character sets or extend in along a single path from the fully immature to the fully mature semaphoront, as would be expected if variation in ontogenetic trajectories was low. In all analyses, the fully immature and fully mature semaphoronts are plotted opposite each other at the

peripheries of the roughly spherical cluster (Fig. 4A–C). There is a qualitatively poor correlation between femoral length and skeletal maturity (i.e., spatial proximity to the fully mature semaphoront), suggesting that femoral length is a poor metric for estimating relative skeletal maturity for many of the individuals in the samples of both *C. bauri* and *Meg. rhodesiensis*. This poor correlation holds for the femoral datasets as well as the full-body *C. bauri* dataset, although size appears to possess a slightly higher correlation with skeletal maturity in the femur of *Meg. rhodesiensis* than in *C. bauri* (Fig. 4A–C). The femoral dataset of *Meg. rhodesiensis* appears to possess slightly less variation than *C. bauri* as indicated by a smaller amount of spread across the graph (Fig. 4B).

The NMDS analysis of the *Branta canadensis* dataset differs considerably from those of the *C. bauri* and *Meg. rhodesiensis* datasets. Instead of a single large cluster with most semaphoronts spread across the graph with no distinct trend with respect to the least and most mature semaphoronts, the unique *B. canadensis* semaphoronts (n = 16) are linked in a roughly arc-shaped path across three-dimensional space from the least mature to most mature semaphoront, consistent with a low level of variation in developmental pathways (Fig. 4D). Further, there is a clear qualitative trend of size increase extending from least to most mature along this path. The *Meleagris gallopavo* NMDS analysis was conducted on a smaller number of unique semaphoronts (n = 8), and as a result there is not a clear path extending from the least mature to most mature semaphoronts; although the plot is suggestive of a similar arc-like shape, missing semaphoronts in the 'middle' (i.e., roughly an equal distance between the least and most mature semaphoronts) make this path incomplete (Fig. 4E).

3. DISCUSSION

Coelophysis bauri and *Megapnosaurus rhodesiensis* possess a large amount of intraspecific variation, both in suites of character states and in size as related to robustness or maturity, compared to living birds. The mature states of these characters are not attained simultaneously during ontogeny, but are staggered in appearance along developmental sequences along which individuals progress towards skeletal maturity in a stepwise fashion. Instead of a single path of semaphoronts leading from the least to most mature in the NMDS analyses, as would be expected in a taxon with all individuals proceeding through developmental stages in a single path in the same sequences, semaphoronts of both *Meg. rhodesiensis* and *C. bauri* appear to be arranged in a cloud of points with no clear trend (Fig. 4A–C). This suggests that an individual may potentially utilize many developmental pathways, each consisting of semaphoronts with character states that conflict with other pathways. Additionally, although size is often used as a proxy for degree of skeletal maturity in many paleontological studies (e.g., Colbert 1990; Raath 1990; Currie and Peng 1993; Currie 2003; Bristowe and Raath 2004; Heckert et al. 2006; Rinehart et al. 2009; Buckley et al. 2010; Carpenter 2010; Manzig et al. 2014) size is overall poorly correlated with skeletal maturity as measured by ontogenetic character states in *Meg. rhodesiensis* and especially in *C. bauri*, with some larger individuals plotting closer to the least mature semaphoronts and some smaller individuals plotting closer to the most mature semaphoronts (Fig. 4A–C). Size also correlates poorly with skeletal maturity as quantified by maturity score in OSA, even though OSA may reconstruct missing data as present (and thus raise the maturity score higher than a strict scoring of the individual would give) (Figs. 1,2). The large number of developmental

pathways reconstructed by OSA suggests that sequence polymorphism (i.e., intraspecific variation in developmental pathways) is a common and widespread aspect of the postnatal development of these early theropods. Ontogenetic sequence analysis reconstructs all developmental sequences that are consistent with the data, and the large number of conflicting developmental pathways consisting of semaphoronts with suites of character states that preclude their belonging in other developmental pathways strongly suggests that variation in the relative order of these developmental characters is widespread throughout the populations of *Coelophysis* and *Megapnosaurus*.

Megapnosaurus rhodesiensis, along with *Coelophysis bauri*, has been suggested to display dimorphism in femoral morphology, with immature individuals and the skeletally mature of one sex lacking robust ossified muscle scars (the 'gracile' morph) and mature individuals of the other sex possessing these scars (the 'robust' morph)(Raath 1977; 1990; Gauthier 1984). If those features were dimorphic in the manner hypothesized, NMDS analyses would plot two clusters of semaphoronts: one cluster, consisting of all larger individuals, around the mature or robust semaphoront, and another cluster surrounding the immature or gracile semaphoront consisting of small- to medium-sized individuals. However, our NMDS analysis of the full-body dataset of *C. bauri* characters, as well as that of the femoral characters, is consistent with the interpretation of these characters as ontogenetic, not sexually dimorphic, with intermediate semaphoronts arranged in a large cluster in between the fully immature and mature semaphoronts rather than forming a bimodal distribution (Fig. 4A–C). As such, these data suggest that gracile individuals are simply less skeletally mature than robust individuals regardless of size, and that an increase in morphological characters used in analyses

(whether qualitative, OSA, or NMDS) effectively eliminates any apparent bimodal variation in character distribution. Histological analysis is outside the scope of this project, but in the future may help to determine whether this lack of correspondence between size and ontogenetic characters is an expression of how body size is related to ontogenetic age, although histological data have been unhelpful in resolving this problem in silesaurids (Griffin and Nesbitt 2016).

High levels of intraspecific variation are present in many early dinosaurs, particularly theropods. In addition to *Megapnosaurus rhodesiensis* and *Coelophysis bauri* (Raath 1979; 1990; Gauthier 1984; Colbert 1989; 1990), variation previously interpreted as a gracile/robust dichotomy has a wide range among early-diverging theropods, including other early neotheropods (the "Shake-N-Bake" coelophysoid, Tykoski 1997; 1998; *'Syntarsus' kayentakatae*, *Dilophosaurus wetherilli*, Tykoski 1998; 2005; Tykoski and Rowe 2004), large ceratosaurs (*Ceratosaurus nasicornis*, Britt et al. 2000) and small ceratosaurs (*Masiakasaurus knopfleri*, Carrano et al. 2002; Lee and O'Connor 2013). Most of these studies have been limited by relatively small sample sizes because of a lack of specimens available (usually, a maximum of n = 5–7), with only a few (3–6) bone scars evaluated. The results of our analyses of features in *Coelophysis* and *Megapnosaurus* utilizing larger sample sizes and higher numbers of features suggest that variation between individuals in suture fusion and bone scar presence in these taxa, with different morphs possessing similar sizes, is the result of a poor correlation between size and skeletal maturity, and is not indicative of sexual dimorphism.

Similar variation, both in robustness of skeletal elements and their relationship with size, is also present in early-diverging dinosaurs outside Theropoda, as well as in

non-dinosaurian dinosauriforms. The Triassic sauropodomorphs *Thecodontosaurus antiques* and *Melanorosaurus readi* have been interpreted as possessing robust/gracile variation in similarly sized limb elements (Heerden and Galton 1997; Benton et al. 2000). Along with some morphological variation in *Plateosaurus engelhardti* (Weishampel and Chapman 1990; Galton 1997; Hofman and Sanders 2014), histological analysis of a large sample of limb elements of *Plateosaurus* has demonstrated that size and histological maturity are poorly correlated in this taxon, with some skeletally mature individuals possessing far smaller body sizes than still-growing, ontogenetically younger individuals (Sander and Klein 2005; Klein and Sander 2007), although a lack of ossified bone scars in the limb elements of this taxon make it less morphologically variable in ontogeny than early theropods. Outside Dinosauria, *Silesaurus opolensis* and *Asilisaurus kongwe* possess variation in femoral scars not fully attributable to size. In the case of *S. opolensis* this variation was interpreted as sexual dimorphism (Piechowski et al. 2014), following Raath's (1977; 1990) interpretation of variation in *Megapnosaurus rhodesiensis*. *Asilisaurus kongwe* possesses similar variation in femoral scars, but these exist on a spectrum, and do not cleanly split into a clear robust/gracile dichotomy although similarly sized femora possess a variety of morphologies. Instead of sexual dimorphism, the variation in *A. kongwe* was interpreted as individual variation in developmental patterns, with sequence polymorphism and variation in the size that relative stages of maturity are reached both playing a role in producing differences between individuals (Griffin and Nesbitt 2016). We follow this interpretation of the variation in *A. kongwe* as well as *S. opolensis* (Griffin and Nesbitt 2016). Because these early-diverging silesaurids and early-diverging theropods phylogenetically bracket Sauropodomorpha, we suggest

that similar intraspecific variation in developmental patterns is present in both *T. antiqus* and *P. engelhardti* ontogeny. Because of the wide distribution of this individual variation in ontogenetic patterns among early-diverging dinosaurs and their closest relatives, this interpretation of our data suggests that polymorphism in both developmental sequence and in body size at skeletal maturity is the ancestral dinosaurian condition.

In contrast, and despite the relatively large sample sizes and number of ontogenetically variable characters examined, the extant birds in our study (*Branta canadensis* and *Meleagris gallopavo*) showed little evidence of widespread sequence polymorphism in OSA, with a low number of potential developmental sequences reconstructed and the majority of specimens represented by semaphoronts on the modal sequences (Figs. 4). Given that the individuals of *B. canadensis* and *Mel. gallopavo* analyzed represent many different populations, and those of *Coelophysis bauri* represent only a few or one populations (Schwartz and Gillette 1994; see Methods), the former would be expected to possess more variation, not less, than the latter. This lack of variation in the OSA of extant birds may be partly the result of low resolution in the relative timing of some of the characters; because extant birds grow quickly, we were unable to control for the relative timing of several developmental characters, all of which OSA reconstructed as appearing in the same developmental 'leap'. It may be that higher resolution of relative timing of ontogenetic events would reveal sequence polymorphism in these characters. However, prior analysis using cladistic ontogeny (a method similar to OSA that does not account for sequence polymorphism) with better resolution on many of the same characters found results consistent with a low amount of sequence polymorphism in *B. canadensis* (Tumarkin-Deratzian et al. 2006), supporting our

hypothesis that the level of intraspecific variation in developmental sequences is low in extant birds relative to early-diverging dinosaurs. Our NMDS analysis supports this hypothesis: instead of a cluster of points, semaphoronts of *B. canadensis* follow a clear path from least to most mature across the three-dimensional space of the NMDS plot (Fig 5D), and NMDS analysis of the *Mel. gallopavo* data is suggestive of this as well (Fig. 5E). Further, size appears to be a relatively good indicator of skeletal maturity in these taxa, with immature semaphoronts representing specimens of smaller size than more mature specimens. Given that variation in ontogeny, especially in size as correlated with maturity, appears to be muted or absent in more derived theropods including several tyrannosaurids (Carr 1999) and *Allosaurus fragilis* (Madsen 1976; Bybee et al. 2006; Supplemental Note 1; Supplemental Fig. 6), we hypothesize that this extreme level of individual variation in ontogenetic trends is absent from the clade Avetheropoda (= Allosauroidea + Coelurosauria), and is constrained to early-diverging dinosaurs and their closest relatives (Fig. 5).

Although most vertebrate species possess some individual variation in growth (Colbert and Rowe 2008), this normal feature of populations appears to play an exaggerated role in early-diverging dinosauriforms, with a larger amount of sequence polymorphism and a wider range of sizes at maturity relative to birds, more derived theropods (see above), and even crocodylians, although the latter does possess intraspecific variation in postnatal ontogeny (Brochu 1992; 1996; Tumarkin-Deratzian et al. 2007). The specific cause(s) of this variation in ontogenetic patterns is difficult to test with the evidence available in the paleontological record. However, evidence supporting the dominant cause as intrinsic or extrinsic, or some combination of the two, is available

for interpretation. Developmental plasticity as a reaction to environmental variables is a common source of variation in body size and occasionally morphology in extant reptiles, including birds, and is usually interpreted as an expression of variation in nutrient acquisition (e.g., Seigel and Ford 1992; Starck and Chinsamy 2002; Bize et al. 2003; Aubret et al. 2004; Hegyi and Török 2007; John-Alder et al. 2007). Therefore, developmental plasticity undoubtedly plays at least some role in the ontogeny of early dinosaurs. However, the wide temporal spread (from the Middle Triassic, *Asilisaurus kongwe* Nesbitt et al. 2010, to the Late Cretaceous, *Masiakasaurus knopfleri* Sampson 2001), large paleolatitudinal range (from tropical paleolatitudes, e.g., *A. kongwe*, *Coelophysis bauri*, to high paleolatitudes, e.g., *Megapnosaurus rhodesiensis*, *Plateosaurus engelhardti*), and varied ecological niches of these taxa (ranging from small- to large-bodied herbivores and carnivores alike) is suggestive of this variation possessing a strong phylogenetic signal (Fig. 5). This indicates that intrinsic factors played the major role in producing this variation in populations, with individuals in a population exposed to roughly similar environments still undergoing different ontogenetic patterns. Because such a high level of variation within a species or population may affect differential survival in an ecologically unstable environment, such as was present in the low latitudes of the Late Triassic (Whiteside et al. 2015) and during the extinction(s) that characterized the Late Triassic (e.g., Olsen et al. 2002; Tanner et al. 2004; Parker and Martz 2010; Atchley et al. 2013; Blackburn et al. 2013), this anomalously high level of intraspecific variation may have contributed to the early success of dinosaurs relative to many pseudosuchian clades in the latest Triassic and through the End Triassic Mass Extinction into the Early Jurassic.

4. METHODS

We evaluated the state of 29 developmental characters, including 10 femoral characters, in 174 unique specimens of *Coelophysis bauri*, 13 developmental characters in the femora of 43 specimens of *Megapnosaurus rhodesiensis*, 38 characters in 72 individuals of *Branta canadensis*, the Canada goose, and 36 characters in 26 individuals of *Meleagris gallopavo*, the wild turkey (see Supplemental Methods for details on ontogenetic characters; Supplemental Data 1–4 for specimen scores for ontogenetic characters). *Branta canadensis* and *Mel. gallopavo* were chosen as representative taxa for modeling the growth of extant birds for 1) their slow growth rate relative to many other birds, making the timing of ontogenetic characters more easily resolved 2) their phylogenetic position relatively close to the most recent common avian ancestor (the last common ancestor of paleognaths and neognaths), and 3) their large numbers in North America, enabling easy access to skeletal growth series with large sample sizes. We measured the maximum proximal/distal widths and maximum lengths of long bones, the anteroposterior widths of acetabula, and the lengths of sacra in *C. bauri* and *Meg. rhodesiensis*, and measured maximum femoral length of both femora in *B. canadensis* and *Mel. gallopavo*. The specimens of *Coelophysis bauri* all were recovered from a single locality, the *Coelophysis* Quarry at Ghost Ranch, New Mexico (Colbert 1989), and all but three specimens of *Megapnosaurus rhodesiensis* come from a single locality in the near the Chitake River, Zimbabwe (Raath 1990). Although a taphonomic study has not been undertaken on the *Meg. rhodesiensis* localities, the *Coelophysis* quarry is thought to have undergone almost no time averaging, and represents individuals buried in only one

to two events (Schwartz and Gillette 1994), making the time and geographic averaging on the *C. bauri* sample potentially less than that of the sample of *B. canadensis* and *Mel. gallopavo*, the skeletons of which do not represent individuals from a single population but were collected across Illinois and Wisconsin, USA over a period of several decades and reposited in Field Museum of Natural History.

Taxonomic Nomenclature. The naming of the Zimbabwean coelophysoid theropod *'Syntarsus' rhodesiensis* (Raath 1977) has caused some confusion: when the name *Syntarsus* was found to belong to a genus of beetle, and therefore taxonomically invalid to apply to a dinosaur, *'S.' rhodesiensis* was placed in the genus *Megapnosaurus* ("big dead reptile"; Ivie et al. 2001). Bristowe and Raath (2004) synonymized *Megapnosaurus* with *Coelophysis*, making the formal name of the Zimbabwean coelophysoid *Coelophysis rhodesiensis*, because *Coelophysis* had taxonomic priority. However, recent phylogenetic analyses have placed *Coelophysis rhodesiensis* as more closely related to *Camposaurus arizonensis* than to *Celophysis bauri* (Ezcurra and Brusatte 2011; You et al. 2014; Martill et al. 2016), making the genus *Coelophysis* paraphyletic. Because synonymizing *Camposaurus* with *Coelophysis* to resolve this problem is unwarranted, we refer to the Zimbabwean coelophysoid theropod as *Megapnosaurus rhodesiensis*.

Regressions to Standardize Size by Femoral Length. Because of the incompleteness of skeletons of *Coelophysis bauri* and *Megapnosaurus rhodesiensis* consisted of overlapping skeletal elements, which made direct numerical comparison of size impossible. We used simple linear regressions in R (www.r-project.org) with the measurement in question as the independent variable and maximum femoral length as the dependent variable to predict the maximum femoral length for those specimens of *C.*

bauri and *Meg. rhodesiensis* for which femoral length could not be directly measured, allowing an approximate size comparison between almost all individuals in the sample with maximum femoral length as the standard (Supplemental Tables 1–4). In the case of one measurement, the maximum mediolateral width of the distal end of the tibia, there were not enough individuals possessing both this measurement and the measurement of maximum femoral length, so a regression between the width of the distal end of the tibia and the maximum length of the tibia, with the resulting estimate for tibial length used to estimate the femoral length. The skeletal proportions of *Coelophysis bauri* and *Megapnosaurus rhodesiensis* are indistinguishable, and measurements from both were used to construct the linear regressions. In order to increase the sample size for the linear regression between the mediolateral width of the distal end of the tibia and the maximum tibial length, we also used measurements from *Gojirasaurus quayi*, a single partial skeleton of a large but otherwise nearly anatomically indistinguishable Triassic coelophysoid with similar proportions. All regressions were statistically significant ($p \leq 0.05$) and the R^2 were acceptable for all regressions (0.792–0.973). A table of all regressions, including independent and dependent variables, sample size, resulting linear equations, p-values and R^2, and included species can be found in the supplemental data (Supplemental Table 5).

Non-Metric Multidimensional Scaling. Non-metric multidimensional scaling is a method of producing an ordination based on a dissimilarity matrix, and represents rank-based, pairwise dissimilarity between samples in two- or three-dimensional space (Kruskal 1964a; 1964b). As such, NMDS functions well with any measure of dissimilarity, including qualitative data such as the discrete numbers used in expressing

character state data, making it an excellent method for describing the similarity or dissimilarity of our datasets of ontogenetic characters. Because NMDS can become stuck on local optima, rather than finding the solution with the true least amount of stress, we conducted multiple runs to ensure a robust result.

We utilized the Claddis package in R (Lloyd 2015) to calculate the pairwise distances in the same taxonomically reduced NEXUS datasets used in OSA (see below) using the MorphDistMatrix command. We then used the resulting Generalized Euclidean Distance matrix (Wills 2001) to conduct NMDS using the command metaMDS in the vegan package in R (Oksanen et al. 2015), using a Euclidean dissimilarity matrix and specifying a three-dimensional solution to reduce stress. In order to reduce the likelihood of missing the true optimally stable solution, we ran the analysis with 1,000 random starts. We plotted the resulting NMDS matrices in three dimensions using the scatterplot3d package in R (Ligges and Mächler 2003).

Body size, using femoral length as a proxy, was not included in the NMDS analyses, but instead semaphoronts were color-coded by femoral length to illustrate the relationship, if any, between maturity and body size in these taxa. If a semaphoront (a set of unique ontogenetic states) was only represented by one specimen in the taxonomically reduced matrix, we used the femoral length for that specimen as the representative femoral length for that semaphoront. If there were multiple specimens with identical suites of character states representing the same semaphoront, the representative femur length for that semaphoront was the mean of the femoral lengths of those specimens. Semaphoronts that lacked specimens with measurements (e.g., the hypothetical immature outgroup semaphoront) were left grey. For *Branta canadensis* and *Meleagris gallopavo*,

almost all the specimens possessed complete right and left femora, and the mean between the lengths of these two elements was used as the femoral length for that individual.

Ontogenetic Sequence Analysis. Ontogenetic Sequence Analysis (OSA) is a parsimony-based, size-independent method of reconstructing all equally parsimonious developmental sequences of discrete ontogenetic character changes in a population, and will therefore reconstruct multiple developmental sequences when sequence polymorphism is present in that population. OSA has normally been used to understand variation and growth in extant organisms (Cubbage and Mabee 1996; Mabee and Trendler 1996; Colbert 1999; Sheil and Greenbaum 2005; Colbert and Rowe 2008; de Jong et al. 2009; Morris 2013), with only two previous studies using this method in extinct taxa (Olori 2013; Griffin and Nesbitt 2016). We followed standard OSA procedure (Colbert and Rowe 2008) to conduct this analysis. First, we constructed a NEXUS file of irreversible ontogenetic characters and combined all operational taxonomic units (OTUs; in this case, individuals) with identical character states into single OTUs. To reduce the amount of missing data in the analysis, we eliminated redundancies in character states of specimens by removing those specimens with missing data if all known characters states were identical to one or more specimens with less missing data using safe taxonomic reduction (Wilkinson 1995) in the Claddis package in R (Lloyd 2015), producing a taxonomically reduced NEXUS file that we used to perform OSA (Supplemental Data 5–9). Additionally, we also constructed a 'reversed' NEXUS file for each file previously constructed, with the coding for mature and immature characters reversed (e.g., '0' becomes '1' for two-state characters, etc.). This step polarizes characters using the most mature outgroup, preventing semaphoronts from

falling along developmental paths that do not extend from the least to most mature semaphoronts (see Colbert and Rowe 2008 for a more detailed explanation). We then used PAUP* (v. 4.0b10, Swofford, 2002) to optimize these developmental events onto trees by running a heuristic search with the tree-bisection-reconnection algorithm, adding specimens randomly and running 300 replicates. The 'normal' dataset was run with the most immature individual as the outgroup OTU, and the 'reversed' dataset with the most mature individual as the outgroup OTU. If completely immature or mature individuals were not present in the dataset, we included an artificial OTU with completely immature/mature character states to provide outgroups to polarize characters; however, all individual character states included in the analysis were observed in the sample. We then visualized the 'normal' and 'reverse' treatment trees returned by PAUP* in MacClade (v. 4.04, Maddison and Maddison 2002), using the "trace all changes" function on both ambiguous and unambiguous changes.

We used this information to construct the OSA reticulating sequence diagrams for each dataset by following standard OSA procedure (Colbert and Rowe 2008), with a few modifications for our paleontological dataset. In order to conservatively estimate the amount of sequence polymorphism, we chose to reconstruct ambiguous changes only along the branch closest to the immature outgroup semaphoront, rather than reconstruct this character change as occurring every place it was ambiguously reconstructed. Missing data can create ambiguities that sometimes result in inflated numbers of developmental sequences, because the same set of specimens can form two adjacent semaphoronts, with one semaphoront having reconstructed a missing character(s) as absent and the other as present, with the change linking the two as part of a sequence. In most cases, this merely

represents the most parsimonious sequence available for these semaphoronts, because the semaphoront reconstructed as ‘mature’ is connected with entirely different specimens, meaning the different optimizations of the missing data merely made a developmental sequence that was already parsimonious more resolved than it otherwise would have been. However, in some instances the ‘mature’ reconstruction of those same specimens merely linked to a more mature semaphoront that the ‘immature’ reconstruction already linked to via another developmental sequence. In this case, the reconstruction of the missing data does not more fully resolve an already-predicted developmental sequence, but instead adds a sequence of equal resolution that only exists because of missing data. To be conservative in estimating amount of sequence polymorphism in the population, we eliminated those semaphoronts that represented the same set of specimens and only added sequences because of different optimizations of missing data. We also modified OSA to accommodate a problem not yet encountered in published studies utilizing OSA: because some specimens with large amounts of missing data in the full-body dataset possessed character suites extremely different from other, more complete specimens, the ‘normal’ treatment placed these specimens in divergent sequences close to the immature outgroup (reconstructing most or all the missing characters as immature), whereas the ‘reverse’ treatment did the opposite, placing these specimens close to the mature outgroup, reconstructing most of the missing data as mature characters. Because the two treatments did not overlap for these specimens, the specimens were left ‘stranded’; that is, without a complete path from the least to most mature semaphoronts. Because the assumptions of OSA require each developmental pathway to connect the two outgroup semaphoronts, we connected the ‘stranded’ semaphoronts to the least or most mature

semaphoronts as needed, resulting in several developmental sequences that are highly unresolved and possess extremely low frequency support weights (see below). Although both reconstruction of these specimens as near to the immature outgroup or near to the mature outgroup are equally consistent with the data, in order to avoid overestimating the number of potential developmental sequences (and therefore the sequence polymorphism in the sample) we arbitrarily chose to eliminate those 'stranded' semaphoronts and associated developmental pathways which were reconstructed as near the mature outgroup, leaving those same specimens that were also reconstructed as semaphoronts near the immature outgroup. The 'raw' OSA diagrams and sequences can be found in the supplemental data (Supp. Figs 1–5).

Frequency support weight—a dimensionless number representing the specimen support for a single semaphoront—was calculated for every semaphoront by standard OSA procedure (Colbert and Rowe 2008). A specimen gives a frequency support weight of 1 if it is only represented by a single semaphoront; otherwise, the support weight given by that specimen is divided evenly between all semaphoronts that represent it. The representative femoral length, resulting in a color for each semaphoront in the OSA reticulating diagram (see key in Figs. 1–3 for color scales for femoral lengths), was determined via the same method as NMDS, except for those semaphoronts with no representative specimen, such as the immature outgroup semaphoront. In these cases, the median of the femoral lengths of all specimens placed in that semaphoront was used as the representative femoral length.

5. REFERENCES

Atchley, S. C., L. C. Nordt, S. I. Dworkin, J. Ramezani, W. G. Parker, S. R. Ash, and S. A. Bowring. 2013. A linkage among Pangean tectonism, cyclic alluviation, climate change, and biologic turnover in the Late Triassic: the record from the Chinle Formation, southwestern United States. Journal of Sedimentary Research 83:1147–1161.

Aubret, F., R. Shine, and X. Bonnet. 2004. Evolutionary biology: adaptive developmental plasticity in snakes. Nature 431:261–262.

Bailleul, A. M., J. B. Scannella, J. R. Horner, and D. C. Evans. 2016. Fusion patterns in the skulls of modern archosaurs reveal that sutures are ambiguous maturity indicators for the Dinosauria. PLoS ONE 11:e0147687. DOI: 10.1371/journal.pone.0147687

Benson, R. B. J., R. J. Butler, M. T. Carrano, and P. M. O'Connor. 2011. Air-filled postcranial bones in theropod dinosaurs: physiological implications and the 'reptile'–bird transition. Biological Reviews 87:168–193.

Benton, M. J., L. Juul, G. W. Storrs, and P. M. Galton. 2000. Anatomy and systematics of the prosauropod dinosaur *Thecodontosaurus antiquus* from the Upper Triassic of southwest England. Journal of Vertebrate Paleontology 20:77–108.

Bize, P., A. Roulin, L.-F. Bersier, D. Pfluger, and H. Richner. 2003. Parasitism and developmental plasticity in Alpine swift nestlings. Journal of Animal Ecology 72:633–639.

Blackburn, T. J., P. E. Olsen, S. A. Bowring, N. M. McLean, D. V. Kent, J. Puffer, G. McHone, E. T. Rasbury, and M. Et-Touhami. 2013. Zircon U-Pb geochronology links the End-Triassic extinction with the Central Atlantic Magmatic Province. Science 340:941–945.

Bristowe, A., and M. A. Raath. 2004. A juvenile coelophysoid skull from the Early Jurassic of

Zimbabwe, and the synonymy of *Coelophysis* and *Syntarsus*. Palaeontologia Africana 40:31–41.

Britt, B. B., D. J. Chure, T. R. Holtz, Jr., C. A. Miles, and K. L. Statdman. 2000. A reanalysis of the phylogenetic affinities of *Ceratosaurus* (Theropoda, Dinosauria) based on new specimens from Utah, Colorado, and Wyoming. Journal of Vertebrate Paleontology 20:32A.

Brochu, C. A. 1992. Ontogeny of the postcranium in crocodylomorph archosaurs. Master's Thesis. University of Texas at Austin: Austin, Texas. 340 pp.

Brochu, C. A. 1996. Closure of neurocentral sutures during crocodilian ontogeny: implications for maturity assessment in fossil archosaurs. Journal of Vertebrate Paleontology 16:49–62.

Brusatte, S. L., G. T. Lloyd, S. C. Wang, and M. A. Norell. 2014. Gradual assembly of avian body plan culminated in rapid rates of evolution across the dinosaur-bird transition. Current Biology 24:2386–2392.

Buckley, L. G., D. W. Larson, M. Reichel, and T. Samman. 2010. Quantifying tooth variation within a single population of *Albertosaurus sarcophagus* (Theropoda: Tyrannosauridae) and implications for identifying isolated teeth of tyrannosaurids. Canadian Journal of Earth Sciences 47:1227–1251.

Bybee, P. J., A. H. Lee, and E.-T. Lamm. 2006. Sizing the Jurassic theropod dinosaur *Allosaurus*: assessing growth strategy and evolution of ontogenetic scaling of limbs. Journal of Morphology 267:347–359.

Carpenter, K. 2010. Variation in a population of Theropoda (Dinosauria): *Allosaurus* from the Cleveland-Lloyd Quarry (Upper Jurassic), Utah, USA. Paleontological Research 14:250–

259.

Carr, T. D. 1999. Craniofacial ontogeny in Tyrannosauridae (Dinosauria, Coelosauria). Journal of Vertebrate Paleontology 19:497–520.

Carrano, M. T., S. D. Sampson, and C. A. Forster. 2002. The osteology of *Masiakasaurus knopfleri*, a small abelisauroid (Dinosauria: Theropoda) from the Late Cretaceous of Madagascar. Journal of Vertebrate Paleontology 22:510–534.

Chiappe, L. M. 2009. Downsized dinosaurs: The evolutionary transition to modern birds. Evolution: Education and Outreach 2:248–256.

Colbert, E. H. 1989. The Triassic dinosaur *Coelophysis*. Museum of Northern Arizona Bulletin 57:1–160.

Colbert, E. H. 1990. Variation in *Coelophysis bauri*; pp. 81–90 *in* K. Carpenter, and P. J. Currie (eds.), Dinosaur Systematics: Perspectives and Approaches. Cambridge University Press, Cambridge, UK, 356 pp.

Colbert, M. W. 1999. Patterns of evolution and variation in the Tapiroidea (Mammalia: Perissodactyla). Ph.D. dissertation. The University of Texas at Austin: Austin, Texas. 464 pp.

Colbert, M. W., and T. Rowe. 2008. Ontogenetic sequence analysis: using parsimony to characterize developmental sequences and sequence polymorphism. Journal of Experimental Zoology Part B, Molecular and Developmental Evolution 310B:398–416.

Cubbage, C. C., and P. M. Mabee. 1996. Development of the cranium and paired fins in the zebrafish *Danio rerio* (Ostariophysi, Cyprinidae). Journal of Morphology 229:121–160.

Currie, P. J., and J.-H. Peng. 1993. A juvenile specimen of *Saurornithoides mongoliensis* from the Upper Cretaceous of northern China. Canadian Journal of Earth Sciences 30:2224–

2230.

de Jong, I. M. L., M. W. Colbert, F. Wittle, and M. K. Richardson. 2009. Polymorphism in developmental timing: intraspecific heterochrony in a Lake Victoria cichlid. Evolution & Development 7:367–394.

Eagle, R. A., T. Tütken, T. S. Martin, A. K. Tripati, H. C. Fricke, M. Connely, R. L. Cifelli, and J. M. Eiler. 2011. Dinosaur Body Temperatures Determined from Isotopic (13C-18O) Ordering in Fossil Biominerals. Science 333:443–445.

Erickson, G. M., K. C. Rogers, and S. A. Yerby. 2001. Dinosaurian growth patterns and rapid avian growth rates. Nature 412:429–432.

Ezcurra, M. D., and S. L. Brusatte. 2011. Taxonomic and phylogenetic reassessment of the early neotheropod dinosaur *Camposaurus arizonensis* from the Late Triassic of North America. Palaeontology 54:763–772.

Galton, P. M. 1997. Comments on sexual dimorphism in the prosauropod dinosaur *Plateosaurus engelhardti* (Upper Triassic, Trossingen). Neues Jahrbuch für Geologie und Paläontologie 11:674–682.

Garn, S. M., C. G. Rohmann, and T. Blumenthal. 1966. Ossification sequence polymorphism and sexual dimorphism in skeletal development. American Journal of Physical Anthropology 24:101–116.

Gauthier, J. A. 1984. A cladistics analysis of the higher systematic categories of the Diapsida. Ph.D. Dissertation. University of California, Berkeley: Berkeley. 564 pp.

Griffin, C. T., and S. J. Nesbitt. 2016. The femoral ontogeny and long bone histology of the Middle Triassic (?late Anisian) dinosauriform *Asilisaurus kongwe* and implications for the growth of early dinosaurs. Journal of Vertebrate Paleontology 36. DOI:

10.1080/02724634.2016.1111224

Heckert, A. B., S. G. Lucas, L. F. Rinehart, J. A. Spielman, A. P. Hunt, and R. Kahle. 2006. Revision of the archosauromorph reptile *Trilophosaurus*, with a description of the first skull of *Trilophosaurus jacobsi*, from the Upper Triassic Chinle Group, West Texas, USA. Palaeontology 49:621–640.

Heerden, J. v., and P. M. Galton. 1997. The affinities of *Melanosaurus*—a Late Triassic prosauropod dinosaur from South Africa. Neues Jahrbuch für Geologie und Paläontologie 12:39–55.

Hegyi, G., and J. Török. 2007. Developmental plasticity in a passerine bird: an experiment with collared flycatchers *Ficedula albicollis*. Journal of Avian Biology 38:327–334.

Hennig, W. E. 1966. Phylogenetic Systematics. University of Illinois Press, Urbana, 263 pp.

Hofmann, R., and P. M. Sander. 2014. The first juvenile specimens of *Plateosaurus engelhardti* from Frick, Switzerland: isolated neural arches and their implications for developmental plasticity in a basal sauropodomorph. PeerJ 2:e458. DOI: 10.7717/peerj.458

Ivie, M. A., S. A. Slipinski, and P. Wegrzynowicz. 2001. Generic homonyms in the Colydiinae (Coleoptera: Zopheridae). Insecta Mundi 15:63–64.

John-Alder, H. B., R. M. Cox, and E. N. Taylor. 2007. Proximate developmental mediators of sexual dimorphism in size: case studies from squamate reptiles. Integrative and Comparative Biology 47:258–271.

Klein, N., and P. M. Sander. 2007. Bone histology and growth of the prosauropod *Plateosaurus engelhardti* MEYER, 1837 from the Norian bonebeds of Trossingen (Germany) and Frick (Switzerland). Special Papers in Paleontology:169–206.

Lee, A. H., and P. M. O'Connor. 2013. Bone histology confirms determinate growth and small

body size in the noasaurid theropod *Masiakasaurus knopfleri*. Journal of Vertebrate Paleontology 33:865–876.

Ligges, U., and M. Mächler. 2003. Scatterplot3d - an R package for visualizing multivariate data. Journal of Statistical Software 8:1–20.

Lloyd, G. T. 2016. Estimating morphological diversity and tempo with discrete character-taxon matrices: implementation,challenges, progress, and future directions. Biological Journal of the Linnean Society. DOI: 10.1111/bij.12746

Mabee, P. M., and T. A. Trendler. 1996. Development of the cranium and paired fins in *Betta splendens* (Teleostei: Percomorpha): intraspecific variation and interspecific comparisons. Journal of Morphology 227:249–287.

Maddison, D. R., and W. P. Maddison. 2002. MacClade 4: Analysis of phylogeny and character evolution. Version 1.04.

Madsen, J. H., Jr. 1976. *Allosaurus fragilis*: a revised osteology. Utah Geological Survey Bulletin 109:1–163.

Manzig, P. C., A. W. A. Kellner, L. C. Weinschütz, C. E. Fragoso, C. S. Vega, G. B. Guimarães, L. C. Godoy, A. Liccardo, J. H. Z. Ricetti, and C. C. Moura. 2014. Discovery of a rare pterosaur bone bed in a Cretaceous desert with insights on ontogeny and behavior of flying reptiles. PLoS ONE 9:e100005. DOI: 10.1371/journal.pone.0100005

Martill, D. M., S. U. Vidovic, C. Howells, and J. R. Nudds. 2016. The oldest Jurassic dinosaur: A basal neotheropod from the Hettangian of Great Britain. PLoS ONE 11:e0145713. DOI: 10.1371/journal.pone.0145713

Morris, Z. 2013. Skeletal ontogeny of *Monodelphis domestica* (Mammalia: Didelphidae): quantifying variation, variability, and technique bias inossification sequence

reconstriction. M.S. thesis. University of Texas at Austin: Austin, Texas. 204 pp.

Nesbitt, S. J. 2011. The early evolution of archosaurs: relationships and the origin of major clades. Bulletin of the American Museum of Natural History 352:1–292.

Nesbitt, S. J., C. A. Sidor, R. B. Irmis, K. D. Angielczyk, R. M. H. Smith, and L. A. Tsuji. 2010. Ecologically distinct dinosaurian sister group shows early diversification of Ornithodira. Nature 464:95–98.

Norell, M. A., and X. Xu. 2005. Feathered dinosaurs. Annual Review of Earth and Planetary Sciences 33:277–299.

O'Connor, P. M., and L. P. A. M. Claessens. 2005. Basic avian pulmonary design and flow-through ventilation in non-avian theropod dinosaurs. Nature 436:253–256.

Oksanen, J., F. G. Blanchet, R. Kindt, P. Legendre, P. R. Minchin, R. B. O'Hara, G. L. Simpson, P. Solymos, M. H. H. Stevens, and H. Wagner. 2015. vegan: Community Ecology Package. R package version 2.3-0.

Olori, J. C. 2013. Ontogenetic sequence reconstruction and sequence polymorphism in extinct taxa: an example using early tetrapods (Tetrapoda: Lepospondyli). Paleobiology 39:400–428.

Olsen, P. E., D. V. Kent, H.-D. Sues, C. Koeberl, H. Huber, A. Montanari, E. C. Rainforths, S. J. Fowell, M. J. Szajna, and B. W. Hartline. 2002. Ascent of dinosaurs linked to an iridium anomaly at the Triassic-Jurassic boundary. Science 296:1305–1307.

Padian, K., A. d. Ricqlès, and J. A. Horner. 2001. Dinosaurian growth rates and bird origins. Nature 412:405–408.

Parker, W. G., and J. W. Martz. 2010. The late Triassic (Norian) Adamanian-Revueltian tetrapod faunal transition in the Chinle Formation of Petrified Forest National Park, Arizona.

Earth and Environmental Science Transactions of the Royal Society of Edinburgh 101:231–260.

Raath, M. A. 1977. The anatomy of the Triassic theropod *Syntarsus rhodesiensis* (Sauischia: Podokesauridae) and a consideration of its biology. Ph.D. dissertation. Rhodes University: Grahamnstown, South Africa. 233 pp.

Raath, M. A. 1990. Morphological variation in small theropods and its meaning in systematics: evidence from *Syntarsus rhodesiensis*; pp. 91–105 *in* K. Carpenter, and P. J. Currie (eds.), Dinosaur Systematics: Perspectives and Approaches. Cambridge University Press, Cambridge, UK.

Rinehart, L. F., S. G. Lucas, A. B. Heckert, J. A. Spielman, and M. D. Celeskey. 2009. The paleobiology of *Coelophysis bauri* (Cope) from the Upper Triassic (Apachean) Whitaker Quarry, New Mexico, with detailed analysis of a single quarry block. New Mexico Museum of Natural History and Science Bulletin 45:1–260.

Sampson, S. D., M. T. Carrano, and C. A. Forster. 2001. A bizarre predatory dinosaur from the Late Cretaceous of Madagascar. Nature 409:504–506.

Sander, P. M., and N. Klein. 2005. Developmental plasticity in the life history of a prosauropod dinosaur. Science 16:1800–1802.

Scanella, J. B., and J. R. Horner. 2010. *Torosaurus* Marsh, 1891, is *Triceratops* Marsh, 1889 (Ceratopsidae: Chasmosaurinae): synonymy through ontogeny. Journal of Vertebrate Paleontology 30:1157–1168.

Schwartz, H. L., and D. D. Gillette. 1994. Geology and taphonomy of the *Coelophysis* quarry, Upper Triassic Chinle Formation, Ghost Ranch, New Mexico. Journal of Paleontology 68:1118–1130.

Seigel, R. A., and N. B. Ford. 1992. Effects of energy input on variation in clutch size and offspring size in a viviparous reptile. Functional ecology 6:382–385.

Sheil, C., and E. Greenbaum. 2005. Reconsideration of skeletal development of *Chelydra serpentina* (Reptilia: Testudinata: Chelydridae): evidence for intraspecific variation. Journal of Zoology 265:235–267.

Starck, J. M., and A. Chinsamy. 2002. Bone microstructure and developmental plasticity in birds and other dinosaurs. Journal of Morphology 254:232–246.

Swofford, D. L. 2003. PAUP*. Phylogenetic Analysis Using Parsimony (*and Other Methods). Version 4. Sinauer Associates, Sunderland, Massachusetts.

Tanner, L. H., S. G. Lucas, and M. G. Chapman. 2004. Assessing the record and causes of the Late Triassic extinctions. Earth-Science Reviews 65:103–139.

Tumarkin-Deratzian, A. R., D. R. Vann, and P. Dodson. 2006. Bone surface texture as an ontogenetic indicator in long bones of the Canada goose *Branta canadensis* (Anseriformes: Anatidae). Zoological Journal of the Linnean Society 148:133–168.

Tumarkin-Deratzian, A. R., D. R. Vann, and P. Dodson. 2007. Growth and textural ageing in long bones of the American alligator *Alligator mississippiensis* (Crocodylia: Alligatoridae). Zoological Journal of the Linnean Society 150:1–39.

Tykoski, R. S. 1998. The osteology of *Syntarsus kayentakatae* and its implications for ceratosaurid phylogeny. M.S. thesis. University of Texas Austin: Austin, Texas. 217 pp.

Tykoski, R. S. 2005. Anatomy, ontogeny, and phylogeny of coelopysoid dinosaurs. Ph.D. dissertation. The University of texas at Austin: Austin, Texas. 553 pp.

Tykoski, R. S., and T. Rowe. 2004. Ceratosauria; pp. 47–70 *in* D. B. Weishampel, P. Dodson, and H. Osmólska (eds.), The Dinosauria, second edition. University of California Press,

Berkeley and Los Angeles, California.

Wagner, G. P., and J. A. Gauthier. 1999. 1,2,3 = 2,3,4: A solution to the problem of the homology of the digits in the avian hand. Proceedings of the National Academy of Science 96:5111–5116.

Weishampel, D. B., and R. E. Chapman. 1990. Morphometric study of *Plateosaurus* from Trossingen (Baden-Württemberg, Federal Republic of Germany); pp. 43–51 *in* K. Carpenter, and P. J. Currie (eds.), Dinosaur systematics: approaches and perspectives. Cambridge University Press, Cambridge, UK.

Whiteside, J. H., S. Lindströmb, R. B. Irmis, I. J. Glasspool, M. F. Schaller, M. Dunlavey, S. J. Nesbitt, N. D. Smith, and A. H. Turner. 2015. Extreme ecosystem instability suppressed tropical dinosaur dominance for 30 million years. Proceedings of the National Academy of Science 112:7909–7913.

Wilkinson, M. 1995. Coping with abundant missing entries in phylogenetic inference using parsimony. Systematic Biology 44:501–514.

Wills, J. C. 2001. Morphological disparity: a primer; pp. 55–144 *in* J. M. Adrian, G. D. Edgecombe, and B. S. Lieberman (eds.), Fossils, Phylogeny, and Form: An Analytical Approach. Kluwer Academic/Plenum Publishers, New York, NY.

Woodward, H. N., F. E. A. Freedman, J. O. Farlow, and J. R. Horner. 2015. *Maiasaura*, a model organism for extinct vertebrate population biology: a large sample statistical assessment of growth dynamics and survivorship. Paleobiology 41:503–527.

You, H.-L., Y. Azuma, T. Wang, Y.-M. Wang, and Z.-M. Dong. 2014. The first well-preserved coelophysoid theropod dinosaur from Asia. Zootaxa 3873:233–249.

6. FIGURES

Figure 1. Ontogenetic sequence analysis reticulating diagram illustrating the 136 reconstructed developmental sequences of the 27 ontogenetic characters of *Coelophysis bauri*. The representative femoral length of each semaphoront is illustrated by color.

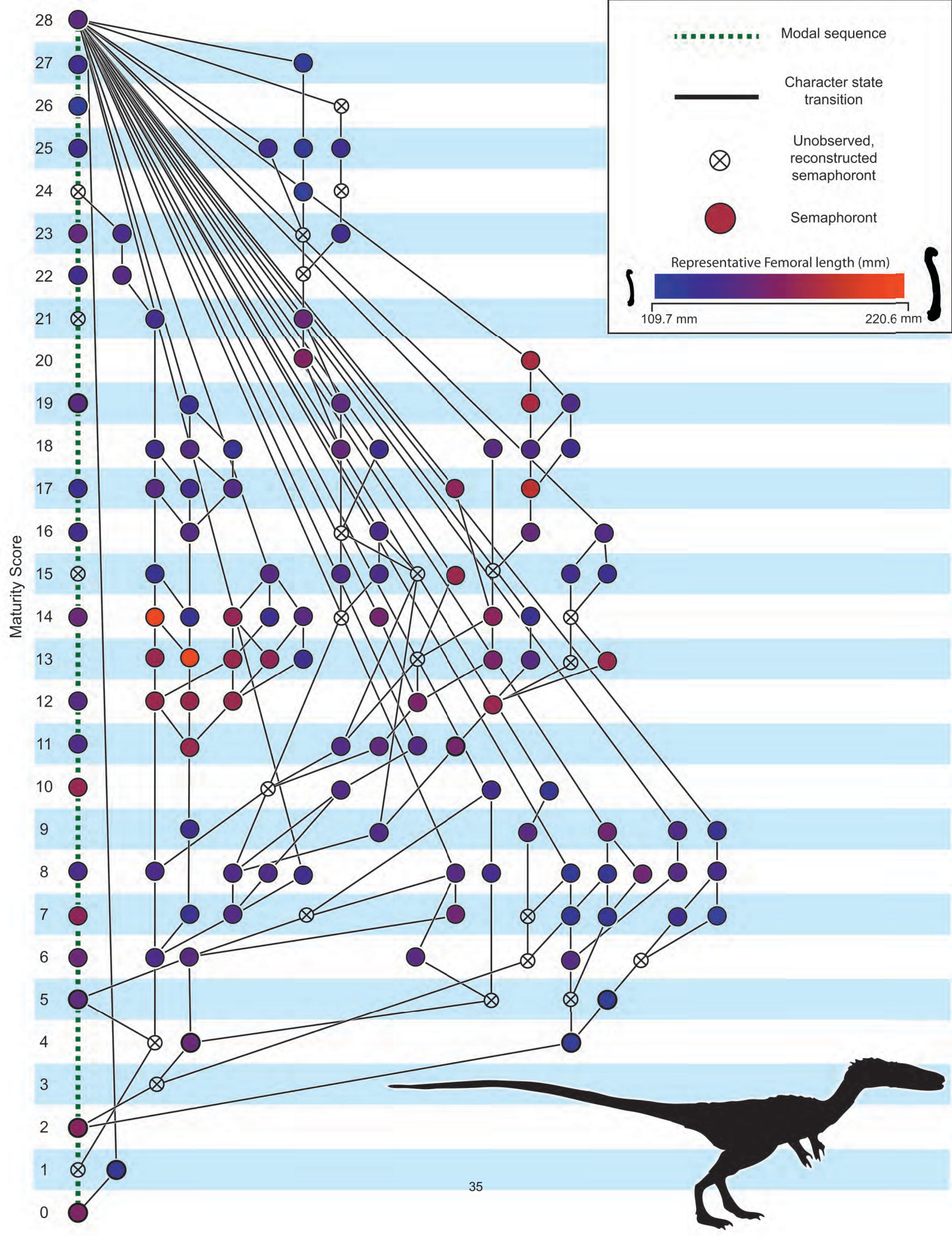
Modal sequence
Character state transition
Unobserved, reconstructed semaphoront
Semaphoront
Representative Femoral length (mm)
109.7 mm
220.6 mm
Maturity Score
28
27
26
25
24
23
22
21
20
19
18
17
16
15
14
13
12
11
10
9
8
7
6
5
4
3
2
1
0

Figure 2. OSA reticulating diagrams of femora of early theropods. **A** Ontogenetic sequence analysis reticulating diagram illustrating the 82 reconstructed developmental sequences of the 10 femoral ontogenetic characters of *Coelophysis bauri*. **B** Ontogenetic sequence analysis reticulating diagram illustrating the 145 reconstructed developmental sequences of the 13 femoral ontogenetic charactersof and for *Megapnosaurus rhodesiensis*. Representative femoral length for each semaphoront is illustrated by color. This figure follows the key in Fig. 1.

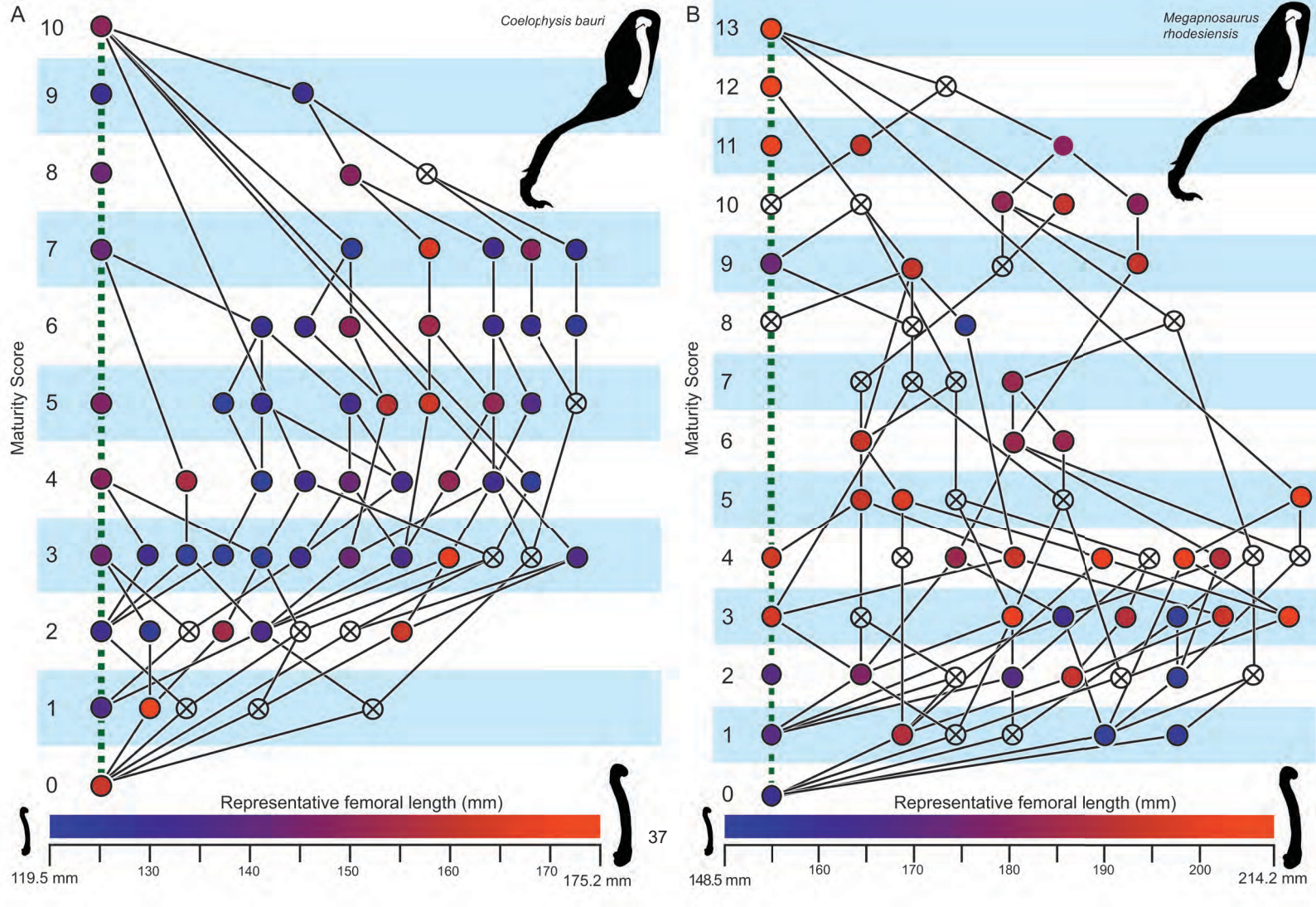
A
Coelophysis bauri
Maturity Score
10
9
8
7
6
5
4
3
2
1
0
Representative femoral length (mm)
37
119.5 mm
130
140
150
160
170
175.2 mm
B
Megapnosaurus rhodesiensis
Maturity Score
13
12
11
10
9
8
7
6
5
4
3
2
1
0
Representative femoral length (mm)
148.5 mm
160
170
180
190
200
214.2 mm

Figure 3. OSA reticulating diagrams of extant avians. **A** Ontogenetic sequence analysis reticulating diagram illustrating the 9 reconstructed developmental sequences of the 36 ontogenetic characters of *Branta canadensis*. **B** Ontogenetic sequence analysis reticulating diagram illustrating the 4 reconstructed developmental sequences of the 35 ontogenetic characters of *Meleagris gallopavo*. Representative femoral length for each semaphoront is illustrated by color. This figure follows the key in Fig. 1.

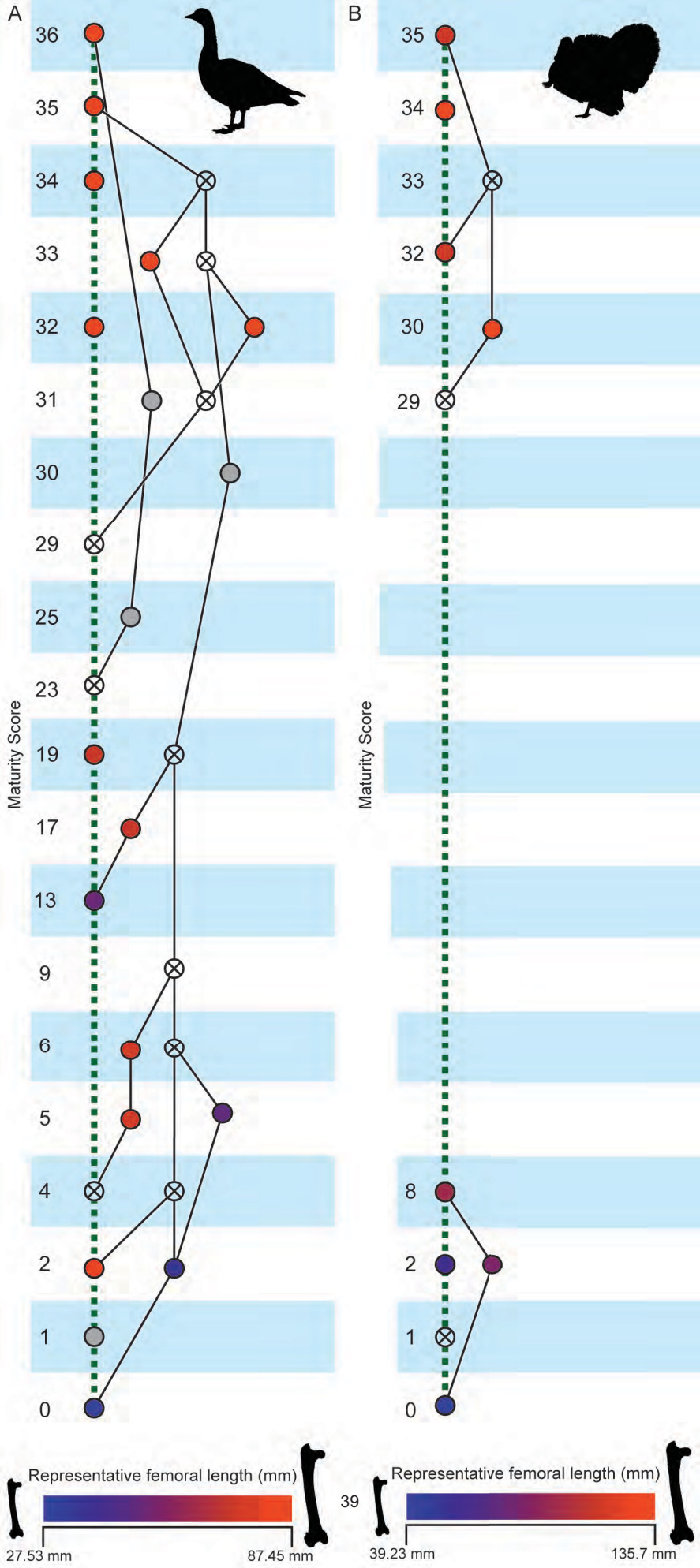
A
B
Maturity Score
Maturity Score
36
35
34
33
32
31
30
29
25
23
19
17
13
9
6
5
4
2
1
0
35
34
33
32
30
29
8
2
1
0
Representative femoral length (mm)
27.53 mm
87.45 mm
39
Representative femoral length (mm)
39.23 mm
135.7 mm

Figure 4. Non-metric multidimensional scaling analysis (NMDS) plots of early theropods and extant birds. **A** NMDS plot of the dataset of the 10 femoral ontogenetic characters of *Coelophysis bauri*. Color indicates femoral size of each specimen using the scale of Fig. 2A. Stress = 0.103. **B** NMDS plot of the dataset of the 13 femoral ontogenetic characters of *Megapnosaurus rhodesiensis*. Color indicates femoral size of each specimen using the scale of Fig. 2B. Stress = 0.048. **C** NMDS plot of the dataset of all 27 ontogenetic characters of *Coelophysis bauri*. Color indicates femoral size of each specimen using the scale of Fig. 1. Stress = 0.212. **D** NMDS plot of the dataset of all 36 ontogenetic characters of *Branta canadensis*. Color indicates femoral size of each specimen using the scale of Fig. 3A. Stress = 0.007. **E** NMDS plot of the dataset of all 35 ontogenetic characters of *Meleagris gallopavo*. Color indicates femoral size of each specimen using the scale of Fig. 3B. Stress < 0.001.

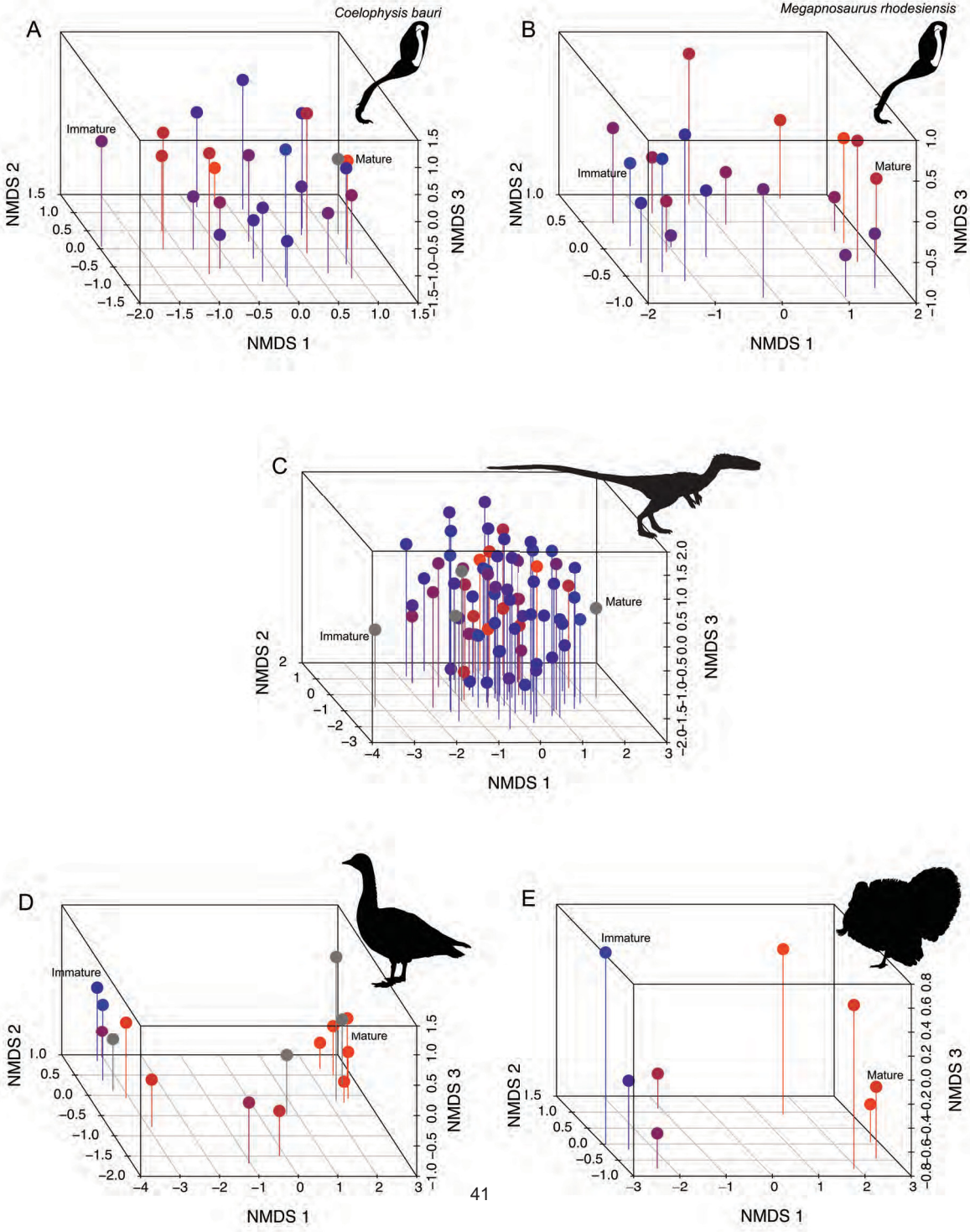
A
Coelophysis bauri
Immature
Mature
NMDS 1
NMDS 2
NMDS 3
B
Megapnosaurus rhodesiensis
Immature
Mature
NMDS 1
NMDS 2
NMDS 3
C
Immature
Mature
NMDS 1
NMDS 2
NMDS 3
D
Immature
Mature
NMDS 1
NMDS 2
NMDS 3
E
Immature
Mature
NMDS 1
NMDS 2
NMDS 3

Figure 5. Intraspecific variation in ontogeny is exaggerated in early-diverging dinosauriforms and dinosaurs relative to the ancestral condition, regardless of period or geographic location, and is absent in more derived theropod dinosaurs, including birds.

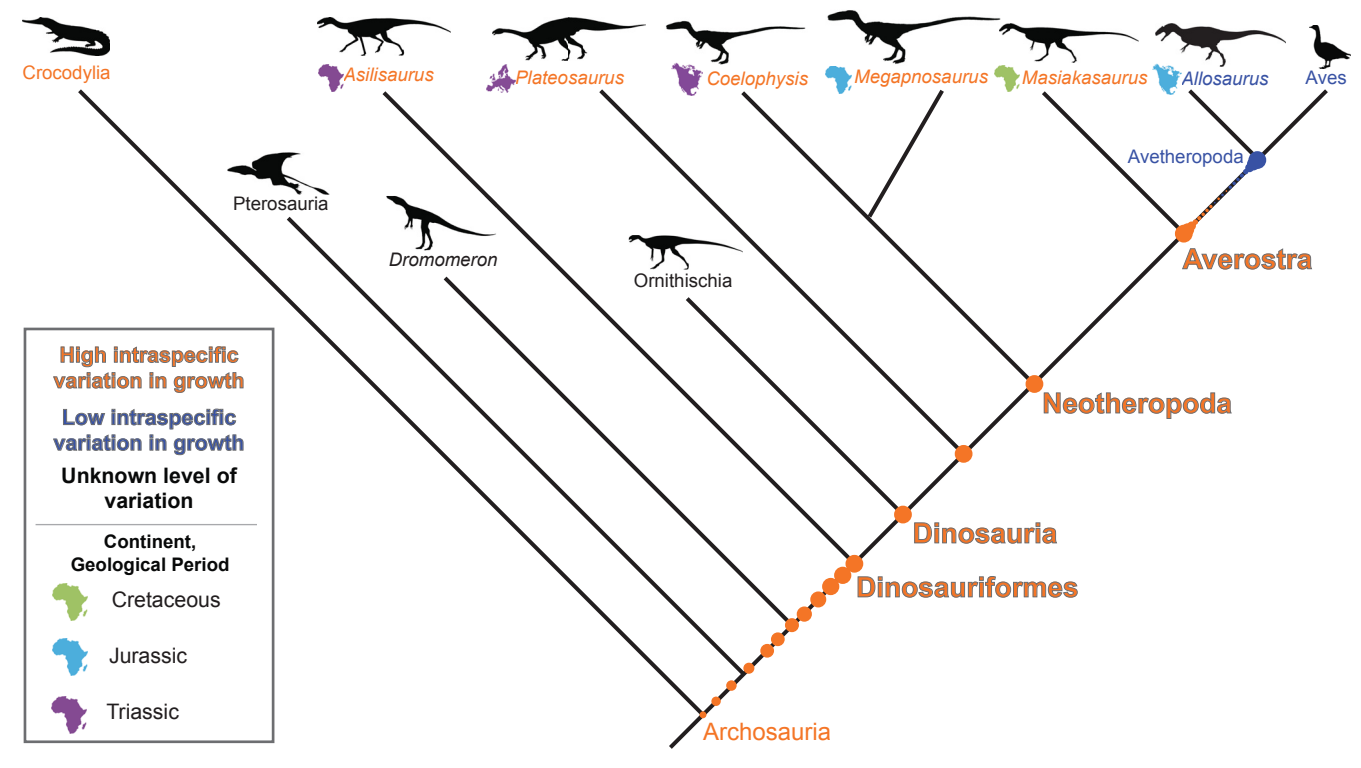
Crocodylia
Asilisaurus
Plateosaurus
Coelophysis
Megapnosaurus
Masiakasaurus
Allosaurus
Aves
Avetheropoda
Pterosaurus
Dromomeron
Ornithischia
Averostra
Neotheropoda
Dinosauria
Dinosauriformes
Archosauria
High intraspecific variation in growth
Low intraspecific variation in growth
Unknown level of variation
Continent, Geological Period
Cretaceous
Jurassic
Triassic

Chapter 2

GROWTH AND VARIATION IN EARLY THEROPODS

C. T. Griffin, Department of Geosciences, Virginia Polytechnic Institute and State University, ctgriff@vt.edu.

Formatted for the *Journal of Anatomy*

ABSTRACT

Understanding ontogenetic patterns is important in vertebrate paleontology because the assessed skeletal maturity of an individual often has implications for paleobiogeography, species synonymy, paleobiology, and body size evolution of major clades. Further, for many groups the only means of confidently determining ontogenetic status of an organism is through the destructive process of histological sampling. Although the ontogenetic patterns of Late Jurassic and Cretaceous dinosaurs are more well understood, knowledge of the ontogeny of the earliest dinosaurs is relatively poor because most species-level growth series known from these groups are small (usually, maximum of n = ~5) and incomplete. To investigate the morphological changes that occur during ontogeny in early dinosaurs, I used ontogenetic sequence analysis (OSA) to reconstruct developmental sequences of morphological changes in the postcranial ontogeny of the early theropods *Coelophysis bauri* and *Megapnosaurus rhodesiensis*, which are both known from large sample sizes (n = 174 and 183, respectively). I found a large amount of sequence polymorphism (i.e. intraspecific variation in developmental patterns) in both taxa and especially in *C. bauri*, which possesses this variation in every element analyzed. *Megapnosaurus rhodesiensis* is similar, but it possesses no variation in the sequence of development of tibial and tarsal ontogenetic characters. Despite the large amount of variation in growth, many characters occur consistently earlier or later in ontogeny and could therefore be important morphological features for assessing the relative maturity of other early-diverging theropods. Additionally, there is a phylogenetic signal to the order in which homologous characters appear in ontogeny, with homologous characters appearing earlier or later in developmental sequences of early-diverging

theropods and the close relatives of dinosaurs, silesaurids. Many of these morphological features are important characters for the reconstruction of archosaurian phylogeny. Because these features vary in presence or appearance with ontogeny, these characters should be used with caution when undertaking phylogenetic analyses in these groups, because a specimen may possess certain character states because of ontogenetic stage, not phylogenetic position.

KEYWORDS: Ontogeny, Triassic, dinosaur, theropod, intraspecific variation

1. INTRODUCTION

Understanding morphological changes undergone by an organism during ontogeny is a well-recognized problem in vertebrate paleontology, especially in extinct reptiles, which often lack easily discernable anatomical indicators of age (Johnson 1977; Galton 1982; Raath, 1990; Bennett 1993; 1996; Brochu 1996; Carr 1999; Irmis 2007; Delfino and Sánchez-Villagra 2010; Piechowski 2014; Griffin and Nesbitt 2016). Because the biology of extinct organisms may differ from their closest extant relatives in unexpected or unique ways, using extant analogues has an important but limited value for understanding how extinct organisms grew, and how those growth patterns have evolved through time (e.g., Irmis 2007). However, ontogenetic studies using extinct taxa, especially in older or rarer groups, are often hampered by a dearth of ontogenetic series of species-level taxa, and those series that are available often have a limited sample size (usually, a maximum of n = ~5).

Studies of Late Jurassic and Cretaceous dinosaurian ontogenies are relatively common and have been utilized with great success to understand such questions as species synonymy (e.g., Carr 1999; Scannella and Horner 2010; Horner and Goodwin

2009) which in turn influences paleodiversity estimates and paleobiogeography, the evolution of growth rates and metabolism (Horner et al. 1999; 2000; 2001; Padian et al. 2001; Erickson et al. 2004; Horner and Padian 2004), and mass-extinction structure and recovery (Codron et al. 2012). However, because of a comparative rarity of ontogenetic series, our understanding of the ontogenies of early-diverging dinosaurs is lacking, and our knowledge becomes increasingly poor in those clades closest to the origin of dinosaurs in the Late Triassic (Langer 2004; Langer and Benton 2006).

The comparatively uncommon ontogenetic studies of Triassic and Early Jurassic dinosaurs usually have focused on osteohistology (Chinsamy 1990; Chinsamy 1993; Ricqlés 1968; Sander et al. 2004; Sander and Klein 2005; Klein and Sander 2007; Knoll et al. 2010; Padian et al. 2004) or allometry (Gay 2005; Rinehart et al. 2009), with only a few studies undertaking a brief analysis of morphological variation in the context of growth (Colbert 1989; 1990; Raath 1990; Genin 1992; Benton et al. 2000; Tykoski 2005). In the latter, postcranial variation generally has been interpreted as evidence of sexual dimorphism, especially in the early neotheropod *Coelophysis*. Variation has been reported in six muscle attachment features of the femur of the Early Jurassic *Megapnosaurus* (= *'Syntarsus'*, Raath 1969; = *Coelophysis*, Bristowe and Raath 2004) *rhodesiensis*, which was interpreted as forming a robust/gracile dichotomy (Raath 1977; 1990). Although this morphological variation was connected to size ('gracile' individuals were on average smaller, and all the smallest individuals were this morph), Raath (1977; 1990) interpreted this pattern as evidence of sexual dimorphism, with the 'robust' morph only appearing at the onset of sexual maturity. The Late Triassic taxon *Coelophysis bauri* also has been interpreted as possessing sexually dimorphic variation. Although a

robust/gracile femoral dichotomy have been touched on in this taxon, differences in skeletal proportions have been the primary evidence put forward in favor of sexual dimorphism (Colbert 1989; 1990; Rinehart et al. 2009), along with some morphological characters (Rinehart et al. 2009). However, several studies have suggested that this dichotomy is less certain. Genin (1992), utilizing a principle compenents analysis, found no evidence of sexual dimorphism in the hindlimb of *C. bauri*, and Griffin and Nesbitt (Chapter 1), utilizing a larger sample size and greater number of morphological characters, argued that this variation in morphology is ontogenetic, rather than sexual dimorphism. A recent study of similar variation in femoral bone scars in the early-diverging dinosauriform *Asilisaurus kongwe* also suggested that this variation was the result of individual variation in ontogeny, and not sexual dimorphism (Griffin and Nesbitt 2016).

In this study, I describe postcranial variation in the early neotheropod dinosaurs *Coelophysis bauri* and *Megapnosaurus rhodesiensis* in detail, and place this variation in the context of ontogenetic change, following Griffin and Nesbitt (Chapter 1). *Coelophysis bauri* and *M. rhodesiensis* provide excellent study taxa to hypothesize on the cause of similar variation in early dinosaurs because: 1) they have been reported to possess a high amount of variation in the presence of bone scars and suture fusions (Colbert 1989; 1990; Raath 1977; 1990; Genin 1992; Chapter 1); 2) they are both early-diverging neotheropods, and therefore in a close phylogenetic position to the common dinosaurian ancestor (Nesbitt et al. 2009b; Nesbitt 2011; Sues et al. 2011); 3) both *C. bauri* and *M. rhodesiensis* are temporally close (Late Triassic and Early Jurassic, respectively; Colbert 1989; Raath 1977) to the origin of dinosaurs in the Late Triassic (Langer and Benton

2006; Brusatte et al. 2010); and 4) they are both known from large ontogenetic series. *Coelopysis bauri* in particular is known from a large number of articulated to partially articulated individuals (at least n = 75), allowing the relative developmental order of ontogenetic events across multiple elements to be determined.

Institutional Abbreviations: **AMNH FARB**, American Museum of Natural History, New York, New York, U.S.A.; **CM**, Carnegie Museum of Natural History, Pittsburgh, Pennsylvania, U.S.A.; **CMNH**, Cleveland Museum of Natural History, Cleveland, Ohio, U.S.A.; **FMNH**, Field Museum of Natural History, Chicago, Illinois, U.S.A.; **GR**, Ghost Ranch Ruth Hall Museum of Paleontology, Abiquiu, New Mexico, U.S.A.; **HMN**, Museum für Naturkunde, Humboldt Universität, Berlin, Germany; **MCZ**, Museum of Comparative Zoology, Harvard University, Cambridge, Massachusetts, U.S.A.; **MNA**, Museum of Northern Arizona, Flagstaff, Arizona, U.S.A.; **NMMNH**, New Mexico Museum of Natural History and Science, Albuquerque, New Mexico, U.S.A.; **QG**, Natural History Museum of Zimbabwe, Bulawayo, Zimbabwe; **SMP VP**, State Museum of Pennsylvania, Harrisburg, Pennsylvania, U.S.A.; **TMP**, Royal Tyrrell Museum of Paleontology, Drumheller, Alberta, Canada; **UCM,** University of Colorado Museum of Natural History, Boulder, Colorado, U.S.A.; **UMNH VP**, Utah Museum of Natural History, Salt lake City, Utah, U.S.A.

2. METHODS

Taxonomic Justification and Nomenclature

The generic name of the Zimbabwean coelophysoid theropod *'Syntarsus' rhodesiensis* (Raath 1977) has been changed several times: when the name *Syntarsus* was

found to be a previously-named beetle genus, and therefore taxonomically invalid to apply to a dinosaur, *'S.' rhodesiensis* was placed in the genus *Megapnosaurus* ("big dead reptile"; Ivie et al. 2001). Bristowe and Raath (2004) synonymized *Megapnosaurus* with *Coelophysis*, making the formal name of the Zimbabwean coelophysoid *Coelophysis rhodesiensis*, because *Coelophysis* had taxonomic priority. However, recent phylogenetic analyses have placed *Coelophysis rhodesiensis* as more closely related to *Camposaurus arizonensis* than to *Coelophysis bauri* (Ezcurra et al. 2011; You et al. 2014; Martill et al. 2016), making the genus *Coelophysis* paraphyletic and therefore taxonomically undesirable. Because synonymizing *Camposaurus* with *Coelophysis* to resolve this problem is unwarranted, I here follow Ivie et al. (2001) in referring to the Zimbabwean coelophysoid theropod as *Megapnosaurus rhodesiensis*. Because the generic name of the Early Jurassic coelophysoid *'Syntarsus' kayentakatae* (Rowe 1989) has not been formally changed to either *Coelophysis* or *Megapnosaurus* (nor should it be, because this would render either generic name used non-monophyletic; Ezcurra et al. 2011; You et al. 2014; Martill et al. 2016), I refer to this taxon with the generic name in quotes. I follow the definition of Coelophysoidea sensu Sereno et al. (2005) as the clade that includes all taxa that share a more recent common ancestor with *Coelophysis bauri* than with *Allosaurus fragilis*.

Measurements and Scoring Ontogenetic Characters

I measured dimensions of long bones, pelves, and tarsal elements with a Cen-Tech 6-inch digital caliper, and if the dimension in question was too large for this caliper to measure I took multiple measurements in the same dimension and added them together. When this was not possible I used a millimeter-graduated measuring tape to

measure the element in question. In order to compare the sizes of different specimens with non-overlapping elements, I used linear regressions to estimate femoral length for all specimens, thereby standardizing all specimen sizes (Supplemental Table 1). In a few cases, a statistically significant regression between a certain measurement (e.g., the maximum width of the distal end of the tibia) and femoral length could not be constructed because of a low sample size, and in these cases I used a linear regression to estimate the length of another element that did have a significant regression with femur length (e.g., tibia length). Although this adds another step of uncertainty to the final estimated femur length, it was only necessary for a few, highly incomplete specimens (Supplementary Data). Because the postcranial anatomy and proportions of *Coelophysis bauri* and *Megapnosaurus rhodesiensis* are so similar (Colbert 1989; Bristowe and Raath 2004), I used measurements from both taxa to construct these linear regressions, as well as a single measurement from the large Triassic neotheropod *Gojirasaurus quayi* (Carpenter 1997), which is extremely morphologically similar to both *C. bauri* and *M. rhodesiensis* in all but size.

The scoring for characters that were either present or absent (e.g., bone scars) was straightforward. Interelemental fusion events are not as easily scored, however, because a suture can possess varying degrees of closure, both across individuals and at different locations on the suture itself. Previous studies have utilized a three-tiered method of scoring suture closures, with the most immature state being an open suture, the intermediate state being a closed suture with a line of suture still visible, and the suture completely obliterated in the most mature state (Brochu 1996; Irmis 2007; Bailleulel et al. 2016). This method of scoring is useful for specimens of extant taxa and three-

dimensional well-preserved fossils, because sutures can show varying states of closure depending the portion of the suture being observed; however, many specimens of *C. bauri* and *M. rhodesiensis* are incompletely preserved, and most specimens of *C. bauri* are preserved in blocks, with matrix obscuring part or most of the specimen. Further, I do not know a priori whether all sutures fuse in their most mature state so as to completely obliterate the line of suture in these taxa. In order to reduce uncertainty, I scored sutures in only two categories. I scored fusion characters as immature in both cases of a completely open suture, and a suture incompletely open so that the three-dimensional line of suture was completely visible and formed a distinct depression between the two elements. The mature state was a suture only visible as a thin line on the surface of the bone, an incompletely obliterated line, or was completely obliterated. This method of scoring suture closure reduces resolution, but still accurately represents states. Additionally, this method is conservative with respect to variation in the sample, reducing variation that may have been introduced by taphonomic or methodological factors rather than biological.

Ontogenetic Sequence Analysis

Ontogenetic sequence analysis (OSA) is a size independent, parsimony-based method of reconstructing all equally parsimonious developmental sequences with all semaphoronts (i.e., discrete morphological ontogenetic stages in a taxon sensu Hennig 1966) of discrete ontogenetic characters within a population (Colbert and Rowe 2008). OSA allows for the testing and quantification of intraspecific variation in growth patterns, and is therefore ideal to reconstruct growth patterns in *Coelophysis bauri* and *Megapnosarus rhodesiensis*, which have been previously reported to possess a high

degree of variability in the presence of morphological characters (Raath 1979; 1990; Colbert 1989; 1990; Chapter 1). To summarize the method, which follows Colbert and Rowe (2008): NEXUS files of irreversible developmental characters are constructed, with specimens as operational taxonomic units (OTUs). Then, a parsimony-based cladistics program (e.g., PAUP*) is used to optimize these characters onto trees, which are then used to construct a reticulating diagram showing all equally parsimonious developmental sequences in the sample. In order to make all sequences link the least mature semaphoront with the most mature, this analysis is run twice: the first time with the most immature semaphoront as the outgroup, and the second with the most mature semaphoront as the outgroup. The trees returned from both analyses are used to construct a single reticulating diagram (e.g., Fig. 14). Because size and skeletal maturity appear to be somewhat disjunctive in early theropods (e.g., Raath 1990; Chapter 1; this study) OSA is preferable to reconstructing the ontogeny of these taxa because it provides a way to reconstruct developmental sequences without utilizing the common assumption that size is correlated with ontogenetic age and maturity.

I examined specimens of *Coelophysis bauri* and *Megapnosaurus rhodesiensis* in person to evaluate developmental character states. In OSA, immature character states are scored as [0], whereas mature character states are scored as [1]. One character (character 2) possessed multiple, ordered, irreversible character states, and for this character the most mature state was scored as [2], with the state possessing intermediate maturity scored as [1] and the least mature state scored as [0]. Missing data were scored as [?], and all characters were treated as irreversible. These data were stored as NEXUS files (supplemental data). For *Coelophysis bauri*, I split the data into a femoral character

dataset, a tibial and tarsal/metatarsal character dataset, and a pelvic character dataset, as well as a dataset that included all ontogenetic characters from all elements in question. Because *'Syntarsus' rhodesiensis* consists largely of disarticulated elements, inter-elemental comparison of growth patterns was not possible to determine with any accuracy, so I split ontogenetic character data for this taxon into a femoral, a tibial-tarsal, and a pelvic data set. Because of disarticulation, the tibial-tarsal dataset of *M. rhodesiensis* lacked the two pedal characters of the tibial and tarsal/metatarsal dataset of *C. bauri*. For all datasets I then eliminated all specimens that, because of missing data, only possessed information for a single character, because these specimens are useless for reconstructing the relative timing of developmental events. I then combined specimens with identical suites of character data into a single operational taxonomic unit (OTU). Some OTUs were redundant with others; that is, the suite of character data they possessed was identical with that of another OTU, but the latter OTU possessed less missing data. These redundant OTUs do not add new sequence information while simultaneously introducing uncertainty into the analysis, because the parsimony program is forced to reconstruct the missing data, so I eliminated them from the initial analysis using the safe taxonomic reduction function in the Claddis package (Lloyd 2016) in R (www.r-project.com). As safe taxonomic reduction (Wilkinson 1995) eliminates all redundant OTUs, so this method reduces uncertainty while retaining the most informative data. In order to run the 'reverse' analysis with the most mature semaphoront as the outgroup, reversal of character states is necessary. For the 'reverse' NEXUS files, all characters scored as [0] were scored as [1], and vice-versa. The only exception was for character 2 (number of fused sacra), for which [0] and [2] were reversed. For datasets

which did not contain an OTU with entirely immature or mature characters, I included an artificial OTU with completely mature or immature character states to provide outgroups (see next paragraph). However, all character states were observed in the sample, and all characters states in these artificial immature and mature outgroup OTUs were observed in specimens.

I conducted OSA using the method of Colbert and Rowe (2008). Using PAUP* (v. 4.0b10, Swofford, 2002), a heuristic search was run on each NEXUS file using a tree-bisection-reconnection algorithm for 300 replicates and adding sequences randomly. When the heuristic search was completed, I collapsed all branches with a minimum length of zero and saved all trees to a .tre file. The 'normal' dataset was run with the most immature individual as the outgroup OTU, and the 'reversed' dataset with the most mature as the outgroup. These trees were then visualized in MacClade (v. 4.04, Maddison and Maddison 2002) with the "trace all changes" function used to see all reconstructed character transformations for all trees. This was done for all 'normal' and 'reverse' datasets, and then reticulating diagrams were constructed for each pair of datasets following standard OSA procedure (Colbert and Rowe 2008). Although I followed the standard OSA method described by Colbert and Rowe (2008), some modifications were necessary to accommodate a dataset with a larger than normal amount of missing data, and to do so I followed the methodology described in Chapter 1.

Additionally, because these data represent a large amount of variation in combination with a fairly large amount of missing data, one further modification to the traditional OSA methodology was required. Some specimens with a large amount of missing data nevertheless possessed suites of characters that were unique with respect to

nearly all other specimens in the sample, especially in the full-body dataset of *Coelophysis bauri*. Because of this missing data, the 'normal' treatment reconstructed these specimens in sequences close to the immature outgroup, but in highly divergent sequences that were different from other reconstructed sequences because of the odd suite of character scores these specimens possessed. The 'reverse' treatment did the opposite, and reconstructed these specimens as being close to the mature outgroup (with missing data reconstructed as mature instead of immature character states) in, again, highly anomalous sequences. Usually, the two treatments result in all semaphoronts linked by developmental sequences which all connect the immature and mature outgroup semaphoronts, following the assumption of OSA that all characters proceed from immature to mature states during ontogeny; therefore, any semaphoront that is not linked to the mature semaphoront in the 'normal' treatment is linked by the 'reverse' treatment, and vice-versa. However, because the same specimens were reconstructed in such different places in the reticulating diagram, and possessed such anomalous suites of character states, they were left 'stranded' and did not form complete developmental sequences. To complete these sequences, I manually connected the least or most mature semaphoront in each incomplete developmental sequence to the mature or immature outgroup semaphoront, respectively. This resulted in a number of developmental sequences that were highly unresolved and possessed very low specimen frequency support weights. Reconstruction of specimens as closer to either the immature or mature outgroup semaphoront are both equally consistent with the data; however, in order to avoid inflating the amount of sequence polymorphism reconstructed in the population by including both reconstructed states of these specimens, I arbitrarily chose to eliminate

the incomplete, manually reconstructed sequence close to the mature outgroup semaphoront, with the semaphoronts representing those same specimens reconstructed as close to the immature outgroup remaining in the final analysis. The 'raw' OSA diagrams and sequences can be found in the supplementary data.

Frequency support weight is a dimensionless number that represents the number of specimens (i.e., specimen support) for a single semaphoront. A specimen lends a support weight of 1 to a semaphoront if that is the only semaphoront which can represent it. If, because of missing data, two semaphoronts are both equally consistent with this specimen, then each of those semaphoronts is lent a weight of 0.5 for this specimen. The combined specimen support in a semaphoront gives that semaphoront's frequency support weight, and that developmental sequence possessing the highest combined frequency support weight—that is, the developmental sequence representing the most specimens—is the modal sequence.

3. DESCRIPTION

Descriptions of Ontogenetic Characters

1. Sacrum, neural spine fusion: (0) all neural spines separate; (1) neural spines fused into single sheet of bone. (Fig. 1A)

In individuals of both *Coelophysis bauri* and *Megapnosaurus rhodesiensis* the neural spines can either be distinct structures or coossified into a single, continuous structure of five sacral neural spines. This variation in fusion has been suggested to be sexual dimorphic, with one sex possessing unfused sacral spines and the other fused spines (Colbert 1989, 1990; Rinehart et al. 2009), but I interpret this character as being variable through ontogeny, following Raath (1990), with unfused spines as the immature

character state and spines fused into a single bony sheet as the mature state. This hypothesis is supported by the existence of individuals with somewhat intermediate character states: in one individual of *C. bauri* (AMNH FARB 7228), although the neural spines are fused into a single sheet, the fusion is relatively incomplete with respect to other individuals, and on the dorsal edge of the structure the individual neural spines are discernable. I scored all individuals with five fused sacral neural spines as [1], even if they were less completely fused than others, because this minor variation in individuals with fused spines was only discernable in exceptionally well-preserved individuals, whereas for most individuals I was only able to determine whether or not the spines were separate or fused together. Because I could only confidently determine the relative degree of fusion in a few individuals, I chose to consider fusion of all degrees as state [1].

2. Sacrum, number of five sacral centra coossified: (0) 0–3 coossified sacral centra; (1) 4 coossified sacral centra; (2) 5 coossified sacral centra. Ordered character. (Fig. 1B, D)

In the largest individuals of *Coelophysis bauri* and *Megapnosaurus rhodesiensis* the centra of the five sacral vertebrae are fused together, with the suture between centra obliterated, producing a smooth continuous surface. However, many individuals possess only four sacrals in this coossified structure, with the posteriormost sacral (sacral 5) remaining unfused. Some individuals of *C. bauri* possess only three fused sacrals, with four and five remaining unfused, and in one individual (TMP 1984.063.0001) lacks fusion between all centra. Because observation of the sacrum is partially obscured by the ilium in some specimens, especially those of *C. bauri*, in these specimens I was only able to determine whether the centra of sacrals 1 and 2 and sacrals 4 and 5 were coossified, with the articulations between sacrals 2, 3, and 4 remaining covered. Because I never

observed an individual with the anterior two or posterior two sacrals fused without fusion between the interior sacrals, and because the position of these interior sacrals was always consistent with their being fused into a single structure, I chose to score these as fused even when the fusions themselves were not visible. Therefore, an individual with observed fusion between sacral centra 1 and 2, and 4 and 5, was scored as [2]. An individual with fusion between sacrals 1 and 2, but not 4 and 5, was scored as [1]. This method of scoring this character is conservative with respect to the amount of variation in the sample, because it will underestimate, rather than overestimate, intraspecific variation in the number of fused sacral centra.

Only a few individuals of *C. bauri* were scored as fully immature [0] for this character, and in two of these individuals the anterior three sacrals were coossified, with sacrals 4 and 5 remaining unfused (AMNH FARB 7230, NMMNH P-42353). However, in TMP 1984.063.0001 all articulations of sacral centra that are visible are unfused, with only the articulation between sacrals 2 and 3 obscured by the ilium. Unlike the other sacral vertebrae in this individual, sacrals 2 and 3 are roughly in life position, consistent with both their being fused, or with their simply being in proper articulation with each other. Therefore, I cannot say with certainty whether there are two fused sacrals in this individual, or none. Two specimens of *M. rhodesiensis* (QG 179; unnumbered) consisted entirely of two unfused sacrals, and these can be confidently identified as either sacrals 2 and 3 or 3 and 4 because the articulations for the sacral ribs are shared between centra (Nesbitt 2011), justifying a score of [0]. If the hypothesized sequence of sacral fusion in *C. bauri* holds for *M. rhodesiensis*, this suggests that these two specimens possess no fused sacrals, because fusions between sacral centra 2 and at least one adjacent centrum

would be expected to be the first fusion event to occur following the order of fusion I have hypothesized above.

Fusion of sacral centra is a synapomorphy of Neotheropoda, with the proximal outgroups of this clade (e.g., *Herrerasaurus*, *Staurikosaurus*, *Saturnalia*) lacking this character state (Nesbitt 2011). Sacral centra are also coossified in ornithischian dinosaurs, some sauropodomorphs, pterosaurs, and several pseudosuchian lineages; however, the sacral centra of the silesaurid *Silesaurus opolensis* lack coossification (Nesbitt 2011), so this character state has evolved independently in multiple archosaurian lineages.

3. Scapula and coracoid, fusion between elements: (0) absent; (1) present. (Fig. 2)

In some individuals of both *Coelophysis* and *Megapnosaurus* the scapula and coracoid have coossified into a single structure, the scapulocoracoid, with the line of suture either completely obliterated or so faint that the elements would be unable to disassociate.

Fusion between the scapula and coracoid is common in the ontogeny of amniotes and is present in many lepidosaurs (Romer 1956), turtles (Lee 1996) crocodylians (e.g., Brochu 1992), phytosaurs (Camp 1930), silesaurids (e.g., *Asilisaurus kongwe*, NMT RB159; *Silesaurus opolensis*, Dzik 2003), and early saurischians (e.g., *Eoraptor lunensis*, Sereno et al. 2013). Given how widespread this character is across Reptilia, it may be the ancestral saurian condition to fuse the scapula and coracoid during ontogeny. Fusion of the scapula and coracoid is the only character I observed to be variable within a single individual: in NMMNH P-42577, the left scapulocoracoid is completely coossified, whereas the right scapula and coracoid are separate from each other. For this specimen, I scored this character as immature, following a preference for scoring characters as

immature until the mature state for that character has unambiguously been reached (see Methods).

4. Humerus, scar of origin of M. triceps brachii caput laterale: (0) absent; (1) present as rugose ridge. (Fig. 3)

A low, rugose ridge effectively acts as the border between the deltopectoral crest and the shaft, extending distally from the proximolateral edge of the deltopectoral crest along the humeral shaft, terminating at roughly the same location that the distal portion of the deltopectoral crest joins the humeral shaft. This feature is present in some individuals of both *Coelophysis bauri* and *Megapnosaurus rhodesiensis* (e.g., AMNH FARB 7223; QG 1).

The broad anterolateral face of the deltopectoral crest is the insertion of the M. deltoideus clavicularis in crocodylians and *Sphenodon* (Dilkes 2000; Meers 2003). Burch (2014) also reconstructed this face as the insertion of the M. deltoideus clavicularis (hypothesized to be homologous with either the propatagialis in avians; Burch 2014) the early theropod *Tawa hallae*, with the low ridge as the origin of the M. triceps brachii caput laterale (TBL), marking the posterior margin of the M. deltoideus clavicularis insertion area. Given that this feature is common in theropods, early sauropodomorphs (*Saturnalia,* Langer et al. 2007), and early-diverging dinosauromorphs (*Dromomeron romeri*, pers. obs., unnumbered Hayden Quarry specimen reposited at GR) I follow Burch's (2014) hypothesis for the identification of the muscle associated with this osteological feature.

5. Humerus, scar of origin of the M. triceps brachii caput mediale: (0) absent; (1) present as rugose ridge. (Fig. 3)

Megapnosaurus rhodesiensis possesses a linear, rugose ridge on the proximal, posteromedial portion of the humeral shaft that is connected at its most distal point to the origination scar of the TBL. Proximal to this point, it extends posteriorly and proximally to the same proximal level as the origin scar of the triceps brachii caput laterale, forming a 'V' shape in posterolateral view from the intersection between the two scars. I did now observe this scar (character 5) in any individual of *Coelophysis bauri*; however, the hypothesized mature state of this character is variable during ontogeny in *Megapnosaurus*, and the preservation of most individuals of *C. bauri* in blocks that only expose one side of the element in question made scoring this character problematic for the majority of individuals. Therefore, possible reasons for the absence of this character state in *C. bauri* include: 1) this character state develops later in ontogeny in *C. bauri* than *M. rhodesiensis*, and all individuals for which the humeri were observed were too immature; 2) the order in which that this character state appears during ontogeny is highly variable in *C. bauri*, and the low humeral sample size for this taxon simply made observing the mature state of this character unlikely; and 3) this character state is autapomorphic for *Megapnosaurus rhodesiensis*. Because this scar is absent in otherwise robust, mature individuals of both *C. bauri* and *'Syntarsus' kyentakatae*, I hypothesize that this character is an autapomorphy of *Megapnosaurus rhodesiensis* and is not present in other coelophysoids regardless of skeletal maturity.

In extant crocodylians and birds, the origin of the M. triceps brachii caput medialis (TBM) is a wide region on the posteromedial potion of the humeral shaft, extending distally from the posteroproximal region of the humerus to cover nearly the entire humeral shaft (Burch 2014). The proximalmost portion of the origin of this muscle

is bifurcated, and I hypothesize that the rugose ridge that extends proximomedially away from the origin scar of the TBL is the osteological correlate for the origin of the lateral branch of the proximal region of the origin of the TBM. Although this muscle has been reconstructed in theropods (Burch 2014), the origin of this muscle has not been previously hypothesized to correspond to a bone scar or other osteological correlate.

6. Humerus, raised lineation along posterior portion of the humeral shaft: (0) absent; (1) present. (Fig. 3)

A raised proximodistally-oriented lineation morphologically similar to the femoral intermuscular lines (see characters 17 and 18) is present along the posterior face of the humerus in *Megapnosaurus rhodesiensis*, originating just distal and posterior to the deltopectoral crest and origin scar of the TBM, and terminating halfway down the humeral shaft. This scar was not observed in any individuals of *Coelophysis bauri*, but like the scar for the origin of the TBM (character 5), this may be the result of sampling or preservational issues. However, similar to the origination scar for the TBM, this scar is absent in otherwise robust, mature individuals of both *C. bauri* and *'Syntarsus' kyentakatae*, so I hypothesize that this character is also an autapomorphy of *Megapnosaurus rhodesiensis*.

The humeri of many theropods (e.g., dromaeosaurids, troodontids, *Tawa hallae*) have been reported to possess a linear groove on the lateral side of the humerus posterior to the deltopectoral crest, and this has been thought to represent the insertion site of the M. latissimus dorsi in these taxa (Jasinoski et al. 2006; Burch 2014). In extant crocodylians and birds the insertion of this muscle is marked by a rugose scar or tuberosity (Meers 2003; Jasinoski et al. 2006), and in birds as a scar or long ridge

(Jasinoski et al. 2006). Because the scar in *M. rhodesiensis* is situated in a similar position to that reconstructed at the insertion of the M. latissimus dorsi for *Tawa hallae* (Burch et al. 2014: Fig. 3), I hypothesize that this scar is the osteological correlate for the insertion of the M. latissimus dorsi in *M. rhodesiensis*.

7. Humerus, deltopectoral crest: (0) gracile and mediolaterally thin; (1) robust and thick in the anterior portion. (Fig. 3)

In *Coelophysis* and *Megapnosaurus* the anteriormost portion of the deltopectoral crest of the humerus possesses two morphologies, gracile and robust, analogous to the two morphologies of the fourth trochanter in these taxa (see character 23) and in *Asilisaurus kongwe* (Griffin and Nesbitt 2016) and *Dromomeron gregorii* (Nesbitt et al. 2009a). In the gracile morph (e.g., QG 517) the deltopectoral crest is smooth to the apex on the anterior portion of the crest, and is relatively poorly extended anteriorly. The robust morph (e.g., QG 543) possesses a large, raised rugose surface on the apex of the deltopectoral crest, similar in morphology to hypertrophied muscle scars, and because of this the crest extends farther anteriorly.

The apex of the deltopectoral crest, along with the area immediately lateral to it, is the insertion of the supracoraoideus in crocodylians (Meers 2003), although in birds it has shifted to the posterior surface of the greater tubercle (Jasinoski et al. 2006). In reconstructing the musculature of *Tawa hallae*, Burch (2014) hypothesized that the apex of the deltopectoral crest remained the insertion of the supracoracoideus in this taxon, and I follow this hypothesis that the apex of the deltopectoral crest, and especially the hypertrophied ossification that is present in some individuals, is the osteological correlate of the supracoracoideus insertion.

8. Ilium and pubis, fusion: (0) absent; (1) present. (Figs. 1D; 4B; 5)

The ilium fuses with the pubis in some individuals of both *Coelophysis bauri* and *Megapnosaurus rhodesiensis*. The suture between these two elements is completely obliterated during this fusion, and a slightly raised area is present at the region of the suture.

Fusion between the ilium and pubis, ilium and ischium (character 9), and pubis and ischium (character 10) has been recognized as an ontogenetic character within coelophysoids and other early diverging non-averostran theropods (Rowe and Gauthier 1990; Tykoski and Rowe 2004; Tykoski 2005). Holtz (1994, p. 1103) found the character "ilium fused with pubis and ischium in adults" to be a synapomorphy of Ceratosauria, a clade that sensu Gauthier (1984) included coelophysoid neotheropods and other early-diverging neotheropods now placed in a grade outside Averostra (Carrano and Sampson 1999; Forster 1999; Carrano et al. 2002; Rauhut 2003; Wilson et al. 2003; Sereno et al. 2004). However, although *'Sytarsus' kayentakatae* is known to coossify its pelvic elements, *Dilophosaurus wetherelli* and *Lilliensternus lilliensterni* are known only from individuals with unfused pelvic elements (Tykoski 2005), as is *Cryolophosaurus ellioti* (Smith et al. 2007), and *Gojirasaurus quayi* (UCM 47221) is only known from an individual possessing completely unfused right pubis. Therefore, how widespread these ontogenetic characters are among early-diverging theropods is poorly constrained. Although *Ceratosaurus nasicornis* completely coossifies its pelvic elements (Marsh 1892), even skeletally mature individuals of *Allosaurus fragilis* lack pelvic coossification (Madsen 1976), suggesting that pelvic fusion may occur during ontogeny in all non-averostran neotheropods. Outside of Theropoda pelvic fusion is rare, with early-diverging

sauropodomorphs (e.g., *Plateosaurus engelhardti*, Galton 1990), silesaurids (*Silesaurus opolensis*, Dzik 2003; *Asilisaurus kongwe*, NMT RB159), and early saurischians (Holtz and Osmólska 2004) lacking fusion of pelvic elements, although the pelvis of the dinosauriform *Marasuchus lilloensis* is completely fused (Sereno and Arcucci 1994).

9. Ilium and ischium, fusion: (0) absent; (1) present. (Figs. 1D; 4B, D)

The ilium and ischium completely coossify in some individuals of both *Coelophysis bauri* and *Megapnosaurus rhodesiensis*, and the homology of this character is discussed in conjunction with the other pelvic ontogenetic characters of the pelvis in the description of character 8.

10. Pubis and ischium, fusion: (0) absent; (1) present. (Figs. 1B, D; 4D)

The pubis and ischium completely coossify in some individuals of both *Coelopysis bauri* and *Megapnosaurus rhodesiensis*. The homology of this character is discussed in conjunction with the other pelvic ontogenetic characters in the description of character 8.

11. Femur, shallow groove on proximal surface: (0) present and deep; (1) faint, and nearly absent. (Fig. 5)

In many smaller or less skeletally mature individuals of *Megapnosaurus rhodesiensis* (e.g., QG 713, 714, 741) the proximal surface of the femur possess a shallow groove. This groove is present between the posteromedial and anterolateral tubera in proximal aspect and extends down the middle of the proximal surface of the femur to just posterodistal to the posterolateral tuber, curving medially slightly near the posterolateral depression (sensu Novas 1996). This groove is so shallow as to be almost

entirely absent in many larger or more robust femora, and all individuals of *Coelopysis bauri* for which this character could be scored possess this morphology.

The presence, absence, and different morphologies of a groove on the proximal surface of the femur have been used as phylogenetic character states in studies of archosaur relationships (Ezcurra 2006; Nesbitt 2011). Many crocodile-line archosaurs, as well as silesaurids, possess a relatively deep straight groove on the proximal surface of the femur, whereas many other pseudosuchians and avemetatarsalians possess a rounded proximal femoral surface, with no groove. Smaller individuals of the aetosaur *Typothorax coccinarum* possess a groove, whereas in larger individuals the proximal femoral surface is smooth, suggesting that this character is ontogenetically variable in this taxon (Nesbitt 2011). Nesbitt (2011) described early-diverging neotheropods (i.e., *Coelophysis bauri*) as possessing a curved groove on the proximal surface of the femur, and it is this groove that I find to be ontogenetically variable in morphology. Because both *Liliensternus liliensterni* (HMN MB.R.2175) and the 'Padian *Coelophysis*' (UCMP 129618) possess this groove, this is not an autapomorphy of *Megapnosaurus rhodesiensis*.

12. Femur, depression on anterolateral face of proximal portion: (0) present; (1) absent. (Fig. 7B)

In many smaller or less skeletally mature femora of *Megapnosaurus rhodesiensis* (e.g., QG 691) there is a shallow depression on the anterolateral face of the proximal portion of the femur. The edge of the depression is sharp posterior to the anterolateral tuber and just distal to the articular surface, forming a well-defined border on the anterior and proximal sides of the depression. However, the depression is poorly defined along the posterior and distal regions, and the surface of the depression grades into the normal

cortical bone, making a distinct border between the depression and normal bone impossible to determine. The depression is deepest anteroproximally, nearest to the distinct edge. No femora of *Coelophysis bauri* possess this feature, even in extremely small and gracile individuals. This either suggests that all observed femora are too skeletally mature to possess the immature morph of this ontogenetic character, or that this character is never present in *C. bauri*.

Raath (1977) referred to this feature as a 'shallow dimple,' interpreting it as a location of ligament attachment homologous with the avian teres ligament (sensu Cracraft 1971). I interpret this shallow pit, along with the anterolateral scar (character 19), as an osteological correlate of the attachment of the iliofemoral ligament, which inserts on the anterolateral face of the proximal end of the femur in *Alligator mississippiensis* (Tsai and Holliday 2014). The shallow 'basin' bordered laterodistally by the anterolateral scar makes up the majority of the insertion surface of the iliofemoral ligament (see discussion for character 19), and the sharp depression in some individuals of *M. rhodesiensis* marks the medioproximal border of this insertion area. The region bordered by these two features is roughly the same shape and relative area as the anterolateral scar of silesaurids, further suggesting that both these features represent parts of the attachment area of the iliofemoralis ligament. Because this pit is largely present in less skeletally mature individuals of *M. rhodesiensis*, and the anterolateral scar is present in mature morphs, relatively few femora possess both structures. I have not observed this feature in its immature state in any other early theropod taxon, though this may be because this feature is present in earlier ontogenetic stages than are preserved for most

other taxa. This feature, or at least its appearance at such a relatively late stage in ontogeny, may therefore be autapomorphic for *Megapnosaurus rhodesiensis*.

13. Femur, anterolateral edge of proximal surface extending anterolaterally: (0) absent; (1) present. (Fig. 8D)

The anterolateral border of the proximal surface of the femur is dorsoventrally continuous with the anterolateral face of the femur in many less mature individuals of both *Coelophysis bauri* (e.g., TMP 1984.063.0001) and *Megapnosaurus rhodesiensis* (e.g., QG 691), but in many robust individuals this articular edge extends anterolaterally, forming a 'lip' overhanging the anterolateral face of the femur in anteromedial or posterolateral view. Although I have observed this feature to be variable *Coelophysis bauri*, it is not nearly as variable as in *Megapnosaurus rhodesiensis*, and preservational issues made scoring this character much easier and more consistent in the latter taxon. Therefore, although this appears to be a feature in the ontogeny of *C. bauri* as well, I only scored this character state for *M. rhodesiensis*. I am not aware of this ontogenetic change being referred to elsewhere in the literature, so establishing any homology for this character is difficult.

14. Femur, trochanteric shelf: (0) absent; (1) present. (Figs. 5; 7; 9F)

In *Coelophysis bauri* and *Megapnosaurus rhodesiensis*, the trochanteric shelf is usually a roughly horizontal rugose ledge, which forms a continuous structure with the posterodistal portion of the anterior trochanter. When present (e.g., AMNH FARB 7228), the shelf trends towards the posterior edge of the femur. The proximal part of the shelf connects abruptly with the bone surface, forming a distinct ledge, but the trochanteric shelf extends much further distally, often intersecting the bone surface at a lower angle to

the lateral edge. The shelf extends laterally away from the femur, often a farther distance than its own proximodistal axis. In those specimens in which the trochanteric shelf is absent (e.g., TMP 1984.063.0001; QG 691) there is a low, subtle mound, continuous with and indistinguishable from the normal subperiosteal bone surface. A similar structure exists in *Tawa hallae* (Nesbitt et al. 2009b, Fig. 2) some specimens of *Dilophosaurus wetherelli* (Welles 1984, Fig 32; A. Marsh pers. comm. 2015) and all specimens of *Allosaurus fragilis* (Madsen 1976, plate 50; pers. obs.). The presence of the trochanteric shelf has been suggested to relate to ontogenetic stage in early dinosaurs and their closest relatives (Raath 1977; 1990; Nesbitt et al. 2009a; Piechowski et al. 2014; Griffin and Nesbitt 2016; Chapter 1).

The trochanteric shelf is the osteological correlate for the insertion of the M. iliofemoralis externus (= M. iliofemoralis is Crocodylia), and has been hypothesized to have originated in Dinosauromorpha (Hutchinson 2001; Nesbitt et al. 2009a). This structure has been identified in early-diverging dinosauromorphs (*Dromomeron gregorii*, Nesbitt et al. 2009a; *D. gigas*, Martínez et al. 2015) and dinosauriforms (*Marasuchus lilloensis*, Sereno and Arcucci 1994; silesaurids, Nesbitt 2011; Piechowski et al. 2014; Griffin and Nesbitt 2016). The posterior portion of the trochanteric shelf has been hypothesized to correspond to the insertion of the M. ischiotrochantericus (Novas 1996; Hutchinson 2001; 2002).

The presence or absence of the trochanteric shelf appears to affect the morphology of the anterior (= 'lesser') trochanter, which is present in all specimens of *Coelophysis bauri* and *Megapnosaurus rhodesiensis* for which the absence or presence of this feature could be observed. The anterior trochanter is the attachment site of the M.

iliotrochanteris caudalis, and this muscle has also been hypothesized to be homologous with the M. iliofemoralis of crocodylians (Hutchinson 2001). Although originally hypothesized to be a dinosauriform synapomorphy (Hutchinson 2001), the anterior trochanter appears to be present in some early-diverging dinosauromorphs (*Dromomeron gregorii*, Nesbitt et al. 2009a; potentially *D. gigas*, Martínez et al. 2015; *Marasuchus lilloensis*, Sereno and Arcucci 1994), but is only present in a continuous structure with the trochanteric shelf. In at least some silesaurids, the anterior trochanter and trochanteric shelf are partly distinct from each other during ontogeny, but the most mature individuals usually possess both in a single continuous structure (*Sileaurus opolensis*, Dzik 2003; Piechowski et al. 2014; *Asilisaurus kongwe*, Griffin and Nesbitt 2016). In *Coelophysis*, the anterior trochanter usually takes two distinct forms. When the trochanteric shelf is absent (e.g., TMP 1984.063.0001), the anterior trochanter is a spike-like structure oriented proximodistally, roughly twice as tall as it is anteroposteriorly wide, with the proximalmost end of the trochanter detached from the femoral surface and narrowed relative to the rest of the structure. Both the posterolateral and anteromedial faces of this structure are flattened, similar to other dinosaurs (e.g., *Tawa hallae*, Nesbitt et al. 2009b; *Allosaurus fragilis*, Madsen 1976) and non-dinosaurian dinosauriforms (e.g., *Silesaurus opolensis*, Dzik 2003; Piechowski et al. 2014). When the trochanteric shelf is present (e.g., AMNH FARB 7228), the anterior trochanter is rugose raised triangular surface continuous with, but distinct from, the femoral surface, and continuous with the trochanteric shelf. The apex of the anterior trochanter, in relation to the surficial distance away from the femoral surface, occurs just medial to the middle of the anterior trochanter in anterolateral view, and this apex is usually continuous with the ridge of the

trochanteric shelf. A few specimens (e.g., *Coelophysis bauri*, AMNH FARB 7244; *Megapnosaurus rhodesiensis*, QG 174) possess small and indistinct trochanteric shelves (see description of character 15), and in these specimens the anterior trochanter is morphologically similar to those in specimens completely lacking trochanteric shelves. The existence of these intermediate morphologies supports my interpretation of this variation as ontogenetic.

15. Femur, size of trochanteric shelf: (0) absent or small, does not extend past posterolateral edge of femur in anterolateral view; (1) large, extends past the posterolateral edge of femur in anterolateral view. (Figs. 5; 7; 9F)

In some specimens (e.g., SMP VP 1072), the trochanteric shelf was extremely large and well developed, whereas in others (e.g., AMNH FARB 7244; QG 174) it was small, poorly developed, and did not extend far posteriorly away from the anterior trochanter in both *Coelophysis bauri* and *Megapnosaurus rhodesiensis*. I split the trochanteric shelf into two morphologies: underdeveloped trochanteric shelves are those that, in anterolateral view, do not extend past the posterolateral edge of the femur, but instead are confined to the area immediately posterolateral to the anterior trochanter. Large, well-developed trochanteric shelves are those that extend past the posterolateral edge of the femur in anterolateral view. This cutoff point (the posterolateral edge of the femur) is not arbitrary, but chosen because the largest trochanteric shelves in the most mature individuals are connected with the linea intermuscularis caudalis (character 18) and insertion scar for the M. caudifemoralis brevis (character 22). In the latter especially, the trochanteric shelf is unable to reach this scar if it does not extend past the edge of the femur, and so the trochanteric shelf must be large enough for the femur to possess mature

character states. I scored this as a separate character from character 14 instead of a single, ordered, multistate character because in some damaged specimens I was able to determine that a trochanteric shelf was present, but was unable to determine its size.

In most individuals scored as [0] for this character, the trochanteric shelf is either completely absent or is simply small while still conforming with the description of the trochanteric shelf given in the description of character 14. However, in a few specimens the trochanteric shelf is present but underdeveloped to an unusual degree, and in these specimens the anterior trochanter retained the morphology normally only in specimens completely lacking a trochanteric shelf. These intermediate morphologies support this character as ontogenetically variable, because a shelf that is present but still developing would be expected for such a feature. Oddly, these underdeveloped shelves have differing morphologies, with some located further away from the anterior trochanter, with a gap between the two structure (AMNH FARB 7244), and others appearing to be posterolateral outgrowths of the anterior trochanter (QG 174c), suggesting that the way in which the trochanteric shelf develops may in itself be variable.

16. Femur, dorsolateral trochanter: (0) ridge-like; (1) mound-like, ossified on to femur. (Figs. 5; 7; 8D; 9D, F)

In *Coelophysis bauri* and *Megapnosaurus rhodesiensis* the dorsolateral trochanter is present in two morphologies. One morphology (e.g., QG 169) is the classic flange-like structure that is normally described as a dorsolateral trochanter in other taxa (see below). This flange is present on the posteriormost portion of the anterolateral face of the 'greater trochanter'. The proximal portion of the dorsolateral trochanter is relatively free from the femoral surface in this morph, but the distal portion of the dorsolateral trochanter is

usually continuous with the 'greater trochanter'. The posterior surface of the dorsolateral trochanter tends to be rounded, with a flattened side facing anterolaterally. The second morph of the dorsolateral trochanter is a large mound extending posterolaterally from the 'greater trochanter', and unlike the flange-like morph is completely continuous with the femoral surface. This mound is often rugose in the most well preserved specimens (e.g., AMNH FARB 7244), and the mound extends from the anterolateral face around to the posteromedial face of the 'greater trochanter.' Similarly, the scar hypothesized to be homologous with the dorsolateral trochanter extended from the anterolateral face to the posteromedial face of the 'greater trochanter' in *Asilisaurus kongwe* (Griffin and Nesbitt 2016). In some specimens the dorsolateral trochanter possesses an intermediate morphology, and a small proximodistally-oriented ridge extends out from a mound, although most of the flange is incorporated into the mound. I therefore hypothesize that the mound morph is the result of the flange morph being fully incorporated into the main body of the femur. Because of this, and because femora possessing the flange-like morph of the dorsolateral trochanter tended to be smaller and less common than those with a robust dorsolateral trochanter, I hypothesize that the gracile flange morph is the immature ontogenetic state of this character, with the robust mound morph being the robust state. Because the intermediate morphology still possesses flange-like characters and is therefore not fully mature, I scored this morphology as immature [0] as well.

The dorsolateral trochanter has been hypothesized to correspond to either the attachment point of one of the branches of the Mm. iliotrochanterici (Rowe 1986; Langer and Benton 2006; Mm. iliotrochanterici = M. pubo-ischio-femoralis internus 2 in crocodylians, Hutchinson 2001) or M. puboischiofemoralis externus (Hutchinson 2001),

and is a derived dinosauriform character (Langer and Benton 2006; Irmis et al. 2007; Nesbitt et al. 2010), synapomorphic for the clade Silesauridae + Dinosauria (Nesbitt 2011). In addition to its presence in theropods, the dorsolateral trochanter has been described in early-diverging ornithischians (e.g., *Lesothosaurus diagnosticus*, Sereno 1991; *Eocursor parvus*, Butler 2010) and saurischians (e.g., *Herrerasaurus ischigualastensis*, Novas 1993, fig. 7; *Saturnalia tupiniquim*, Langer 2003), as well as several silesaurids (*Sacisaurus agudoensis*, Ferigolo and Langer 2006; Langer and Ferigolo 2013; *Eucoelophysis baldwini,* Nesbitt et al. 2007; *Silesaurus opolensis*, Nesbitt 2011; an unnamed silesaurid, TMM 31100-1303, Griffin and Nesbitt 2016). The dorsolateral trochanter is absent in the smallest specimens of *Silesaurus opolensis*, leading Nesbitt et al. (2007) and Piechowski et al. (2014) to consider its presence and morphology related to growth. The Middle Triassic silesaurid *Asilisaurus kongwe* has been reported to possess a thin scar corresponding to the location of the dorsolateral trochanter in other silesaurids (Griffin and Nesbitt 2016), although all specimens referable to *A. kongwe* lack the distinct flange-like dorsolateral trochanter present in other members of this clade. Additionally, the presence of this scar is variable among femoral specimens of *A. kongwe*, which lead Griffin and Nesbitt (2016) to follow others (Nesbitt et al. 2007; Piechowski et al. 2014) in considering the morphology of the dorsolateral trochanter to be an ontogenetically variable character.

Ancestrally, avian-line archosaurs possessed three branches of the puboischiofemoralis externus (PIFE 1, 2, and 3), but along the line to Neornithes PIFE 1 and 3 were lost or strongly reduced, leaving PIFE 2 (= m. obturatorius medialis, OM) as the main insertion in this group (Hutchinson 2001). The PIFE muscles, or their avian

homologues, have been reconstructed to insert on the lateral of the 'greater trochanter' in dinosaurs (Hutchinson 2001; Carrano and Hutchinson 2002), and this is conserved in neornithines. I follow Hutchinson (2001) in his hypothesis that the dorsolateral trochanter is the osteological correlate of the PIFE musculature insertion.

17. Femur, linea intermuscularis cranialis: (0) absent; (1) present. (Figs. 7B; 8B)

The linea intermuscularis cranialis is a thin, raised proximodistally-oriented lineation on the anterior or anterolateral face of the femoral shaft, created from the intersection of the M. femorotibialis externus and M. femorotibialis internus (Crocodylia, = M. femorotibialis lateralis, Mm. femorotibialis medialis and intermedius in Aves; Hutchinson 2001), and is considered to be derived for archosaurs (Hutchinson 2001). In *Coelophysis bauri* and *Megapnosaurus rhodesiensis* the linea intermuscularis cranialis connects to the anterodistal edge of the anterior trochanter (usually in the robust morph that also possesses a trochanteric shelf) and extends distally to roughly halfway down the shaft of the femur before terminating. The presence of this character has been noted to be variable in extinct (Nesbitt et al. 2009a; Griffin and Nesbitt 2016; Chapter 1) and extant (Tumarkin-Deratzian et al. 2006; 2007) archosaurs.

18. Femur, linea intermuscularis caudalis: (0) absent; (1) present. (Figs. 7B; 8D; 9D, F)

Like the morphologically similar linea intermuscularis cranialis, the linea intermuscularis caudalis is an archosaur synapomorphy, and is a lineation formed at the border between muscles; in this case the M. femorotibialis externus and M. adductor femoris 1 & 2 (Crocodylia; = avian M. femorotibialis lateralis and Mm. puboischiofemorales medialis and lateralis, respectively, Hutchinson 2001; The M. adductor femoris 1 & 2 has been hypothesized to be homologous with the M. pubo-

ischio-trochantericus in *Sphenodon*, Schachner et al. 2011). The linea intermuscularis caudalis usually extends down the posterior face of the femoral shaft (Hutchinson 2001); in *C. bauri* and *M. rhodesiensis* it extends from the posterior edge of the trochanteric shelf down about two-thirds of the femoral shaft, and so extends further distally than the linea intermuscularis cranialis. Like character 17, the presence of the linea intermuscularis caudalis has been noted to be variable in ontogeny in both extinct (Nesbitt et al. 2009a; Griffin and Nesbitt 2016; Chapter 1) and extant (Tumarkin-Deratzian et al. 2006; 2007) archosaurs.

19. Femur, 'anterolateral scar': (0) absent; (1) present. (Figs. 7D; 8D)

In femora of both *Coelophysis bauri* and *Megapnosaurus rhodesiensis* there is a thin, raised, mediolaterally oriented linear scar across the anterolateral face of the proximal part of the femur, proximal to the anterior trochanter. This scar is proximodistally widest at its lateral edge, where is merges with the posterolateral end of the 'greater trochanter' proximal to the dorsolateral trochanter, but as it trends medially it becomes proximodistally narrower and more linear. This scar usually intersects the distal part of the anterolateral tuber at its proximodistal midpoint. Because the area directly proximal to the ridge is lower (i.e., deeper) than the ridge itself, this causes the appearance of shallow 'basins' (distinct from character 12) between this scar and the proximal surface of the femur in anterolateral aspect, as well as between this scar and the anterior trochanter. In *C. bauri*, this ridge is usually more distal than in *M. rhodesiensis*, resulting in the two 'basins' in *M. rhodesiensis* appearing to be roughly equal in area. In those individuals where the scar does not reach medially enough to intersect with the

anterolateral tuber (e.g., QG 733), there appears to be a single 'basin', into which the scar extends into laterally.

In at least some silesaurids, the anterolateral scar (= 'dorsolateral ossification', Piechowski et al. 2014) is a raised, disc-shaped feature on the anterolateral face of the femoral head consisting of course bone fibers, and is hypothesized to have been variable in ontogeny (*Silesaurus opolensis*, Piechowski et al. 2014; *Asilisaurus kongwe*, Griffin and Nesbitt 2016; the anterolateral scar is also present in the unnamed Otis Chalk silesaurid, Griffin and Nesbitt 2016). Because this feature is not known from any extant reptile, homologizing this structure with attachments for a known muscle(s) or ligament(s) is difficult. Piechowski et al. (2014) suggested that this structure is an ossified extension of the dorsolateral trochanter, because the two structures are closely associated or even continuous in *S. opolensis*. Griffin and Nesbitt (2016) hypothesized that this structure is the insertion of the iliofemoral ligament (= pubofemoral ligament of Aves, Tsai and Holliday 2014), citing the similar location between this insertion site in the femur of *Alligator mississipiensis* (Tsai and Holliday 2014) and the anterolateral trochanter of *Asilisaurus kongwe*. Given that the dorsolateral trochanter and anterolateral scar are closely associated but usually separate in all silesaurids for which it has been described, I follow Griffin and Nesbitt (2016) by not considering this scar to be an extension of the dorsolateral trochanter in silesaurids, but a separate structure.

Although the location of this femoral scar and the anterolateral scar of silesaurids is similar, the two have differing morphologies. The scar described in *C. bauri* and *M. rhodesiensis* is linear, ossified, and continuous with the cortical bone, whereas the anterolateral scar of silesaurids is a less well-attached, fibrous disc-shaped structure that

takes up a proportionally larger area of the anterolateral face of the femur (Griffin and Nesbitt 2016). However, similar to the anterolateral scar of some silesaurids, including a few individuals of *Silesaurus opolensis* (Piechowski et al. 2014) this scar in *C. bauri* and *M. rhodesiensis* connects with the posterolateral edge of the femur, at the proximal region of the dorsolateral trochanter. A similar scar with an 'intermediate' morphology has been reported (Novas 1993, Fig. 7B) in *Herrerasaurus ischigualastensis*: instead of a lineation across the anterolateral face of the proximal end of the femur, in *H. ischigualastensis* the scar retains a disc-like or semicircular morphology. However, this scar is shifted laterally relative to the silesaurid condition to a position on the anterolateral face of the femur similar to that in *C. bauri* and *M. rhodesiensis*, with the wide edge of the scar continuing into the posterolateral edge of the 'greater trochanter'. Therefore, I hypothesize that this linear scar in *C. bauri* and *M. rhodesiensis*, the semicircular scar in *H. ischigualastensis*, and the anterolateral scar of silesaurids are all homologous, and I use the term 'anterolateral scar' when referring to these structures. The linear morphology of the anterolateral scar in coelophysoids may be an osteological correlate of the distal edge of the attachment of the iliofemoralis ligament, as opposed to the condition in silesaurids (and possibly *Herrerasaurus*) where the entire attachment appears to be ossified. If this is the case, then the 'basin' proximal to the anterolateral scar may take up the majority of the area of insertion of the iliofemoralis ligament, a hypothesis supported by the presence of a sharp depression in this region in *M. rhodesiensis* (see character 12).

20. Femur, 'obturator ridge' (sensu Raath 1977): (0) absent; (1) present. (Fig. 9)

The presence of a rounded elongate tubercle on the posteromedial face of the 'greater trochanter', identified by Raath (1977) as the 'obturator ridge', is variable in

femora of *Coelophysis bauri* and *Megapnosaurus rhodesiensis*. In some exceptionally preserved specimens of *C. bauri* this scar has a rugose texture, and in those individuals of *M. rhodesiensis* and *C. bauri* lacking this feature, thin lineations marking the muscle attachment are often present on the cortical surface. The ridge extends anteriorly and slightly distally from the posterolateral edge of the 'greater trochanter' (directly medial to the dorsolateral trochanter) across the posteromedial face of the proximal part of the femur, terminating on the medial part of the femoral neck distal to the femoral head. This scar is probably homologous with the 'posterior portion of the dorsolateral trochanter' in *Asilisaurus kongwe* (Griffin and Nesbitt 2016), the presence of which is also variable in ontogeny.

This tubercle in *M. rhodesiensis* has been hypothesized to be the insertion of a portion of the Mm. puboischiofemoralis externi (PIFE; Raath 1977), which, given this muscle complex's hypothesized homology with lepidosaurian muscles (M. pubofemoralis pars ventralis, M. ischiofemoralis anterior, and M. ischiofemoralis posterior, Schachner et al. 2011) is ancestral for all crown saurians. The three heads of the PIFE musculature in crocodylians has been hypothesized to be homologous with the Mm. obturatorius medialis (OM) et lateralis (OL) of birds (Hutchinson 2001). Scars for the insertion of the PIFE or its homologues have been identified in many pseudosuchian archosaurs (e.g., 'rauisuchians', Dutuit 1979; crocodylomorphs, Walker 1970; Crush 1984; Hutchinson 2001; extant crocodylians, Hutchinson 2001; Schachner et al. 2011) as well as avemetatarsalians (e.g., pterosaurs, sauropodomorphs, early-diverging saurischians, Hutchinson 2001; theropods, Andrews 1921; Raath 1977; Martill et al. 2000; neornithines, Ballman 1969; Hutchinson 2001). In birds a scar, ridge or groove, known as

the ‘obturator ridge’, marks insertion of the OM. Therefore, based on the location of this scar on the distal part of the ‘greater trochanter’, this may be the osteological correlate of part of the PIFE. However, given that in most extant archosaurs the branches of the PIFE musculature share a single insertion on the lateral surface of the ‘greater trochanter’, extending onto the posterolateral or posterior surface in only some extant archosaurs (Hutchinson 2001), the anterior extent of this scar along the posteromedial face of the proximal end of the femur suggests that a different muscle(s), if any, may have inserted on the ‘obturator ridge’.

21. Femur, scar proximal to ‘obturator ridge’: (0) absent; (1) present. (Fig. 9)

A ridge extends distolaterally from the lateral portion of the posteromedial tuber across the facies articularis antitrochanterica to the posterolateral edge of the ‘greater trochanter’, converging with the lateral portion of the ‘obturator ridge’, in some individuals of both *Coelophysis bauri* and *Megapnosaurus rhodesiensis*. This scar is similar in morphology to the ‘obturator ridge’, but is usually not as prominent (Fig. 9 C–F).

22. Femur, insertion scar of caudifemoralis brevis: (0) absent; (1) present. (Figs. 8D; 9)

A low, rugose, ridged scar connects posterolaterally to the posterior part of the trochanteric shelf and proximal part of the linea intermuscularis caudalis (or where these features would be in more immature individuals), extending to the proximal portion of the fourth trochanter in *Coelophysis bauri* and *Megapnosaurus rhodesiensis*. In well-preserved specimens that lack this feature (e.g., QG 169), small lineations are present on the surface of the cortical bone in this region. The presence of this scar is variable in the ontogeny of *Asilisaurus kongwe* (Griffin and Nesbitt 2016).

This ridge is the insertion scar of the caudifemoralis brevis (CFB; = caudifemoralis pars pelvica in Aves, Hutchinson 2001), which inserts slightly proximal and lateral to the insertion of the caudifemoralis longus (CFL; the insertion of which the fourth trochanter is the osteological correlate) in extant archosaurs (Hutchinson 2001). Like the CFL, the CFB is present in crown group saurians (Hutchinson 2001; Schachner et al. 2011).

23. Femur, fourth trochanter: (0) gracile and thin; (1) robust and thickened in the posteromedial portion of the apex of the trochanter. (Fig. 9)

Analogous to the deltopectoral crest of the humerus (character 7), the fourth trochanter of the femur is present in all individuals of *Coelophysis bauri* and *Megapnosaurus rhodesiensis* with either gracile or robust morphology. In the gracile morph (e.g., QG 174 B; MCZ 4332) the superficial apex, which is oriented proximodistally along almost the entirety of the fourth trochanter and gives the trochanter its distinctive bladed appearance, lacks scarring and a rugose texture. In contrast, the superficial apex ('blade') of the robust morph of the fourth trochanter (e.g., NMMNH P-425386) is anteroposteriorly thicker and in well-preserved individuals possesses a relatively more rugose texture. Because this gracile/robust morphology extends along the proximodistal length of the fourth trochanter, this character can be scored even when only a small portion of the fourth trochanter has been preserved. The morphology of the fourth trochanter has been noted to vary during ontogeny in early bird-line archosaurs (Nesbitt et al. 2009a; Griffin and Nesbitt 2016).

24. Tibia, tuberosity on anterior and anteromedial portion of the cnemial crest: (0) absent; (1) present. (Fig. 10).

Both *Coelophysis* and *Megapnosaurus*, as well as *'Syntarsus' kayentakatae*, possess a low tuberosity on the anterior and anteromedial portion of the cnemial crest of the proximal part of the tibia. This ossified muscle scar, a low rugose mound extending anteriorly from the distal three-fourths of the cnemial crest, can be most clearly observed in medial view. In individuals without the scar, the anterior edge of the cnemial crest is straight or even slightly posteriorly concave; those possessing this feature have rugose and more well-developed cnemial crests that extend further anteriorly.

Raath (1977) mentioned this scar in his description of *Megapnosaurus rhodesiensis*, and hypothesized that the muscles of the triceps femoris insert here. In *Alligator mississippiensis* the triceps femoris consists of the M. iliotibialis 1 (= M. iliotibialis cranialis, Aves), 2 and 3 (=M. iliotibialis lateralis, Aves), M. ambiens, Mm. femorotibialis externus (= M. femorotibialis lateralis, Aves) and internus (= Mm. femorotibialis intermedius medialis, Aves; all homology hypotheses from Carrano and Hutchinson 2002). Given that these muscles insert on the anteroproximal part of the tibia in *Alligator mississippiensis*, the anterior portion of the cnemial crest in extant birds, and have been reconstructed to insert on the anterior portion of the cnemial crest in *Tyrannosaurus rex* (Carrano and Hutchinson 2002; Hutchinson et al. 2005), I hypothesize that this tuberosity on the cnemial crest of coelophysoids is the osteological correlate of the insertion of the triceps femoris group.

25. Tibia, scar on the posterior portion of the medial surface of the proximal end of the tibia: (0) absent; (1) present. (Fig. 10)

Both *Coelophysis bauri* and *Megapnosaurus rhodesiensis* possess a scar on the posterior portion of the medial surface of the proximal end of the tibia. This rugose area,

slightly raised from the surrounding bone, is most clearly visible in medial view and is morphologically similar to the mound on the cnemial crest (character 24), although it is less prominent. A rugose area in a similar location on the tibia has been suggested to represent the insertion of the M. flexor tibialis internus 3 (FTI3; = avian M. flexor cruris medialis) and M. flexor tibialis externus (FTE; = avian M. flexor cruris lateralis pars pelvica) in *Tyrannosaurus rex* (Carrano and Hutchinson 2002; Hutchinson et al. 2005). The FTI3 and FTE share a tendon for insertion in extant archosaurs, and so this scar is probably the insertion of both muscles.

26. Astragalus and calcaneum, fusion: (0) absent; (1) present. (Fig. 11)

The astragalus and calcaneum fuse to form one continuous structure, the astragalocalcaneum, in *Coelophysis* and *Megapnosaurus,* but this fusion is much more common in individuals of *Coelophysis bauri*. Although in most archosaurian lineages the articulation between the astragalus and calcaneum remains free, many taxa along the line to birds fuse these elements in an astragalocalcaneum, including pterosaurs, early diverging dinosauromorphs, and the early ornithischian *Heterodontosaurus* (Nesbitt 2011), as well as early neotheropods (Rowe and Gauthier 1990). This fusion is widespread among early-diverging neotheropods, including *Camposaurus arizonensis* (Ezcurra and Brusatte 2011), *'Syntarsus' kyentakatae* and the Shake-N-Bake taxon (Tykoski 2005), *Ceratosaurus nasicornis* (Madsen and Welles 2000), *Aucasaurus arrigoid* (Coria et al. 2002), *Masiakasaurus knopfleri* (Carrano et al. 2002), and *Xenotarsosaurus bonapartei* (Martinez et al. 1986), among others. Tykoski (2005) considered this fusion to be variable in ontogeny, but appearing at a relatively early stage

of growth in early theropods. Therefore, this character could be ontogenetically informative across a wide phylogenetic range.

27. Tibia and astragalus, fusion: (0) absent; (1) present. (Figs. 11; 12)

The tibia and astragalus fuse to form a tibiotarsus during ontogeny in several early neotheropods, including *Coelophysis bauri* and *Megapnosaurus rhodesiensis* (e.g., Tykoski and Rowe 2004). However, this coossification is markedly different than other fusion events described for these taxa, including the formation of the astragalocalcaneum. In most suture fusions in *Coelophysis bauri* and *Megapnosaurus rhodesiensis* (e.g., character 26, QG 805), the subperiosteal surfaces of the elements in question remain visible and unmodified with the exception of the area immediately (~ 4 mm) around the suture. In contrast, the fusion of the tibia and astragalus in these taxa results in the posterior surface of the tibia and astragalus becoming covered by continuous rugose bone, which extends from the posteroproximal parts of the malleoli to the posteroproximal portion of the astragalus. In those individuals in which this has occurred (e.g., AMNH FARB 7247; CM 81770), no line of suture is visible in posterior aspect between the astragalus and tibia, because it is covered by the rugose layer of bone. This layer of bone often does not extend far around the medial sides of the astragalus or calcaneum, however, and a normal suture (unless obliterated) can occasionally be observed on these surfaces in individuals that possess a fused astragalus and tibia (as well as a fused fibula and tarsus; see character 28). Although fusion between the astragalus and tibia is visible in anterior aspect, the line of suture is never obliterated. Determining whether fusion has occurred in an individual, or whether there is simply tight articulation, is often difficult for individuals of *C. bauri* remaining in blocks of matrix, because only

the anterior view of the tibia and tarsus is visible, and such individuals must be scored as missing data (?) for this character. One individual of *M. rhodesiensis* (QG 767) possesses the covering of rugose bone on the posterior surface of the distal end of the tibia but the astragalus has been disarticulated. However, the two elements were apparently 'fused', even though the astragalus could be broken off, because some of the rugose bone that would have covered the astragalus is still attached to the tibia extending distally from its posterodistal surface. The break along the distal surface of this rugose bone appears to be fresh, and so occurred after fossilization. This suggests that the fusion between the astragalus and tibia (as well as between the tarsus and fibula, and tibia and fibula; see characters 28 and 29) may not be a normal sutural fusion, with both elements becoming completely coossified and impossible to break apart without damaging the elements. Because, if this break had not occurred, these elements would have appeared to be as completely fused as other individuals for which this character has been scored as fused, I scored this individual (QG 767) as [1] for this character.

Although previous work has identified tibiotarsal fusion in *M. rhodesiensis* (Raath 1977; 1990) and *C. bauri*, in the latter Colbert (1989; 1990) suggested that this fusion represents individual and not ontogenentic variation because of the poor correlation between size and individuals that possess what would be considered the mature state (fused) of this character. However, body size is not a good correlate for skeletal maturity in this taxon because of individual variation in ontogenetic patterns (Chapter 1), nor in early sauropodomorphs (*Plateosaurus engelhardti*, Sander and Klein 2005) and close dinosaurian relatives (*Asilisaurus kongwe*, Griffin and Nesbitt 2016).

Fusion between the tibia and astragalus is widespread among early-diverging neotheropods, but is not as commonly described as astragalocalcaneum fusion (character 26). In addition to *M. rhodesiensis* and *Coelophysis bauri*, *Camposaurus arizonensis* (Tykoski 2005; Ezcurra and Brusatte 2011), *'Syntarsus' kayentakatae* (Rowe 1986; Tykoski 2005; this study), the Shake-N-Bake taxon (Tykoski 2005), *Ceratosaurus nasicornis* (Gilmore 1920; Madsen and Welles 2000), *Xenotarsosaurus bonapartei* (Martínez et al. 1986), *Masiakasaurus knopfleri* (Carrano et al 2002) have all been reported to possess fused tibiotarsi; however, with the exception of *'Syntarsus' kayentakatae* I have not examined these specimens in person, and so cannot comment on whether the tibiotarsal fusion is similar to the fusion described here for *Coelophysis bauri* and *M. rhodesiensis*. *Lepidus praecisio* (Nesbitt and Ezcurra 2015), *Liliensternus iliensterni* and *Dilophosaurus wetherelli* (Tykoski 2005) have all been reported to lack fusion between the tibia and astragalocalcaneum, either indicating that this character was lost in these taxa, or that these specimens represent skeletally immature individuals.

28. Fibula and tarsus, fusion: (0) absent; (1) present. (Fig. 11)

The fibula and tarsus fuse in a similar manner as the tibia and astragalus in *Coelophysis* and *Megapnosaurus*, except that the fusion between the tarsus (= astragalocalcaneum) and fibula is often more complete (that is, the line of suture is nearly or completely absent) in anterior view. The fibula is mostly articulated with the calcaneum in these taxa, but a small part of the proximolateral region of the astragalus also articulated with the fibula; fusion between the fibula and astragalus occurred in conjunction with all instances of fibular fusion with the calcaneum, and in all cases the astragalus was already coosified with the calcaneum when this fusion occurred. For these

reasons, I refer to this fusion as between the fibula and tarsus, and not just the fibula and calcaneum, although this is the same event in practice. This character occurs in many of the same taxa as fusion between the tibia and astragalus (character 27).

29. Fibula and tibia, fusion of distal ends: (0) absent; (1) present. (Fig. 12)

In a few individuals of *Coelophysis bauri* (e.g, AMNH FARB 7234),but not *Megapnosaurus*, the fusion between the tibia, fibula, and tarsus is so extensive that fusion between the tibia and fibula occurs as well. In these individuals, the rugose bone that covers the posterodistal surfaces of the tibia and fibula is so extensive that it forms a continuous surface between these two elements. The coossification is less obvious in anterior view, analogous to the fusion between the tibia and astragalus (character 27). Fusion between the tibia and fibula is rare, and I only observed this in five specimens of *C. bauri* (AMNH FARB 7238, AMNH FARB 7234, SMP 858, TMP 1984.63.6, and TMP 1984.63.21). In other individuals the two elements were very closely associated, and may have even been partly coossified, but I did not score this character as 'fused' unless the rugose bone was continuous across the suture. Fusion between the tibia and fibula has not been reported in other early neotheropods, and I did not observe it in *'Syntarsus' kayentakatae*.

30. Fibula, ridge on medial face of proximal end: (0) absent; (1) present.

On some fibulae of *Megapnosaurus*, the medial surface of the proximal end is flat and slightly concave laterally with a shallow sulcus. However, other fibulae possess a ridge on the proximal border of this sulcus (which is usually deeper in these individuals) extending from a posteroproximal position on the medial face anterodistally. Rowe and Gauthier (1990) refer to the development of this sulcus as ontogenetic, but for

Megapnosaurus the ridge was more often variable than the sulcus it bordered, and the absence or presence of the ridge was more easily diagnosed than the relative depth of the sulcus. The ridge also distally borders a shallow, less well-defined sulcus, and both sulci are deepest near the ridge, and tend to shallow away from it. Even individuals without the ridge still preserve thin lineations on the cortical bone of this area, and Rowe and Gauthier (1990) hypothesize that the sulcus is the site of origin of a portion of the pedal flexor musculature.

Nesbitt et al. (2009b) found this ridge on the medial face of the proximal end of the fibula to be a synapomorphy of Neotheropoda (character 314, ACCTRAN optimization), and so it would be expected to be present and ontogenetically variable in *Coelophysis* as well. However, the medial surface of the proximal end of the fibula was covered in all individuals of *Coelophysis bauri* for which I attempted to score this character, and so this character was not scored for *C. bauri*.

31. Tarsal III and metatarsal III, fusion: (0) absent; (1) present. (Fig. 13)

Tarsal III fuses completely to the proximal surface of metatarsal III in some individuals of both *Coelophysis* and *Megapnosaurus* (e.g., MCZ 9433; QG 1029). This results in tarsal III forming a rounded mound extending proximally from the surface of metatarsal III; the proximal surface of metatarsal III without tarsal III is relatively flat. The coossification of these two elements is so complete that it is difficult to determine where one element begins and another ends.

Rowe (1986), Colbert (1989; 1990), and Rowe and Gauthier (1990) all considered tarsals II and III to be present in at least some coelophysoid theropods, and for coossification to occur between them as well as their respective metatarsals (although

Colbert [1990] did not consider this to be a function of size or age). However, Tykoski (2005) did not consider any tarsal II to be present in these early neotheropods, and therefore did not consider these taxa to possess fused tarsals or tarsal II fused to metatarsal II. Tykoski (2005) also reports that tarsal III slightly covers the proximal end of metatarsal II in *'Syntarsus' kayentakatae*, and that tarsal III–metatarsal III fusion is present in the Shake-N-bake taxon. Nesbitt (2011) found that lacking an ossified tarsal II is a synapomorphy of the clade Aurythrosuchus + Archosauria, and I follow this in interpreting tarsal II as being unossified in *Coelophysis* and *Megapnosaurus*.

32. Metatarsal II and metatarsal III, fusion at proximal ends: (0) absent; (1) present. (Fig. 13)

The proximal ends of metatarsals II and III fuse completely in some individuals of both *Coelophysis* and *Megapnosaurus*, and although this fusion has been reported to be related to size in *Megapnosaurus* (Raath 1969; 1977), Colbert (1990) did not consider this fusion to be related to size or age in *Coelophysis*. This fusion has been interpreted as ontogenetic in early theropods by others (Rowe 1989; Tykoski 2005). *'Syntarsus' kyentakatae* (MNA V2623) exhibits this fusion, as do other specimens referred to this taxon, although one individual exhibits this fusion of the metatarsals on the right pes, but not the left (TMM 43688-1, Tykoski 2005). The proximal ends of metatarsals II and III are not known from many other early-diverging neotheropods, although the shafts of these elements are pressed together tightly in the holotype of *Segisaurus halli*, suggesting they may have been fused in this individual (Tykoski 2005).

Neurocentral suture fusion

Neurocentral sutures fuse during ontogeny, combining the neural arch and centrum into one continuous structure. This has been used with success as a morphological indicator of maturity in extant crocodylians, which possess a posterior to anterior sequence of suture closures during ontogeny, with the axis suture closure indicative of the attainment of skeletal maturity (Brochu 1996). This pattern has also been observed in the ontogeny of phytosaurs, crocodilian-like Triassic archosauriforms (Irmis 2007). However, Irmis (2007) noted that this pattern does not appear to be widespread throughout Archosauria, and that the utility of this pattern (or even the closure of neurocentral sutures themselves) for determining ontogenetic stage should be evaluated for each clade. Nevertheless, many studies of archosaurian ontogeny have used neurocentral suture fusion to assess the level of maturity attained by an individual with varying degrees of confidence (e.g., Hutt et al. 2001; Carrano et al. 2005; Makovicky et al. 2005; Fowler et al 2011; Hofman and Sander 2014; Griffin and Nesbitt 2016). However, I have observed individuals of *Branta canadensis* (e.g., FMNH 496812) and *Meleagris gallopavo* (e.g., FMNH 461781) that possessed fully closed neurocentral sutures with immature body sizes, skeletal characters (Chapter 1), and bone textures (Tumarkin-Deratzian et al. 2006), suggesting that closure of neurocentral sutures may not necessitate cessation of growth.

I did not use neurocentral suture fusion as an ontogenetic character in my OSA analyses, although I did make note of the state of the sutures in the individuals that I scored for other ontogenetic characters. In all specimens of *C. bauri* I observed the neurocentral sutures were entirely fused in all vertebrae, regardless of the size of the individual or the location of the element(s) in the vertebral column. Vertebrae of

Megapnosaurus rhodesiensis, in contrast, commonly possess open neurocentral sutures, although many possess closed sutures as well. Unfortunately, the vast majority of the vertebrae attributable to *M. rhodesiensis* are isolated elements, making the determination of a pattern(s) of neurocentral suture fusion impossible. However, all the distalmost caudals I observed possessed closed neurocentral sutures, and one specimen (QG 408) was comprised of four dorsal vertebrae in a series, with the anterior two vertebrae possessing closed neurocentral sutures and the posterior vertebra possessing an open suture. Size does not appear to be strongly related to suture fusion in *M. rhodesiensis*, although I did not quantitatively evaluate this relationship, and comparing size across different vertebral elements is inexact. Additionally, the large amount of sequence polymorphism in other ontogenetic characters (Chapter 1; this study) suggests that multiple sequences of neurocentral stuture fusion may occur in different individuals of this taxon.

4. RESULTS

Ontogenetic sequence analysis

Ontogenetic sequence analyses of *Megapnosaurus* and *Coelophysis* strongly suggest that sequence polymorphism is present in the ontogenetic trajectories of these taxa. The OSA of the full dataset of 27 ontogenetic characters of *Coelophysis bauri* returned 100,400 trees in both the 'normal' and 'reverse' treatments, which maximized the ability of PAUP* to store trees, and this resulted in 161 equally parsimonious developmental sequences. Twenty-three semaphoronts were eliminated by reduction, bringing the number of reconstructed developmental sequences down to 136 (Fig. 14). The modal sequence of this analysis consisted of 22 developmental steps and possessed a

frequency support weight of 21.82, which was 1.31% the total weight of all sequences, representing only 12.57% the support weight of all semaphoronts.

Ontogenetic sequence analysis (OSA) for the ten femoral ontogenetic characters of *Coelophysis bauri* resulted in 22,756 trees in the 'normal' treatment and 2,436 trees in the 'reverse' treatment, returning 90 equally parsimonious developmental sequences. Two semaphoronts (i.e., unique sets of ontogenetic character states sensu Hennig 1966) were eliminated during reduction of the *C. bauri* femoral OSA, bringing the number of developmental sequences down to 82 (Fig. 15A). The modal sequence of the *C. bauri* femoral OSA consisted of 9 developmental steps and possessed a frequency support weight of 28.09, which was only 1.62% the combined support weight of all sequences, though this support weight is 32% of the combined weight of all semaphoronts included in the analysis. For *Megapnosaurus rhodesiensis*, the 'normal' treatment returned 651 trees and the 'reverse' treatment 178 trees, resulting in 145 developmental sequences for the 13 femoral characters (Fig. 15B). No semaphoronts were reduced from the *Megapnosaurus rhodesiensis* OSA. The support weight of the modal sequence of the *M. rhodesiensis* femoral OSA was 21.63 and consisted of 10 developmental steps, with this support weight only 0.94% the combined weight of all sequences in the analysis, although the support weight of this sequence is 49.63% the weight of all semaphoronts combined because of the lower number of specimens, and therefore semaphoronts, in the analysis.

The ontogenetic sequence analysis of eight ontogenetic characters of the tibia, fibula, tarsus, and pes of *Coelophysis bauri* returned 36,097 trees in the 'normal' treatment and 488,107 in the 'reverse' treatment, which produced 35 distinct ontogenetic

sequences (Fig. 16A). The modal sequence, like all sequences returned by this analysis, consisted of 8 developmental steps and possessed a specimen frequency support weight of 29.06, which was 3.04% the combined weight of all sequences, representing 42.0% the weight of all semaphoronts in the analysis. Because almost all specimen of *Megapnosaurus rhodesiensis* were disarticulated, I was only able to use six characters to analyze the growth of the tibia and tarsus of this taxon and excluded the two pedal characters used in the analysis of *C. bauri*. This tibiotarsal OSA of *Megapnosaurus* returned 4 trees in both 'normal' and 'reverse' treatments, with only a single ontogenetic sequence of four developmental steps (Fig. 16B) with a frequency support weight of 73.

The ontogenetic sequence analysis of the *C. bauri* pelvic and sacral ontogenetic characters returned 53 trees in the 'normal' treatment and 103,337 trees in the 'reverse' treatment, with a total of 16 ontogenetic sequences reconstructed for the 5 ontogenetic characters (Fig. 16D). The modal sequence was composed of 6 steps (as character 2 is an ordered, multistate character), and possessed a frequency support weight of 28.77, which was 8.13% the total weight of all sequences combined and 42.0% the weight of all semaphoronts in the analysis. An analysis of the same characters in *Megapnosaurus rhodesiensis* returned only 9 trees in 'normal' treatment and 5 in 'reverse' treatment, resulting in only 3 distinct ontogenetic sequences (Fig. 16E). The modal sequence consisted of four steps and, with a weight of 26.01, was 34.7% the weight of all ontogenetic sequences and represented 89.69% the weight of all semaphoronts.

Finally, the OSA of the four ontogenetic characters of the humerus of *Megapnosaurus rhodesiensis* returned 2 trees in both the 'normal' and 'reverse' treatments, resulting in only 2 developmental sequences (Fig. 16C). The modal sequence,

which consisted of four developmental steps, possessed a frequency support weight of 16.34, making it 54.7% of the combined weight of both sequences and 91.0% the weight of all semaphoronts in the analysis.

5. DISCUSSION

Ontogenetic variation in *Coelophysis* and *Megapnosaurus*

Both *Coelophysis bauri* and *Megapnosaurus rhodesiensis* possess a large amount of variation in the sequence of developmental events undergone during postnatal ontogeny, as well as in the body sizes at which these events occur (Chapter 1; Figs. 14–16). Sequence polymorphism was reconstructed for the ontogenetic characters of all elements analyzed, as well as the relative timing of events across elements in *C. bauri*, with the exception of four ontogenetic characters analyzed in the tibia and tarsus of *M. rhodesiensis* (characters 26—29), which appeared to possess no variation in their relative order of appearance. Although sample size is important for detecting sequence polymorphism (de Jong et al. 2009; Griffin and Nesbitt 2016), the large number of individuals used in the analysis of these four characters in *M. rhodesiensis* would appear to preclude this lack of variation as an artifact of low sample size. Therefore, *M. rhodesiensis* appears to lack sequence polymorphism in this portion of the skeleton, although the characters of other elements analyzed, especially the femur, possess sequence polymorphism. Additionally, sequence polymorphism is greater in some elements than in others in both taxa, although in some cases this may be an expression of differing sample sizes because there were relatively few specimens and characters used in the analyses of humeral and pelvic ontogeny in *Megapnosaurus rhodesiensis*. Therefore, the characters and elements chosen for analysis can play an important role in the amount

of sequence polymorphism interpreted to be possessed by the population in question. Sequence polymorphism may be high for some characters, whereas the relative developmental sequence of other characters may be the same, and a large number of ontogenetic characters as well as a large sample size of individuals enables a higher level of confidence in interpreting of sequence polymorphism as being present or absent in a population. The large number of both ontogenetic characters and individuals utilized in this study allow the presence of sequence polymorphism to be confidently hypothesized for these taxa, as well as the absence of sequence polymorphism in some of the tibiotarsal characters of *M. rhodesiensis*.

OSA reconstructs all equally parsimonious developmental pathways, and is therefore an excellent method of quantifying the amount of sequence polymorphism in a population for any set of ontogenetic characters (Colbert and Rowe 2008). However, just because a developmental sequence is constructed does not mean that any single individual necessarily underwent this individual sequence during life, and in fact the actual number of developmental sequences in a population could be lower than predicted by OSA. However, OSA cannot distinguish between 'real' developmental sequences and those that are equally parsimonious and simply reconstructed from the data. This difficulty does not exist in a sample with a low amount of sequence polymorphism because the modal sequence represents nearly all individuals in a population and is therefore almost certainly a 'real' sequence undergone by those individuals in life. However, with increasing amounts of sequence polymorphism this certainty lessens for any one sequence, including the modal sequence. This difficulty explains the differences in modal sequences between characters for any single element and the sequence of those

characters in the modal sequence of the multi-elemental OSA of characters of *C. bauri* characters (Fig 17); because there is so much sequence polymorphism in this taxon, the modal sequences for each analysis only make up a relatively small portion of the total weight of all sequences, and therefore relatively small differences in the number of individuals preserved and used for OSA may result in this difference in modal sequences. Therefore, although OSA is an excellent way to quantify the amount of sequence polymorphism in a population, for a population with a large amount of sequence polymorphism the confidence that any one sequence was actually undergone by an individual in the population is less than that of a population with very low levels of sequence polymorphism. However, at least some reconstructed sequences must have been utilized by individuals in the population given the assumptions of OSA (see Methods).

Body size commonly is used as a proxy for ontogenetic age and skeletal maturity, with larger individuals though to represent a more advanced ontogenetic stage than smaller individuals, and individuals of different size having attained the same ontogenetic stage and level of skeletal maturity (e.g., Colbert 1990; Chinnery and Weishampel 1998, Benton et al. 2000; Hunt 2001; Currie 2003; Bybee et al. 2006; Heckert et al. 2006; Buckley et al. 2010; Carpenter 2010; Piechowski et al. 2014; Griffin and Nesbitt 2016). Using this assumption, Raath (1977; 1990) and Colbert (1989) hypothesized that the differences in femoral muscle scars between individuals of similar size was sexual and not ontogenetic, because the individuals were assumed to be at roughly the same ontogenetic stage. However, ontogenetic age, body size, and skeletal maturity as determined by morphological ontogenetic characters may all be somewhat disjunctive, with similarly sized individuals possessing differing levels of skeletal maturity in early

dinosaurs (Chapter 1). For example, TMP 1984.063.0001, a relatively large individual of *Coelophysis bauri* (measured femoral length = 158.1 mm), possesses a suite of entirely immature character states (Fig. 18), whereas MNA V3318 is a smaller individual (measured femoral length = 124.7 mm) possessing many mature character states (Fig. 19), and the smallest known individual of *M. rhodesiensis* (estimated femoral length = 111.95 mm) possesses a large, robust trochanteric shelf (character 14–1; 15–1). Some studies have suggested that using size as a direct correlate for relative maturity may be less well supported than is usually assumed. *Plateosaurus engelhardti* has been reported to possess enormous variation in size unrelated to ontogenetic age as determined by histology (Sander and Klein 2005; Klein and Sander 2007), and skeletal maturity as determined by morphological characters has been reported to be somewhat disconnected to size in *Alligator mississippiensis* (Brochu 1992). The latter study is especially relevant to the current discussion, because it involves skeletal features (including bone scars) that develop during ontogeny in an extant archosaur. In *A. mississippiensis*, there is a very rough correlation between size and skeletal maturity in the whole body, with the smallest individuals consistently less mature than the largest, much variation exists in the sample, and the assumption that larger individuals are always more skeletally mature than smaller individuals does not hold. In assessing the ontogenetic stage of individual elements, the signal becomes more muddied, with an up to twofold difference in size between smaller mature individuals and larger, mature individuals. Notably, this variation does not seem to be related to sexually dimorphic differences (Brochu 1992). A similarly poor correlation between ontogenetically variable characters and body size has been reported for has been reported for many early-diverging dinosaurs and dinosauriforms (e.g.,

Benton et al. 2000; Britt et al. 2000; Carrano et al. 2002; Tykoski 2005; Griffin and Nesbitt 2016; Chapter 1; see discussion below), although preliminary analyses of similar (or even homologous) ontogenetic characters are far better correlated with size in extant birds (Chapter 1). Future, extensive histological investigation of *C. bauri* and *M. rhodesiensis* will determine whether size is a good indicator of ontogenetic age (with differences is skeletal maturity reflecting variation in absolute timing of ontogenetic characters), but this study is beyond the scope of this paper. Although some preliminary reports suggest that this relationship holds (Chinsamy 1990; Werning 2013), others suggest that histology among several early dinosauriforms may not be informative as to ontogenetic age (Nesbitt et al. 2013; Griffin and Nesbitt 2016).

Neurocentral suture fusion of all vertebrae apparently occurs very early in ontogeny among the majority of individuals of *Coelophysis bauri*, because all vertebrae that could be confidently identified as belonging to this taxon possessed fused sutures, regardless of body size or ontogenetic character states. In contrast, most of the vertebrae of *Megapnosaurus rhodesiensis* possess open neurocentral sutures, with the exception of the distalmost caudal vertebrae. Because one partial series of trunk vertebrae possessed fused neurocentral sutures in the anterior vertebrae, the sequence of vertebral fusion may proceed anteriorly from the caudal vertebrae and posteriorly from the dorsals in this taxon, with the posterior dorsals or sacrals the last the fuse their neurocentral sutures. However, the large amount of sequence polymorphism in other elements in this taxon may suggest that more than one sequence of neurocentral suture fusion exists within the population.

Differences between *Coelophysis* and *Megapnosaurus*

The most obvious difference between *Coelophysis bauri* and *Megapnosaurus rhodesiensis* is the ontogenetic characters used for these taxa. Four ontogenetic characters were variable in *M. rhodesiensis* but were not in *C. bauri*: the scar on the humerus for the origin of the M. triceps brachii caput mediale (character 5–1); the shallow groove on the proximal surface of the femur (character 11–0); the depression on the anterolateral face of the proximal portion of the femur (character 12–0); and the anterolateral edge of the proximal surface of the femur extending anterolaterally (character 13–1). Because these characters are ontogenetically variable, it may be that all observed specimens of *C. bauri* were simply at the incorrect ontogenetic stage to possess these character states. If this is the case, this difference in characters still represent a difference in taxa, because unlike the other ontogenetic characters, the ontogenetic sequence of these characters is so different that they can be misinterpreted as absent in one taxon. If all the characters apparently absent from *C. bauri* were all the immature or mature states, this would suggest that the observed individuals of *C. bauri* are too immature/mature, respectively, to possess these states, and would therefore leave open the possibility that these characters were present in *C. bauri* but unobserved because of a sample that does not include the individuals possessing the requisite stages of maturity to observe these states. However, this is not the case: two of the anomalous character states are the mature state, whereas for the other two characters it is the immature state that is absent in the *C. bauri* sample. This suggests that these are clear morphological differences between the taxa, and that *C. bauri* would lack these anatomical features regardless of the level of maturity attained. Whereas all neurocentral sutures of the vertebrae of *C. bauri* appear to be closed, most of those of *M. rhodesiensis* are open. Whether or not these taxa possess the

same sequence(s) of neurocentral suture fusion is not testable with these data, but this difference is presumably a result of *C. bauri* completing all neurocentral suture fusion at a younger age, or at least at a smaller size, relative to *M. rhodesiensis*. Although the complete fusion of neurocentral sutures indicates the attainment of skeletal maturity and cessation of growth in extant crocodylians (Brochu 1996; Irmis 2007), the absence of open nuerocentral sutures in any individual of *C. bauri*, no matter the size or suite of ontogenetic character states, suggests that this is not universal means of determining whether skeletal growth has ceased in an individual.

These data also suggest that *Coelophysis bauri* and *Megapnosaurus rhodesiensis* grew differently, with slightly different ontogenetic sequences reconstructed for the same elements and characters for these taxa, although the majority of the features that changed during ontogeny are the same, and they reached roughly similar sizes at maturity. Most strikingly, *M. rhodesiensis*, unlike *C. bauri*, appears to lack sequence polymorphism in the ontogenetic characters of the tibia and tarsus. This is also in contrast to the other elements of *M. rhodesiensis* analyzed, which do possess sequence polymorphism. Because of the relatively large sample size of tibiae and tarsi used in this analysis this lack of variation in growth sequences is probably not simply a result of a low sample size. Therefore, the characters and elements selected for analysis are important for determining whether sequence polymorphism is prevalent in a taxon, because a taxon with a large amount of overall variation in growth may not possess much sequence polymorphism in a certain element or region. Additionally, the developmental sequence of certain characters may be invariable, even when the sequence of these characters with respect to other characters is. In order to properly assess the amount of sequence

polymorphism in a taxon, it is preferable to include as many ontogenetic characters across as many elements and anatomical regions as possible. Additionally, the known individuals of *M. rhodesiensiss* are larger on average than those of *C. bauri* (Fig. 20)

Implications for growth in early dinosaurs and their close relatives

How the earliest dinosaurs changed morphologically during ontogeny is poorly understood. Therefore, assessing the relative ontogenetic stage attained by an individual before death based on gross morphological features has been difficult for these taxa, and although osteohistology is useful for determining skeletal maturity (e.g., Horner et al. 1999; 2000; Erickson et al., 2000; Erickson et al., 2004), this a destructive process that may be uninformative depending on the element sampled and osteohistological features present (e.g., annual growth lines). Even with the large amount of sequence polymorphism that is present in early-diverging dinosauriforms (Griffin and Nesbitt 2016; Chapter 1), some ontogenetic characters reach mature character states at consistently earlier developmental stages than others in *Coelophysis bauri* (Fig. 21). If this average relative order is conserved across early dinosaurs (that is, if certain characters consistently reach their mature state earlier or later in developmental sequences across these taxa, then these characters may be important indicators of the level of maturity attained by an individual), even if known from only partial or fragmentary remains. Additionally, an individual complete enough to possess a suite of character states may be compared with the OSAs of *C. bauri* and *Megapnosaurus rhodesiensis* to assist in the determination of relative maturity of that individual, provided that the developmental characters utilized are phylogenetically bracketed for the taxon being assessed.

Properly understanding the morphological changes undergone during ontogeny is also important for reconstructing evolutionary relationships. The difficulty of important phylogenetic characters being ontogenetically variable has been touched on in many studies—a skeletally immature specimen of a given taxon may be recovered in a very different, often more basal phylogenetic position relative to a mature specimen of the same taxon. Therefore, understanding what phylogenetic characters are variable in ontogeny, and how the scoring of these characters influences the phylogenetic placement of taxa that may only be known from immature individuals, is important to properly reconstructing evolution (Butler and Zhao 2009; Evans et al. 2011; Fowler et al. 2011; Tsuihiji et al. 2011; Campione et al. 2013; Tsai and Fordyce 2014). This problem has been especially noted in early dinosaurs and their relatives, which possess many phylogenetically important characters that are variable during growth (Tykoski 2005; Griffin and Nesbitt 2016).

Although there is variation in the order at which mature characters states are reached, comparing modal sequences across taxa may help determine what ontogenetically variable phylogenetic characters are more useful, and which should be used with caution. In comparing the order of appearance of homologous femoral ontogenetic characters between three early-diverging dinosauriforms with excellent growth series, *Coelophysis bauri*, *Megapnosaurus rhodesiensis,* and the silesaurid *Asilisaurus kongwe* (Griffin and Nesbitt 2016), some characters consistently appear earlier in ontogeny than others, and the order of appearance during ontogeny is relatively conserved (Fig. 22). For example, the anterior trochanter is present in all known individuals of *C. bauri* and *M. rhodesiensis*, and in all but the least mature known

specimen of *A. kongwe*. Therefore, this character state is probably one of the first, if not the first, ontogenetically variable phylogenetic character to appear during ontogeny, and will probably not influence the results of a phylogenetic analysis even if many immature specimens are included in the analysis. Conversely, a character like the insertion scar of the M. caudifemoralis brevis (character 22) may present more problems for phylogenetic analysis, because this character appears in a range of ontogenetic orders in these taxa, all later in ontogeny. In this case, a taxon only known from skeletally immature individuals is more likely to appear to lack this character (and others like it) because of ontogenetic stage, and not because of a real phylogenetic signal. Additionally, because many phylogenetic characters for early dinosaurs and other archosaurs are based on the morphology of muscle scars (e.g., dorsolateral trochanter, anterior trochanter, trochanteric shelf, fourth trochanter; Nesbitt 2011), which changes during ontogeny, these characters should be used with caution in cladistic analyses of archosaurs and their closest relatives.

ACKNOWLEDGEMENTS

I thank the curators and collections staff at AMNH, CM, CMNH, FMNH, GR, MCZ, MNA, NMMNH, QG, SMP, TMP, UCM, and UMNH. This study was enriched by discussions with R. Irmis, P. Makovicky, N. Smith, M. McClain, S. Werning, K. Padian, K. Stein, A. Pritchard, and Z. Morris. I thank S. Nesbitt, M. Stocker, M. Colbert, and L. Freeman for their helpful reviews of the manuscript. This study was supported by the Jurassic Foundation, the Geological Society of America Graduate Student Research Grants, and the Charles E. and Frances P. Sears Research Scholarship.

6. REFERENCES

Andrews, C. W. 1921. On some remains of a theropodous dinosaur from Scotland: limb bone of a ceratosaur theropod from Skye. Scottish Journal of Geology 31:177–182.

Bailleul, A. M., J. B. Scannella, J. R. Horner, and D. C. Evans. 2016. Fusion patterns in the skulls of modern archosaurs reveal that sutures are ambiguous maturity indicators for the Dinosauria. PLoS ONE 11:e0147687. DOI: 10.1371/journal.pone.0147687

Ballman, P. 1969. Les oiseaux Miocènes de La Grive-Saint-Alban (Isère). Gèobios 2:157–204.

Bennett, S. C. 1993. The ontogeny of *Pteranodon* and other pterosaurs. Paleobiology 19:92–106.

Bennett, S. C. 1996. Year-classes of pterosaurs from the Solnhofen Limestone of Germany: taxonomic and systematic implications. Journal of Vertebrate Paleontology 16:432–444.

Benton, M. J., L. Juul, G. W. Storrs, and P. M. Galton. 2000. Anatomy and systematics of the prosauropod dinosaur *Thecodontosaurus antiquus* from the Upper Triassic of southwest England. Journal of Vertebrate Paleontology 20:77–108.

Bristowe, A., and M. A. Raath. 2004. A juvenile coelophysoid skull from the Early Jurassic of Zimbabwe, and the synonymy of *Coelophysis* and *Syntarsus*. Palaeontologia Africana 40:31–41.

Britt, B. B., D. J. Chure, T. R. J. Holtz, C. A. Miles, and K. L. Stadtman. 2000. A reanalysis of the phylogenetic affinities of *Ceratosaurus* (Theropoda, Dinosauria)

based on new specimens from Utah, Colorado, and Wyoming. Journal of Vertebrate Paleontology 20:32A.

Brochu, C. A. 1992. Ontogeny of the postcranium in crocodylomorph archosaurs. Master's thesis. University of Texas at Austin: Austin, Texas. 340 pp.

Brochu, C. A. 1996. Closure of neurocentral sutures during crocodilian ontogeny: implications for maturity assessment in fossil archosaurs. Journal of Vertebrate Paleontology 16:49–62.

Brusatte, S. L., S. J. Nesbitt, R. B. Irmis, R. J. Butler, M. J. Benton, and M. A. Norell. 2010. The origin and early radiation of dinosaurs. Earth-Science Reviews 101:68–100.

Buckley, L. G., D. W. Larson, M. Reichel, and T. Samman. 2010. Quantifying tooth variation within a single population of *Albertosaurus sarcophagus* (Theropoda: Tyrannosauridae) and implications for identifying isolated teeth of tyrannosaurids. Canadian Journal of Earth Sciences 47:1227–1251.

Burch, S. H. 2014. Complete forelimb myology of the basal theropod dinosaur *Tawa hallae* based on a novel robust muscle reconstruction method. Journal of Anatomy 225:271–297.

Butler, R. J. 2010. The anatomy of the basal ornithischian dinosaur *Eocursor parvus* from the lower Elliot Formation (Late Triassic) of South Africa. Zoological Journal of the Linnean Society 160:648–684.

Butler, R. J., and Q. Zhao. 2009. The small-bodied ornithischian dinosaurs *Micropachycephalosaurus hongtuyanensis* and *Wannanosaurus yansiensis* from the Late Cretaceous of China. Cretaceous Research 30:63–77.

Bybee, P. J., A. H. Lee, and E.-T. Lamm. 2006. Sizing the Jurassic theropod dinosaur *Allosaurus*: assessing growth strategy and evolution of ontogenetic scaling of limbs. Journal of Morphology 267:347–359.

Camp, C. L. 1930. A study of the phytosaurs with description of new material from western North America. Memoirs of the University of California 10:161.

Campione, N., K. S. Brink, E. A. Freedman, and C. T. McGarrity. 2013. '*Glishades ericksoni*', an indeterminate juvenile hadrosaurid from the Two Medicine Formation of Montana: implications for hadrosauroid diversity in the latest Cretaceous (Campanian-Maastrichtian) of western North America. Palaeodiversity and Palaeoenvironments 93:65–75.

Carpenter, K. 1997. A giant coelophysoid (Ceratosauria) theropod from the Upper Triassic of New Mexico. (With 8 figures and 3 tables in the text). Neues Jahrbuch für Geologie und Paläontologie 205:189–208.

Carpenter, K. 2010. Variation in a population of Theropoda (Dinosauria): *Allosaurus* from the Cleveland-Lloyd Quarry (Upper Jurassic), Utah, USA. Paleontological Research 14:250–259.

Carr, T. D. 1999. Craniofacial ontogeny in Tyrannosauridae (Dinosauria, Coelosauria). Journal of Vertebrate Paleontology 19:497–520.

Carrano, M. T., and J. R. Hutchinson. 2002. Pelvic and hindlimb musculature of *Tyrannosaurus rex* (Dinosauria: Theropoda). Journal of Morphology 253:207–228.

Carrano, M. T., J. R. Hutchinson, and S. D. Sampson. 2005. New information of *Segisaurus halli*, a small theropod dinosaur from the Early Jurassic of Arizona. Journal of Vertebrate Paleontology 25:835–849.

Carrano, M. T., and S. D. Sampson. 1999. Evidence for a paraphyletic 'Ceratosauria' and its implications for theropod dinosaur evolution. Journal of Vertebrate Paleontology 19:36A.

Carrano, M. T., S. D. Sampson, and C. A. Forster. 2002. The osteology of *Masiakasaurus knopfleri*, a small abelisauroid (Dinosauria: Theropoda) from the Late Cretaceous of Madagascar. Journal of Vertebrate Paleontology 22:510–534.

Chinnery, B. J., and D. B. Weishampel. 1998. *Montanoceratops cerorhynchus* (Dinosauria: Ceratopsia) and relationships among basal neoceratopsians. Journal of Vertebrate Paleontology 18:569–585.

Chinsamy, A. 1990. Physiological implications of the bone histology of *Syntarsus rhodesiensis* (Saurischia: Theropoda). Palaeontologia Africana 27:77–82.

Chinsamy, A. 1990. Physiological implications of the bone histology of *Syntarsus rhodesiensis* (Saurischia: Theropoda). Palaeontologia Africana 27:77–82.

Chinsamy, A. 1993. Bone histology and growth trajectory of the prosauropod dinosaur *Massospondylus carinatus* Owen. Modern Geology 18:319–329.

Codron, D., C. Carbone, D. W. H. Müller, and M. Clauss. 2012. Ontogenetic niche shifts in dinosaurs influenced size, diversity and extinction in terrestrial vertebrates. Biology Letters 8:620–623.

Colbert, E. H. 1989. The Triassic dinosaur *Coelophysis*. Museum of Northern Arizona Bulletin 57:1–160.

Colbert, E. H. 1990. Variation in *Coelophysis bauri*; pp. 81–90 *in* K. Carpenter, and P. J. Currie (eds.), Dinosaur Systematics: Perspectives and Approaches. Cambridge University Press, Cambridge, UK, 356 pp.

Colbert, M. W., and T. Rowe. 2008. Ontogenetic sequence analysis: using parsimony to characterize developmental sequences and sequence polymorphism. Journal of Experimental Zoology Part B, Molecular and Developmental Evolution 310B:398–416.

Coria, R. A., L. M. Chiappe, and L. Dingus. 2002. A new close relative of *Carnotaurus sastrei* Bonaparte 1985 (Theropoda: Abelisauridae) from the Late Cretaceous of Patagonia. Journal of Vertebrate Paleontology 22:460–465.

Cracraft, J. 1971. The functional morphology of the hind limb of the Domestic Pigeon, *Columba livia*. Bulletin of the American Museum of Natural History 144:171–268.

Crush, P. J. 1984. A Late Upper Triassic sphenosuchid crocodilian from Wales. Palaeontology 27:131–157.

Currie, P. J. 2003. Cranial anatomy of tyrannosaurid dinosaurs from the Late Cretaceous of Alberta, Canada. Acta Palaeontologica Polonica 48:191–226.

de Jong, I. M. L., M. W. Colbert, F. Wittle, and M. K. Richardson. 2009. Polymorphism in developmental timing: intraspecific heterochrony in a Lake Victoria cichlid. Evolution & Development 7:367–394.

Delfino, M., and M. R. Sánchez-Villagra. 2010. A survey of the rock record of reptilian ontogeny. Seminars in Cell & Developmental Biology 21:432–440.

Dilkes, D. W. 2000. Appendicular myology of the hadrosaurian dinosaur *Maiasaura peeblesorum* from the Late Cretaceous (Campanian) of Montana. Transactions of the Royal Society of Edinburgh: Earth Sciences 90:87–125.

Dutuit, J.-M. 1979. Un pseudosuchien du Trias continental marocain. Annales de Paléontologie (Vertébrés) 65:55–68.

Dzik, J. 2003. A beaked herbivorous archosaur with dinosaur affinities from the early Late Triassic of Poland. Journal of Vertebrate Paleontology 23:556–574.

Erickson, G. M., P. J. Mackovicky, P. J. Currie, M. A. Norell, S. A. Yerby, and C. A. Brochu. 2004. Gigantism and comparative life-history parameters of tyrannosaurid dinosaurs. Nature 430:772–775.

Erickson, G. M., and T. A. Tumanova. 2000. Growth curve of *Psittacosaurus mongoliensis* Osborn (Ceratopsia: Psittacosauridae) inferred from long bone histology. Zoological Journal of the Linnean Society 130:551–566.

Evans, D. C., C. M. Brown, M. J. Ryan, and K. Tsogtbaatar. 2011. Cranial ornamentation and ontogenetic status of *Homalocephale calathocercos* (Ornithischia: Pachycephalosauria) from the Nemegt Formation, Mongolia. Journal of Vertebrate Paleontology 31:84–92.

Ezcurra, M. D. 2006. A review of the systematic position of the dinosauriform archosaur *Eucoelophysis baldwini* Sullivan & Lucas, 1999 from the Upper Triassic of New Mexico, USA. Geodiversitas 28:649–684.

Ezcurra, M. D., and S. L. Brusatte. 2011. Taxonomic and phylogenetic reassessment of the early neotheropod dinosaur *Camposaurus arizonensis* from the Late Triassic of North America. Palaeontology 54:763–772.

Ferigolo, J., and M. C. Langer. 2006. A Late Triassic dinosauriform from south Brazil and the origin of the ornithischian predentary bone. Historical Biology 19:1–11.

Forster, C. A. 1999. Gondwanan dinosaur evolution and biogeographic analysis. Journal of African Earth Sciences 28:169–185.

Fowler, D. W., H. N. Woodward, E. A. Freedman, P. L. Larson, and J. R. Horner. 2011. Reanalysis of "*Raptorex kriegsteini*": A juvenile tyrannosaurid dinosaur from Mongolia. PLoS ONE 6:e21376. DOI: 10.1371/journal.pone.0021376

Galton, P. M. 1982. Juveniles of the stegosaurian dinosaur *Kentrosaurus* from the Upper Jurassic of Tanzania, East Africa. Journal of Vertebrate Paleontology 2:47–62.

Galton, P. M. 1990. Basal sauropodomorpha – prosauropoda; pp. 320–344 *in* D. B. Weishampel, P. Dodson, and H. Osmólska (eds.), The Dinosauria. University of California Press, Berkeley.

Gauthier, J. A. 1984. A cladistics analysis of the higher systematic categories of the Diapsida. Ph.D. dissertation. University of California, Berkeley: Berkeley, CA. 564 pp.

Gay, R. 2005. Sexual dimorphism in the Early Jurassic theropod dinosaur *Dilophosaurus* and a comparison with other related forms; pp. 277–283 *in* K. Carpenter (ed.), The Carnivorous Dinosaurs. Indiana University Press, Indianapolis, IN.

Genin, D. 1992. Hind limb proportions and ontogenetic changes in the theropod dinosaur, *Coelophysis bauri*. Master's thesis. Northern Illinois University: DeKalb, IL. 107 pp.

Gilmore, C. W. 1920. Osteology of the carnivorous Dinosauria in the United States National Museum, with special reference to the genera *Antrodemus* (*Allosaurus*) and *Ceratosaurus*. Bulletin of the U.S. National Museum 110:1–154.

Griffin, C. T., and S. J. Nesbitt. 2016. The histology and femoral ontogeny of the Middle Triassic (?late Anisian) dinosauriform *Asilisaurus kongwe* and implications for the growth of early dinosaurs. 2016. DOI: 10.1080/02724634.2016.1111224

Heckert, A. B., S. G. Lucas, L. F. Rinehart, J. A. Spielman, A. P. Hunt, and R. Kahle. 2006. Revision of the archosauromorph reptile Trilophosaurus, with a description of the first skull of Trilophosaurus jacobsi, from the Upper Triassic Chnle Group, West Texas, USA. Palaeontology 49:621–640.

Hennig, W. E. 1966. Phylogenetic Systematics. University of Illinois Press, Urbana, 263 pp.

Hofmann, R., K. Stein, and P. M. Sander. 2014. Constraints on the lamina density of laminar bone architecture of large-bodied dinosaurs and mammals. Acta Palaeontologica Polonica 59:287–294.

Holtz, T. R. J. 1994. The phylogenetic position of the Tyrannosauridae: implications for theropod systematics. Journal of Paleontology 68:1100–1117.

Holtz, T. R. J., and H. Osmólska. 2004. Saurischia; pp. 21–24 *in* D. B. Weishampel, P. Dodson, and H. Osmólska (eds.), The Dinosauria, Second Edition. University of California Press, Berkeley.

Horner, J. A., and K. Padian. 2004. Age and growth dynamics of *Tyrannosaurus rex*. Proceedings of the Royal Society B: Biological Sciences 271:1875–1880.

Horner, J. A., K. Padian, and A. d. Ricqlès. 2001. Comparative osteohistology of some embryonic and perinatal archosaurs: developmental and behavioral implications for dinosaurs. Paleobiology 27:39–58.

Horner, J. A., A. d. Ricqlès, and K. Padian. 1999. Variation in dinosaur skeletochronology indicators: implications for age assessment and physiology. Paleobiology 25:295–304.

Horner, J. A., A. d. Ricqlès, and K. Padian. 2000. Long bone histology of the hadrosaurid dinosaur *Maiasaura peeblesorum*: growth dynamics and physiology based on an ontogenetic series of skeletal elements. Journal of Vertebrate Paleontology 20:109–123.

Horner, J. R., and M. B. Goodwin. 2009. Extreme cranial ontogeny in the Upper Cretaceous dinosaur *Pachycephalosaurus*. PLoS ONE 4:e7626. DOI: 10.1371/journal.pone.0007626

Hunt, A. P. 2001. The vertebrate fauna, biostratigraphy, and biochronology of the type Revueltian land-vertebrate faunachron, Bull Canyon Formation (Upper Triassic), east-central New Mexico. New Mexico Geological Society 52nd Field Conference Guidebook:123–151.

Hutchinson, J. R. 2001. The evolution of femoral osteology and soft tissues on the line to extant birds (Neornithes). Zoological Journal of the Linnean Society 131:169–197.

Hutchinson, J. R., F. C. Anderson, S. S. Blemker, and S. L. Delp. 2005. Analysis of hindlimb muscle moment arms in *Tyrannosaurus rex* using a three-dimensional

musculoskeletal computer model: implications for stance, gait, and speed. Paleobiology 31:676–701.

Hutt, S., D. Naish, D. M. Martill, M. J. Barker, and P. Newbery. 2001. A preliminary account of a new tyrannosauroid theropod from the Wessex Formation (Early Cretaceous) of southern England. Cretaceous Research 22:227–242.

Irmis, R. B. 2007. Axial skeleton ontogeny in the parasuchia (Archosauria: Pseudosuchia) and its implications for ontogenetic determination in archosaurs. Zoological Journal of the Linnean Society 131:169–197.

Irmis, R. B., S. J. Nesbitt, K. Padian, N. D. Smith, A. H. Turner, D. Woody, and A. Downs. 2007. A Late Triassic dinosauromorph assemblage from New Mexico and the rise of dinosaurs. Science 317:358–361.

Ivie, M. A., S. A. Slipinski, and P. Wegrzynowicz. 2001. Generic homonyms in the Colydiinae (Coleoptera: Zopheridae). Insecta Mundi 15:63–64.

Jasinoski, S. C., A. P. Russell, and P. J. Currie. 2006. An integrative phylogenetic and extrapolatory approach to the reconstruction of dromaeosaur (Theropoda: Eumaniraptora) shoulder musculature. Zoological Journal of the Linnean Society 146:301–344.

Johnson, R. 1977. Size independent criteria for estimating relative age and the relationships among growth parameters in a group of fossil reptiles (Reptilia: Ichthyosauria). Canadian Journal of Earth Sciences 14:1916–1924.

Klein, N., and P. M. Sander. 2007. Bone histology and growth of the prosauropod *Plateosaurus engelhardti* MEYER, 1837 from the Norian bonebeds of Trossingen (Germany) and Frick (Switzerland). Special Papers in Paleontology:169–206.

Knoll, F. K., K. Padian, and A. d. Ricqlès. 2010. Ontogenetic change and adult body size of the early ornithischian dinosaur *Lesothosaurus diagnosticus*: implications for basal ornithischian taxonomy. Gondwana Research 17:171–179.

Langer, M. C. 2003. The pelvic and hind limb anatomy of the stem-sauropodomorph *Saturnalia tupiniquim* (Late Triassic, Brazil). PaleoBios 23:1–30.

Langer, M. C. 2004. Basal Saurischia; pp. 25–46 *in* D. B. Weishampel, P. Dodson, and H. Osmólska (eds.), The Dinosauria, Second Edition. University of California Press, Berkeley, CA.

Langer, M. C., and M. J. Benton. 2006. Early dinosaurs: a phylogenetic study. Journal of Systematic Palaeontology 4:309–358.

Langer, M. C., and J. Ferigolo. 2013. The Late Triassic dinosauromorph *Sacisaurus agudoensis* (Caturrita Formation; Rio Grande do Sul, Brazil): anatomy and affinities; pp. 353–392 *in* S. J. Nesbitt, J. B. Desojo, and R. B. Irmis (eds.), Anatomy, Phylogeny, and Palaeobiology of Early Archosaurs and their Kin. Geological Society, London, UK.

Langer, M. C., M. A. G. Franca, and S. Gabriel. 2007. The pectoral girdle and forelimb anatomy of the stem-sauropodomorph *Saturnalia tupiniquim* (Upper Triassic, Brazil). Special Papers in Paleontology 77.

Lee, M. S. Y. 1996. The homologies and early evolution of the shoulder girdle in turtles. Proceedings of the Royal Society B: Biological Sciences 263:111–117.

Lloyd, G. T. 2016. Estimating morphological diversity and tempo withdiscrete character-taxon matrices: implementation,challenges, progress, and future directions. Biological Journal of the Linnean Society. DOI: 10.1111/bij.12746

Maddison, D. R., and W. P. Maddison. 2002. MacClade 4: Analysis of phylogeny and character evolution. Version 1.04.

Maddison, D. R., and S. P. Welles. 2000. *Ceratosaurus* (Dinosauria, Theropoda): a revised osteology. Utah Geological Survey, Miscellaneous Publications 00–2:1–80.

Madsen, J. H. J. 1976. *Allosaurus fragilis*: a revised osteology. Utah Geological Survey Bulletin 109:1–163.

Makovicky, P. J., S. Apesteguía, and F. L. Agnolín. 2005. The earliest dromaeosaurid theropod from South America. Nature 437:1007–1011.

Marsh, O. C. 1884. Principal characters of American Jurassic dinosaurs, part VIII: The order Theropoda. American Journal of Science 27:329–340.

Martill, D. M., E. Frey, H.-D. Sues, and A. Cruickshank, R. 2000. Skeletal remains of a small theropod dinosaur with associated soft structures from the Lower Cretaceous Santana Formation of northeastern Brazil. Canadian Journal of Earth Sciences 37:891–900.

Martill, D. M., S. U. Vidovic, C. Howells, and J. R. Nudds. 2016. The oldest Jurassic dinosaur: A basal neotheropod from the Hettangian of Great Britain. PLoS ONE 11:e0145713. DOI: 10.1371/journal.pone.0145713

Martínez, R. N., C. Apaldetti, G. A. Correa, and D. Abelín. 2015. A Norian lagerpetid dinosauromorph from the Quebrada del Barro Formation, northwestern Argentina Ameghiniana 53:1–13.

Martínez, R. N., O. Giménez, J. Rodríguez, and G. Bochatey. 1986. *Xenotarsosaurus bonapartei* nov. gen. et sp. (Carnosauria, Abelisauridae), un nuevo Theropoda de

la Formación Bajo Barreal, Chubut, Argentina. Simposio de Evolucion de los vertebrados Mesozoicos: IV Congreso Argentino de paleontologia y bioestratigrafia 2:23–31.

Meers, M. B. 2003. Crocodylian forelimb musculature and its relevance to Archosauria. The Anatomical Record 274A:891–916.

Nesbitt, S. J. 2011. The early evolution of archosaurs: relationships and the origin of major clades. Bulletin of the American Museum of Natural History 352:1–292.

Nesbitt, S. J., P. M. Barrett, S. Werning, C. A. Sidor, and A. J. Charig. 2013. The oldest dinosaur? A Middle Triassic dinosauriform from Tanzania. Biology Letters 9. DOI: 10.1098/rsbl.2012.0949

Nesbitt, S. J., and M. D. Ezcurra. 2015. The early fossil record of dinosaurs in North America: A new neotheropod from the base of the Upper Triassic Dockum Group of Texas. Acta Palaeontologica Polonica 60:513–526.

Nesbitt, S. J., R. B. Irmis, and W. G. Parker. 2007. A critical re-evaluation of the Late Triassic dinosaur taxa of North America. Journal of Systematic Palaeontology 5:209–243.

Nesbitt, S. J., R. B. Irmis, W. G. Parker, N. D. Smith, A. H. Turner, and T. Rowe. 2009. Hindlimb osteology and distribution of basal dinosauromorphs from the Late Triassic of North America. Journal of Vertebrate Paleontology 29:498–516.

Nesbitt, S. J., C. A. Sidor, R. B. Irmis, K. D. Angielczyk, R. M. H. Smith, and L. A. Tsuji. 2010. Ecologically distinct dinosaurian sister group shows early diversification of Ornithodira. Nature 464:95–98.

Nesbitt, S. J., N. D. Smith, R. B. Irmis, A. H. Turner, A. Downs, and M. A. Norell. 2009. A complete skeleton of a Late Triassic saurischian and the early evolution of dinosaurs. Science 326:1530–1533.

Novas, F. E. 1993. New information on the systematics and postcranial skeleton of *Herrerasaurus ischigualastensis* (Theropoda: Herrerasauridae) from the Ischigualasto Formation (Upper Triassic) of Argentina. Journal of Vertebrate Paleontology 13:400–423.

Novas, F. E. 1996. Dinosaur monophyly. Journal of Vertebrate Paleontology 16:723–741.

Padian, K., J. A. Horner, and A. d. Ricqlès. 2004. Growth in small dinosaurs and pterosaurs: the evolution of archosaurian growth strategies. Journal of Vertebrate Paleontology 24:555–571.

Padian, K., A. d. Ricqlès, and J. A. Horner. 2001. Dinosaurian growth rates and bird origins. Nature 412:405–408.

Piechowski, R., M. Tałanda, and J. Dzik. 2014. Skeletal variation and ontogeny of the Late Triassic Dinosauriform *Silesaurus opolensis*. Journal of Vertebrate Paleontology 34:1383–1393.

Raath, M. A. 1969. A new coelurosaurian dinosaur from the Forest Sandstone of Rhodesia. Arnoldia 4:1–25.

Raath, M. A. 1977. The anatomy of the Triassic theropod *Syntarsus rhodesiensis* (Sauischia: Podokesauridae) and a consideration of its biology. Ph.D. dissertation. Rhodes University: Grahamnstown, South Africa. 233 pp.

Raath, M. A. 1990. Morphological variation in small theropods and its meaning in systematics: evidence from *Syntarsus rhodesiensis*; pp. 91–105 *in* K. Carpenter,

and P. J. Currie (eds.), Dinosaur Systematics: Perspectives and Approaches. Cambridge University Press, Cambridge, UK.

Rauhut, O. W. M. 2003. The interrelationships and evolution of basal dinosaurs. Special Papers in Paleontology 69:1–214.

Ricqlés, d. A. 1968. Recherches paléohistologiques sur les os longs des Tétrapodes. I. Origine du tissu osseux plexiforme des Dinosauriens Sauropodes. Annales de Paléontologie (Vertébrés) 54:133–145.

Rinehart, L. F., S. G. Lucas, A. B. Heckert, J. A. Spielman, and M. D. Celeskey. 2009. The paleobiology of *Coelophysis bauri* (Cope) from the Upper Triassic (Apachean) Whitaker Quarry, New Mexico, with detailed analysis of a single quarry block. New Mexico Museum of Natural History and Science Bulletin 45:1–260.

Romer, A. 1956. Osteology of the reptiles. University of Chicago Press, Chicago, 772 pp.

Rowe, T. 1986. Homology and evolution of the deep dorsal thigh musculature in birds and other Reptilia. Journal of Morphology 189:327–346.

Rowe, T. 1989. A new species of the theropod dinosaur *Syntarsus* from the Early Jurassic Kayenta Formation of Arizona. Journal of Vertebrate Paleontology 9:125–136.

Rowe, T., and J. Gauthier. 1990. Ceratosauria; pp. 151–168 *in* D. B. Weishampel, P. Dodson, and H. Osmólska (eds.), The Dinosauria. University of California Press, Berkeley.

Sander, P. M., and N. Klein. 2005. Developmental plasticity in the life history of a prosauropod dinosaur. Science 16:1800–1802.

Sander, P. M., N. Klein, E. Buffetaut, V. Cuny, V. Suteethorn, and J. L. Loeuff. 2004. Adaptive radiation in sauropod dinosaurs: bone histology indicates rapid evolution of giant body size through acceleration. Organisms Diversity and Evolution 4:165–173.

Scanella, J. B., and J. R. Horner. 2010. *Torosaurus* Marsh, 1891, is *Triceratops* Marsh, 1889 (Ceratopsidae: Chasmosaurinae): synonymy through ontogeny. Journal of Vertebrate Paleontology 30:1157–1168.

Schachner, E. R., P. L. Manning, and P. Dodson. 2011. Pelvic and hindlimb myology of the basal archosaur *Poposaurus gracilis* (Archosauria: Poposauroidea). Journal of Morphology 272:1464–1491.

Sereno, P. C. 1991. *Lesothosaurus*, "fabrosaurids," and the early evolution of Ornithischia Journal of Vertebrate Paleontology 11:168–197.

Sereno, P. C., and A. B. Arcucci. 1994. Dinosaurian precursors from the Middle Triassic of Argentina: *Marasuchus lilloensis*, gen. nov. Journal of Vertebrate Paleontology 14:53–73.

Sereno, P. C., R. N. Martínez, and O. A. Alcobar. 2013. Osteology of *Eoraptor lunensis* (Dinosauria, Sauropodomorpha). Journal of Vertebrate Paleontology 32:83–179.

Sereno, P. C., M. Wilkinson, and J. L. Conrad. 2004. New dinosaurs link southern landmasses in the Mid–Cretaceous. Proceedings of the Royal Society B: Biological Sciences 271:1325–1330.

Smith, N. D., P. J. Makovicky, W. R. Hammer, and P. J. Currie. 2007. Osteology of *Cryolophosaurus ellioti* (Dinosauria: Theropoda) from the Early Jurassic of

Antarctica and implications for early theropod evolution. Zoological Journal of the Linnean Society 151:377–421.

Sues, H.-D., S. J. Nesbitt, D. S. Berman, and A. C. Henrici. 2011. A late-surviving basal theropod dinosaur from the latest Triassic of North America. Proceedings of the Royal Society B: Biological Sciences 278:3459–3464.

Swofford, D. L. 2003. PAUP*. Phylogenetic Analysis Using Parsimony (*and Other Methods). Version 4. Sinauer Associates, Sunderland, Massachusetts.

Tsai, C.-H., and R. E. Fordyce. 2014. Disparate heterochronic processes in baleen whale evolution. Evolutionary Biology 41:299–307.

Tsai, H. P., and C. M. Holliday. 2014. Articular soft tissue anatomy of the archosaur hip joint: structural homology and functional implications. Journal of Morphology. DOI: 10.1002/jmor.20360

Tsuihiki, T., M. Watabe, K. Togtbaater, T. Tsubamoto, R. Barsbold, S. Suzuki, A. H. Lee, R. Ridgley, Y. Kawahara, and L. M. Witmer. 2011. Cranial osteology of a juvenile specimen of *Tarbosaurus bataar* (Theropoda, Tyrannosauridae) from the Nemegt Formation (Upper Cretaceous) of Bugin Tsav, Mongolia. Journal of Vertebrate Paleontology 31:1–21.

Tumarkin-Deratzian, A. R., D. R. Vann, and P. Dodson. 2006. Bone surface texture as an ontogenetic indicator in long bones of the Canada goose *Branta canadensis* (Anseriformes: Anatidae). Zoological Journal of the Linnean Society 148:133–168.

Tumarkin-Deratzian, A. R., D. R. Vann, and P. Dodson. 2007. Growth and textural ageing in long bones of the American alligator *Alligator mississippiensis* (Crocodylia: Alligatoridae). Zoological Journal of the Linnean Society 150:1–39.

Tykoski, R. S. 2005. Anatomy, ontogeny, and phylogeny of coelopysoid dinosaurs. Ph.D. dissertation. The University of texas at Austin: Austin, Texas. 553 pp.

Tykoski, R. S., and T. Rowe. 2004. Ceratosauria; pp. 47–70 *in* D. B. Weishampel, P. Dodson, and H. Osmólska (eds.), The Dinosauria, second edition. University of california Berkeley Press, Berkeley.

Walker, A. D. 1970. A revision of the Jurassic reptile *Hallopus victor* (Marsh), with remarks on the classification of crocodiles. Philosophical Transactions of the Royal Society B 257:323–372.

Welles, S. P. 1984. *Dilophosaurus wetherilli* (Dinosauria, Theropoda) osteology and comparisons. Palaeontographica Abteilung A 185:85–180.

Werning, S. 2013. Evolution of bone histological characters in amniotes, and the implications for the evolution of growth and metabolism. Ph.D. dissertation. University of California, Berkeley: Berkeley. 445 pp.

Wilkinson, M. 1995. Coping with abundant missing entries in phylogenetic inference using parsimony. Systematic Biology 44:501–514.

Wilson, J. A., P. C. Sereno, S. Srivastava, D. K. Bhatt, A. Khosla, and A. Sahni. 2003. A new abelisaurid (Dinosauria, Theropoda) from the Lameta Formation (Cretaceous, Maastrichtian) of India. Contributions from the Museum of paleontology, University of Michigan 31:1–42.

You, H.-L., Y. Azuma, T. Wang, Y.-M. Wang, and Z.-M. Dong. 2014. The first well-preserved coelophysoid theropod dinosaur from Asia. Zootaxa 3873:233–249.

8. FIGURES

Figure 1. Sacra and pelves of *Megapnosaurus rhodesiensis* and *Coelophysis bauri*. **A** Photograph and **B** line drawing of the sacrum, right ischium, and partial right pubis of *Coelophysis bauri* (CMNH 10971) possessing a combination of mature and immature character states, in ventrolateral view. **C** Photograph and **B** line drawing of the sacrum and left pelvis of *Megapnosaurus rhodesiensis* (QG 1) possessing mature character states in left lateral view. Scale bar is 1 cm. Abbreviations: **acet**, acetabulum; **il**, ilium; **isch**, ischium; **pub**, pubis; **sac**, sacrum.

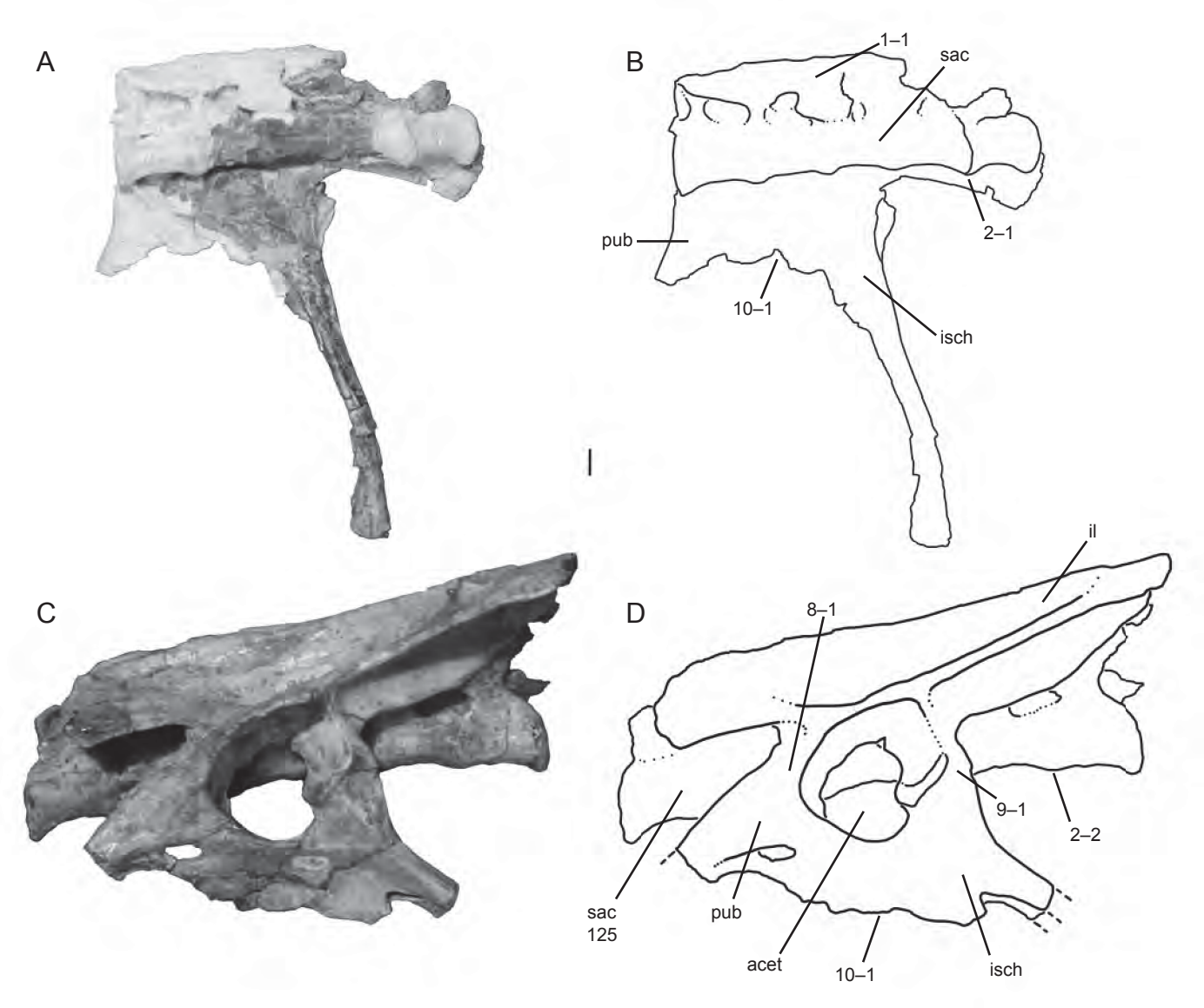
A
B
1–1
sac
pub
2–1
10–1
isch
C
D
il
8–1
9–1
2–2
sac
125
pub
acet
10–1
isch

Figure 2. Scapulae and a coracoid of *Megapnosaurus rhodesiensis* in lateral view. **A** Photograph and **B** line drawing of a right scapula (QG 528) possessing the immature character state. **C** Photograph and **D** line drawing of a left scapulocoracoid (QG 1) possessing the mature character state. Scale bar is 1 cm. Abbreviations: **cor**, coracoid; **scap**, scapula.

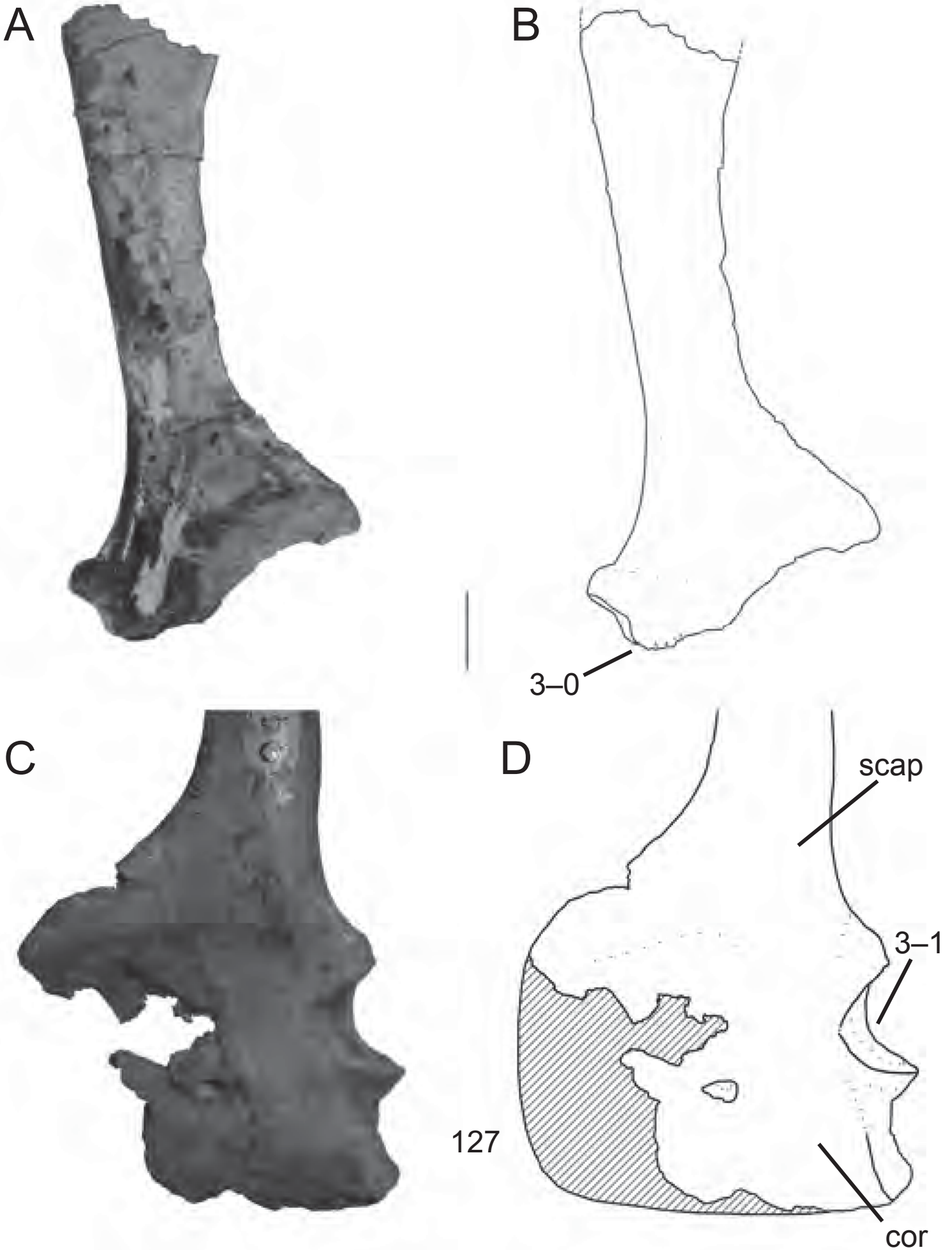
A
B
3–0
C
D
scap
3–1
cor

Figure 3. Humeri of *Megapnosaurus* rhodesiensis. **A** Photograph and **B** line drawing of a left humerus (QG 517) possessing immature character states in lateral view. **C** Photograph and **D** line drawing of a right humerus (QG 548) possessing a combination of mature and immature character states in posterior view. **E** Photograph and **F** line drawing of a left humerus (QG 543) possessing mature character states in posterior view. Scale bar is 1 cm.

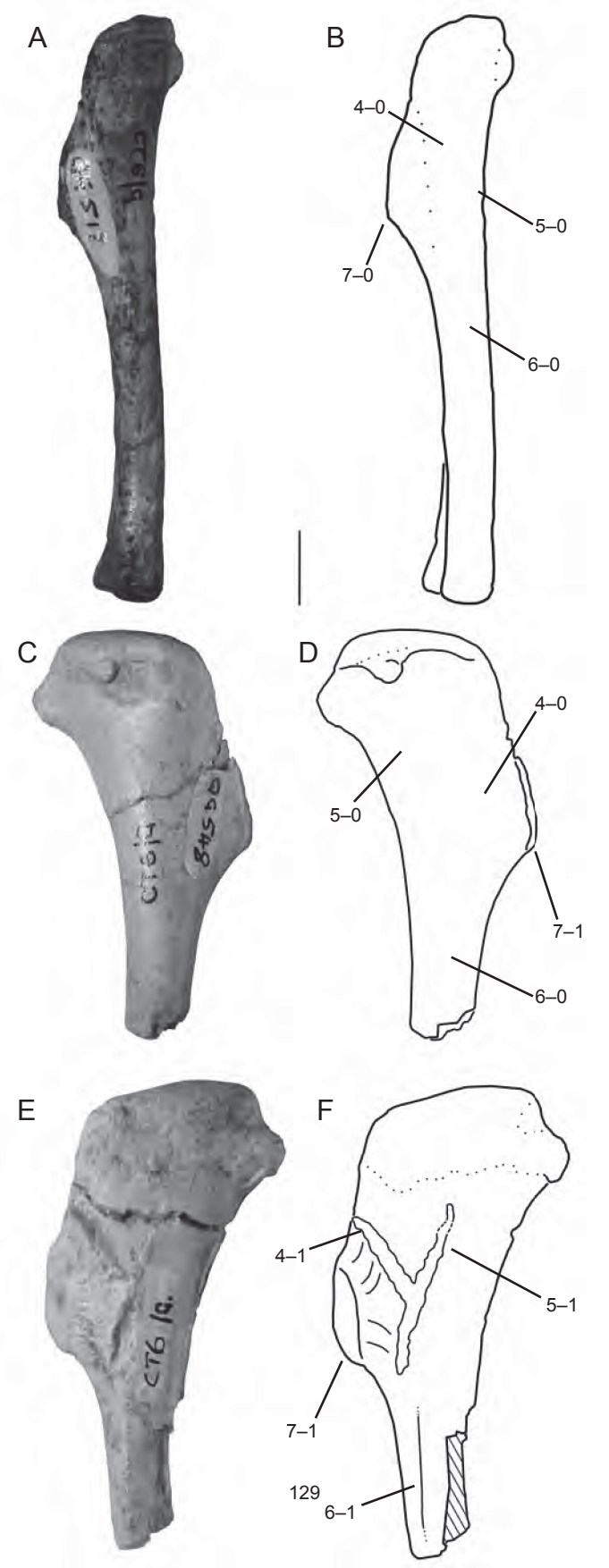
A
B
4–0
5–0
7–0
6–0
C
D
4–0
5–0
7–1
6–0
E
F
4–1
5–1
7–1
129
6–1

Figure 4. Ilium and ischium of *Megapnosaurus rhodesiensis*. **A** Photograph and **B** line drawing of left ilium (QG 691) possessing immature character states in lateral view. **C** Photograph and **D** line drawing of left ischium (QG 691) possessing immature character states in lateral view. Scale bar is 1 cm.

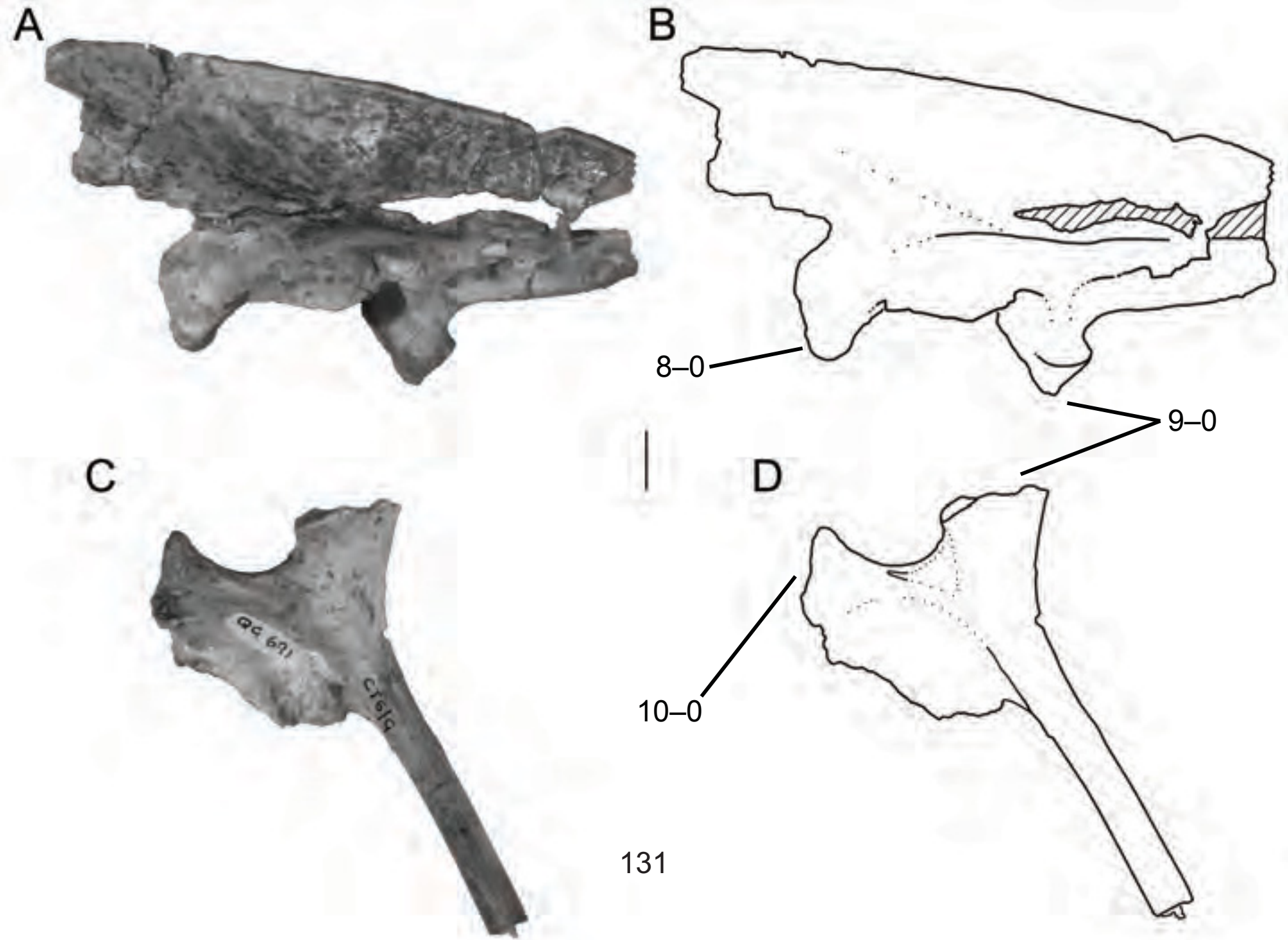
A
B
8–0
9–0
C
D
10–0
QC 671
CT6|9

Figure 5. A Photograph and **B** line drawing of articulated pubes, left ilium, and left femur of *Coelophysis bauri* (AMNH FARB 7244) in anterior view, possessing a combination of mature and immature character states. Non-target skeletal elements and matrix are lightened in Photoshop to highlight relevant skeletal elements. Scale bar is 1 cm. Abbreviations: **fem**, femur; **il**, ilium, **pub**, pubis.

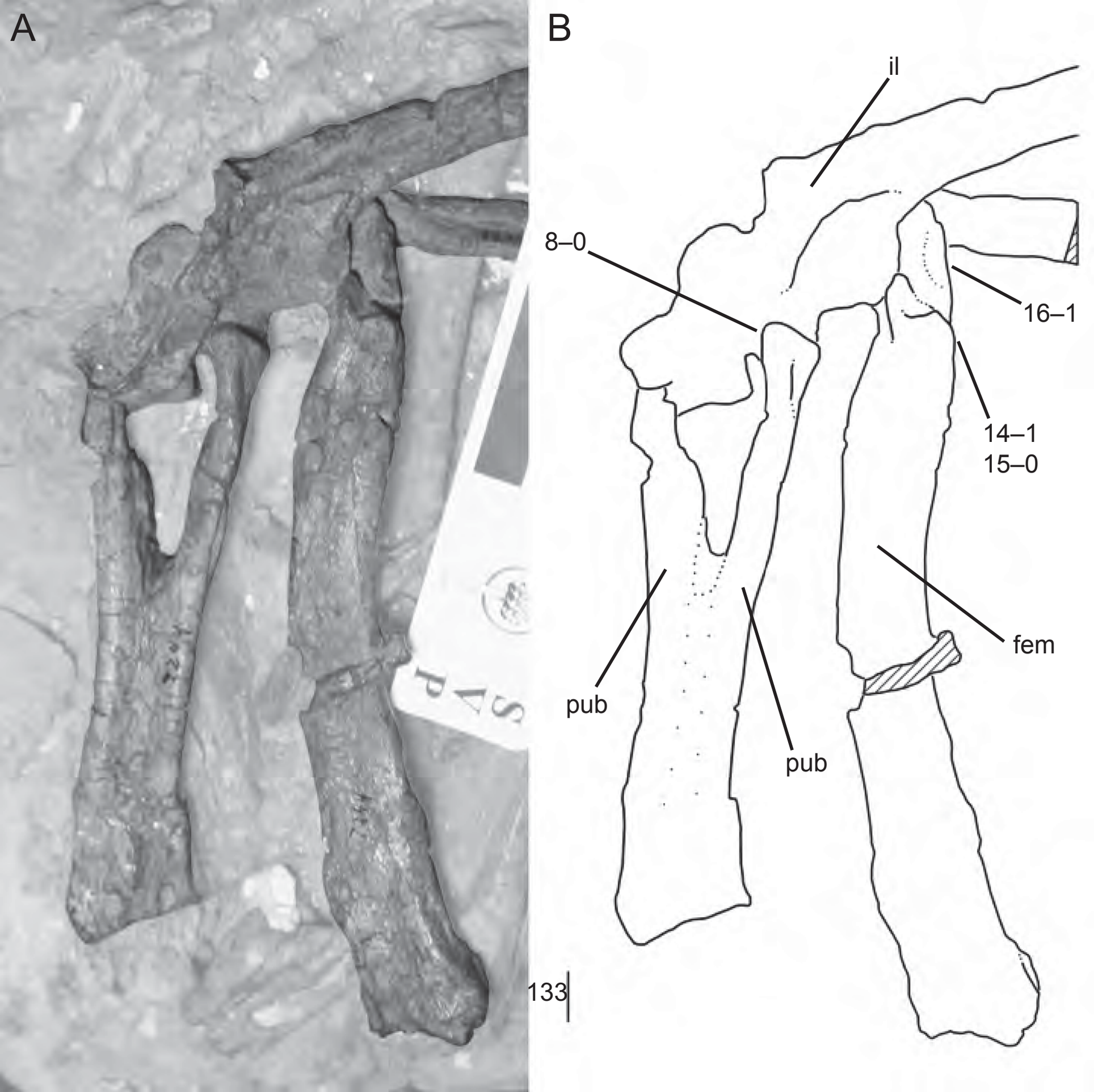
A
B
il
8–0
16–1
14–1
15–0
fem
pub
pub
133

Figure 6. Proximal ends of femora of *Megapnosaurus rhodesiensis* in proximal view. **A** Photograph and **B** line drawing of right femur (QG 174B) possessing the immature character state. **C** Photograph and **D** line drawing of left femur (QG 3A) possessing the mature character state. Scale bar is 1 cm.

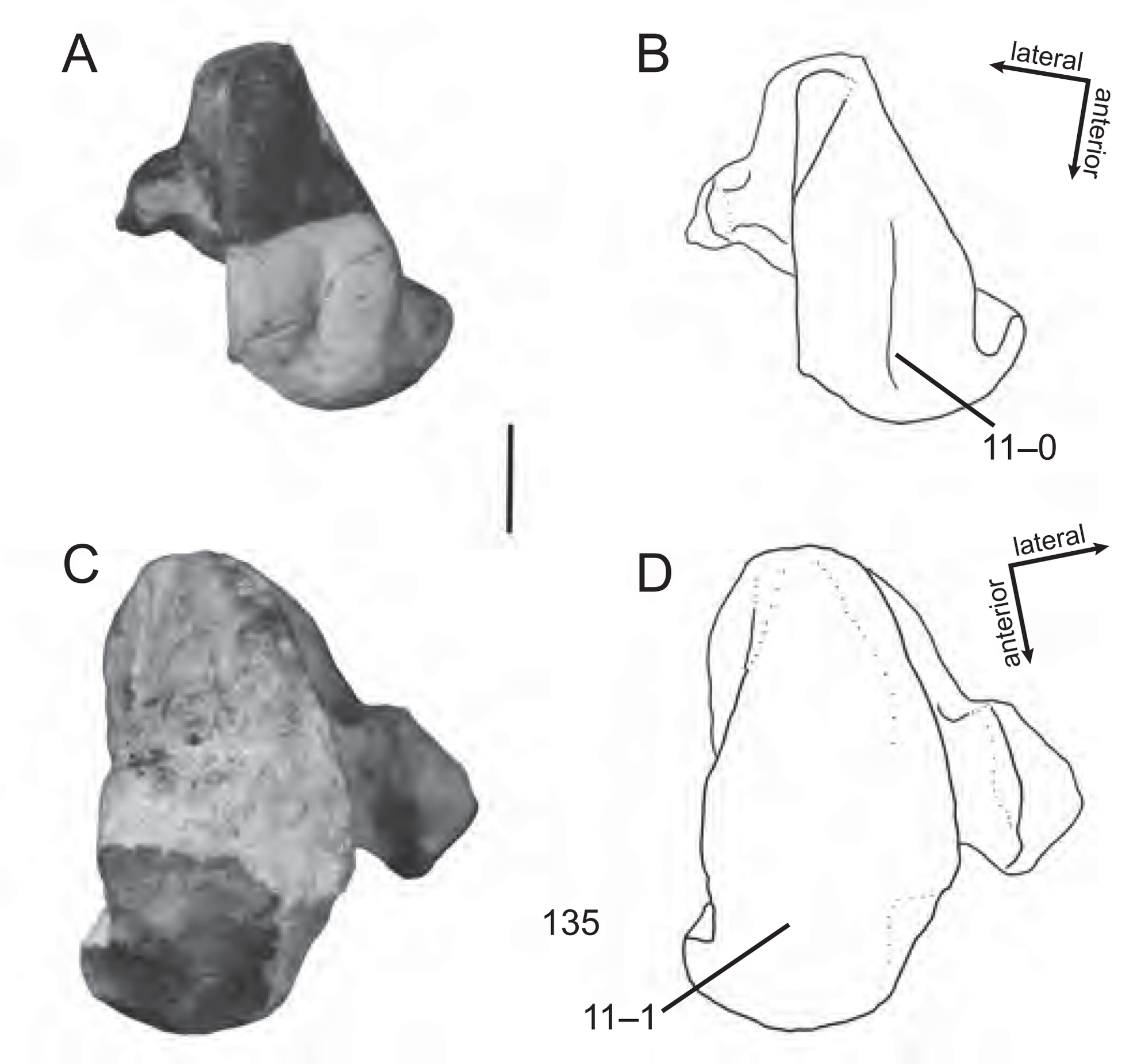
A
B
lateral
anterior
11–0
C
D
lateral
anterior
135
11–1

Figure 7. Proximal ends of left femora of *Megapnosaurus rhodesiensis* in anterolateral view. **A** Photograph and **B** line drawing of femur (QG 691) possessing immature character states. **C** Photograph and **D** line drawing of femur (QG 727) possessing mature character states. Scale bar is 1 cm. Abbreviations: **at**, anterior trochanter; **m**, mound; **ts**, trochanteric shelf.

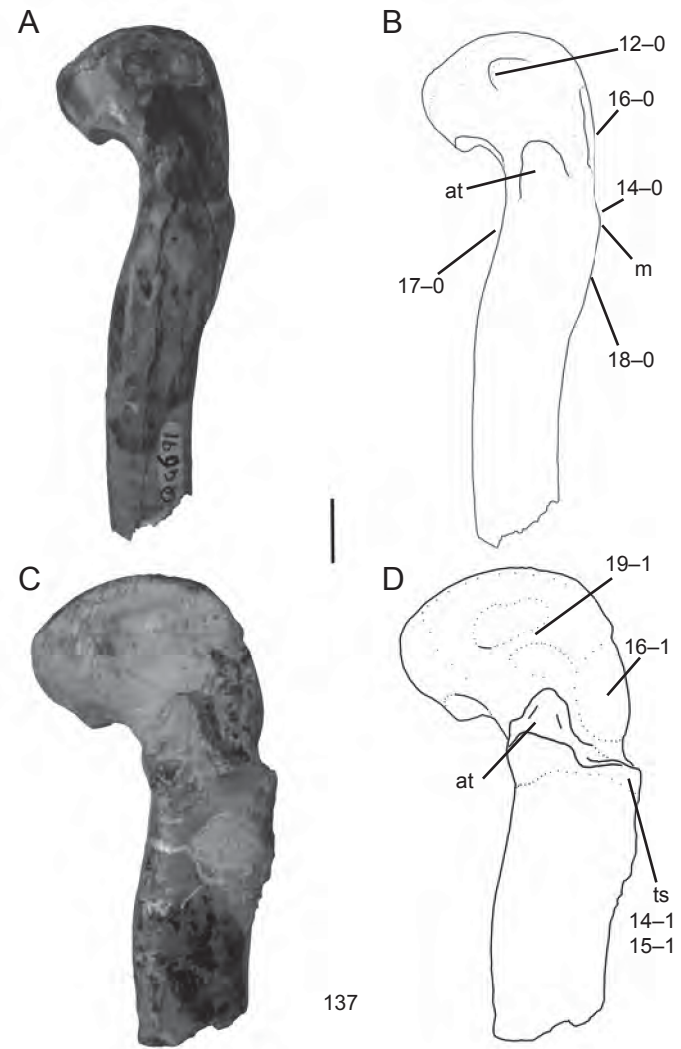
A
B
12–0
16–0
at
14–0
m
17–0
18–0
C
D
19–1
16–1
at
ts
14–1
15–1

Figure 8. Proximal end of left femur of *Megapnosaurus rhodesiensis* (QG 727) showing mature character states. **A** Photograph and **B** line drawing of femur in anteromedial view. **C** Photograph and **D** line drawing of femur in posterolateral view. Scale bar is 1 cm. Abbreviations: **at**, anterior trochanter; **ts**, trochanteric shelf.

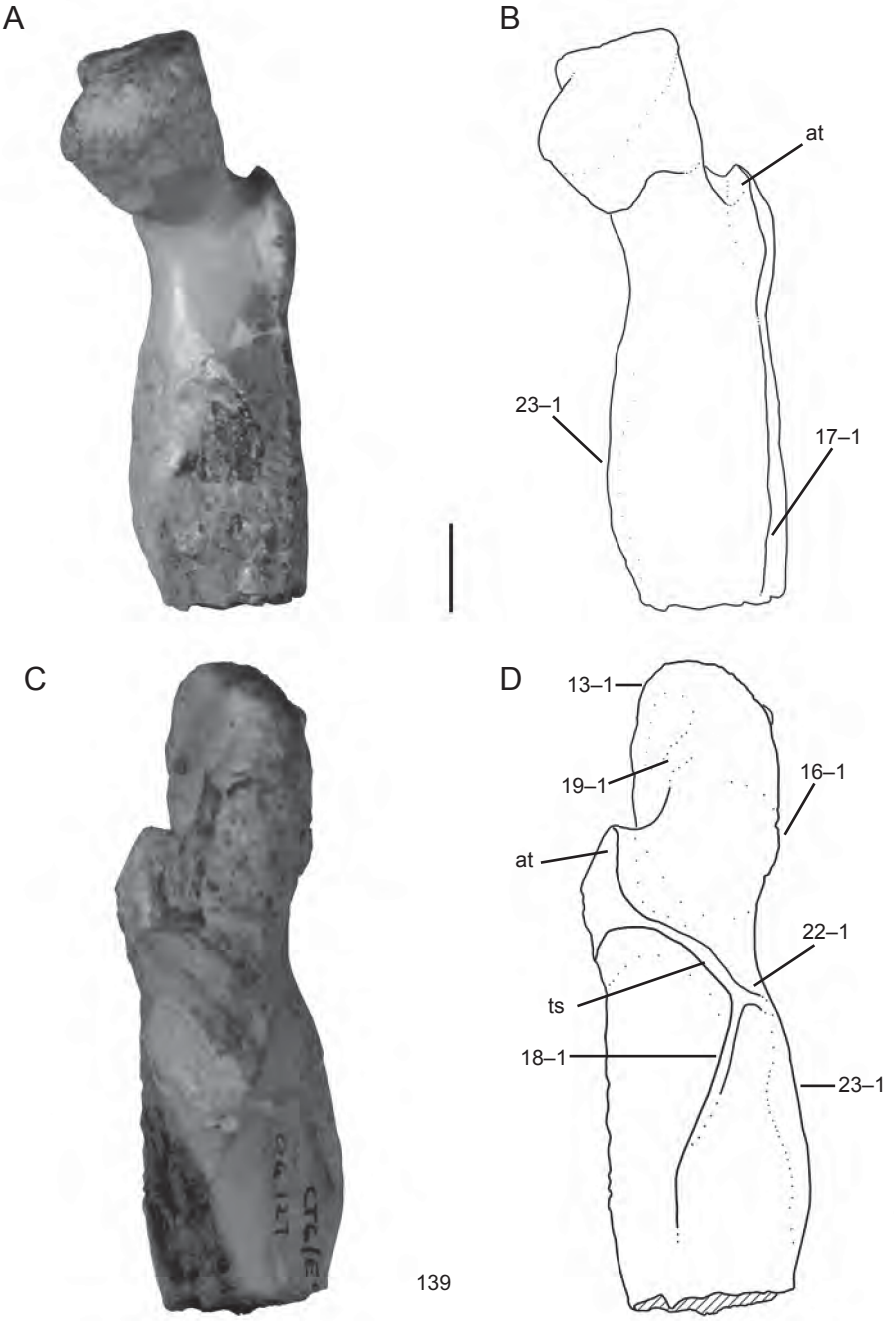
A
B
at
23–1
17–1
C
D
13–1
19–1
16–1
at
22–1
ts
18–1
23–1

Figure 9. Femora of *Megapnosaurus rhodesiensis* and *Coelophysis bauri* in posteromedial view. **A** Photograph and **B** line drawing of left femur of *Megapnosaurus rhodesiensis* (QG 691) possessing immature ontogenetic character states. **C** Photograph and **D** line drawing of left femur of *Megapnosaurus rhodesiensis* holotype (QG 1) possessing mature ontogenetic character states. **E** Photograph and **F** line drawing of right femur of *Coelophysis bauri* (NMMNH P-42351) possessing mature ontogenetic character states, with non-target skeletal elements and matrix lightened in Photoshop to highlight the femur. Scale bar is 1 cm. Abbreviations: **4th**, fourth trochanter; **at**, anterior trochanter; **ts**, trochanteric shelf.

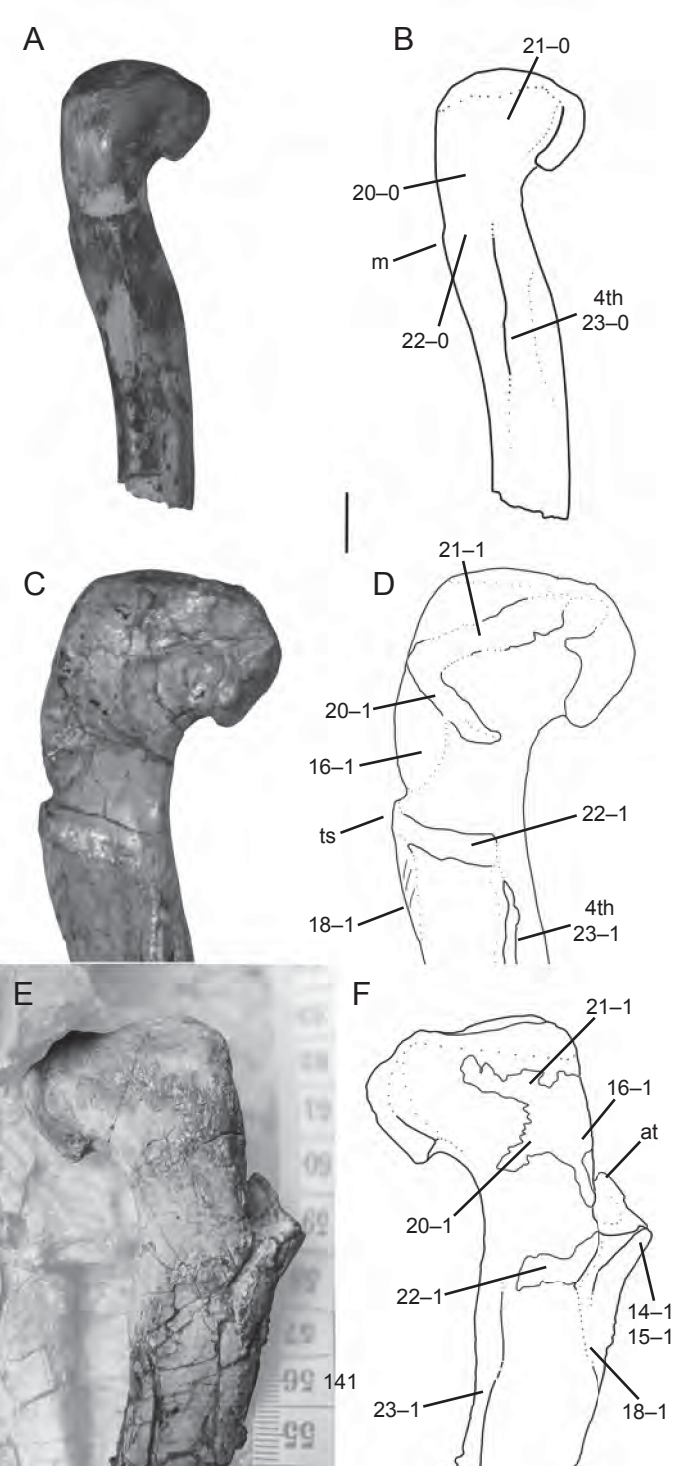
A
B
21–0
20–0
m
22–0
4th
23–0
C
D
21–1
20–1
16–1
ts
22–1
18–1
4th
23–1
E
141
F
21–1
16–1
at
20–1
22–1
14–1
15–1
23–1
18–1

Figure 10. Proximal ends of left tibiae of *Megapnosaurus rhodesiensis* in medial view. **A** Photograph and **B** line drawing of tibia (QG 790) possessing immature character states. **A** Photograph and **B** line drawing of tibia (QG 800) possessing mature character states. Scale bar is 1 cm. Abbreviation: **cn**, cnemial crest.


A
CT6LL

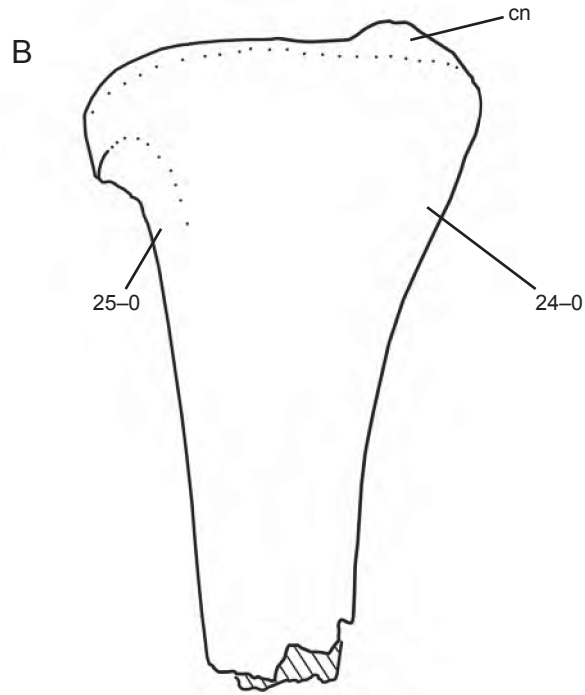
B
cn
25–0
24–0


C

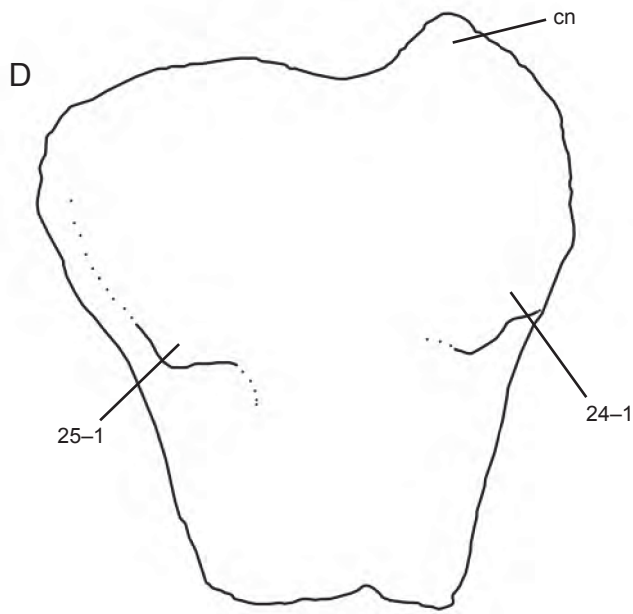
D
cn
25–1
24–1

Figure 11. Distal ends of tibiae and fibulae, with astragali and calcanea, of *Megapnosaurus rhodesiensis* possessing a combination of mature and immature character states. **A** Photograph and **B** line drawing of right tibia, fibula, astragalus, and calcaneum (QG 177) in posterior view. Note that tibia is partially coossified with astragalus (character 27), but is still scored as the immature state. **C** Photograph and **D** line drawing of left tibia, fibula, astragalus, and calcaneum (QG 805) in anterior view. Note that the distal end of the fibula is partially coossified with both the tibia and calcaneum (characters 28, 29), but these characters still scored as the immature states. Scale bar is 1 cm. Abbreviations: **ast**, astragalus; **calc**, calcaneum; **fib**, fibula; **tib**, tibia.

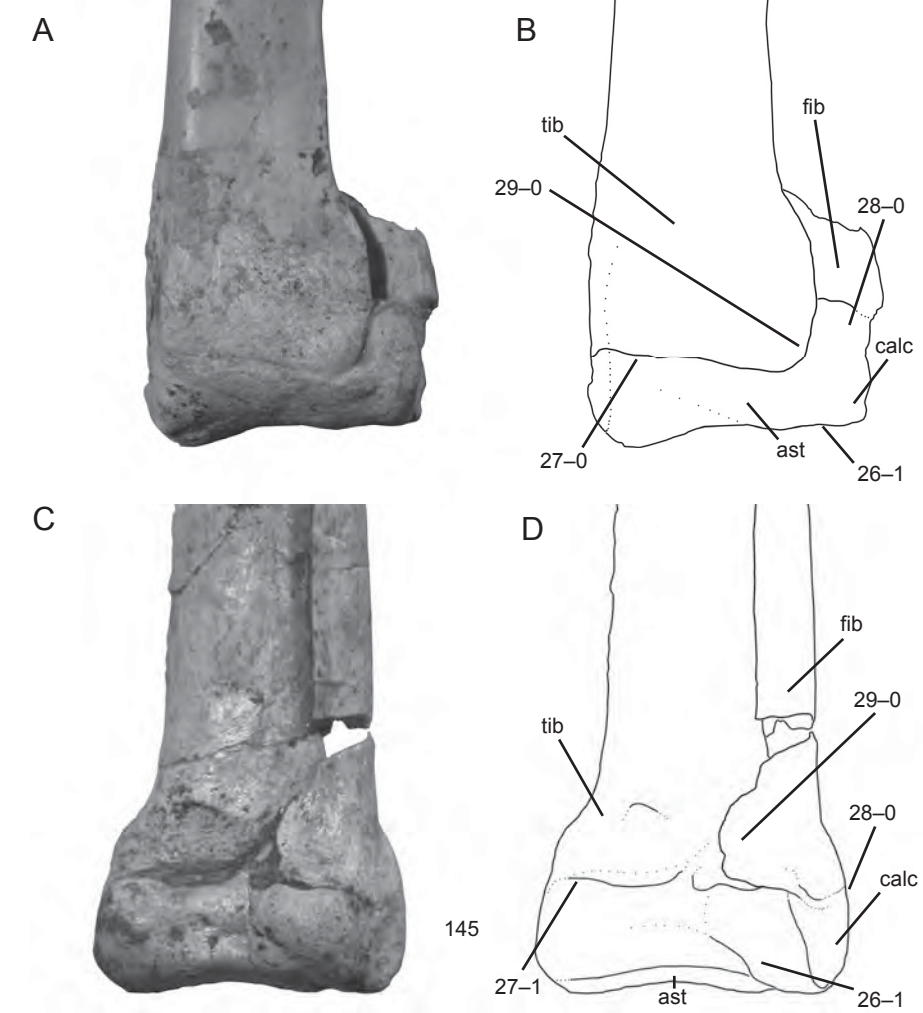
A
B
tib
fib
29–0
28–0
calc
27–0
ast
26–1
C
D
fib
29–0
tib
28–0
calc
27–1
ast
26–1

Figure 12. Right calcaneum and left astragalus of *Megapnosaurus rhodesiensis* showing immature character states. **A** Photograph and **B** line drawing of calcaneum (QG 816) possessing immature character states in anterior view. **C** Photograph and **D** line drawing of astragalus (QG 820) possessing immature character states in anterior view.

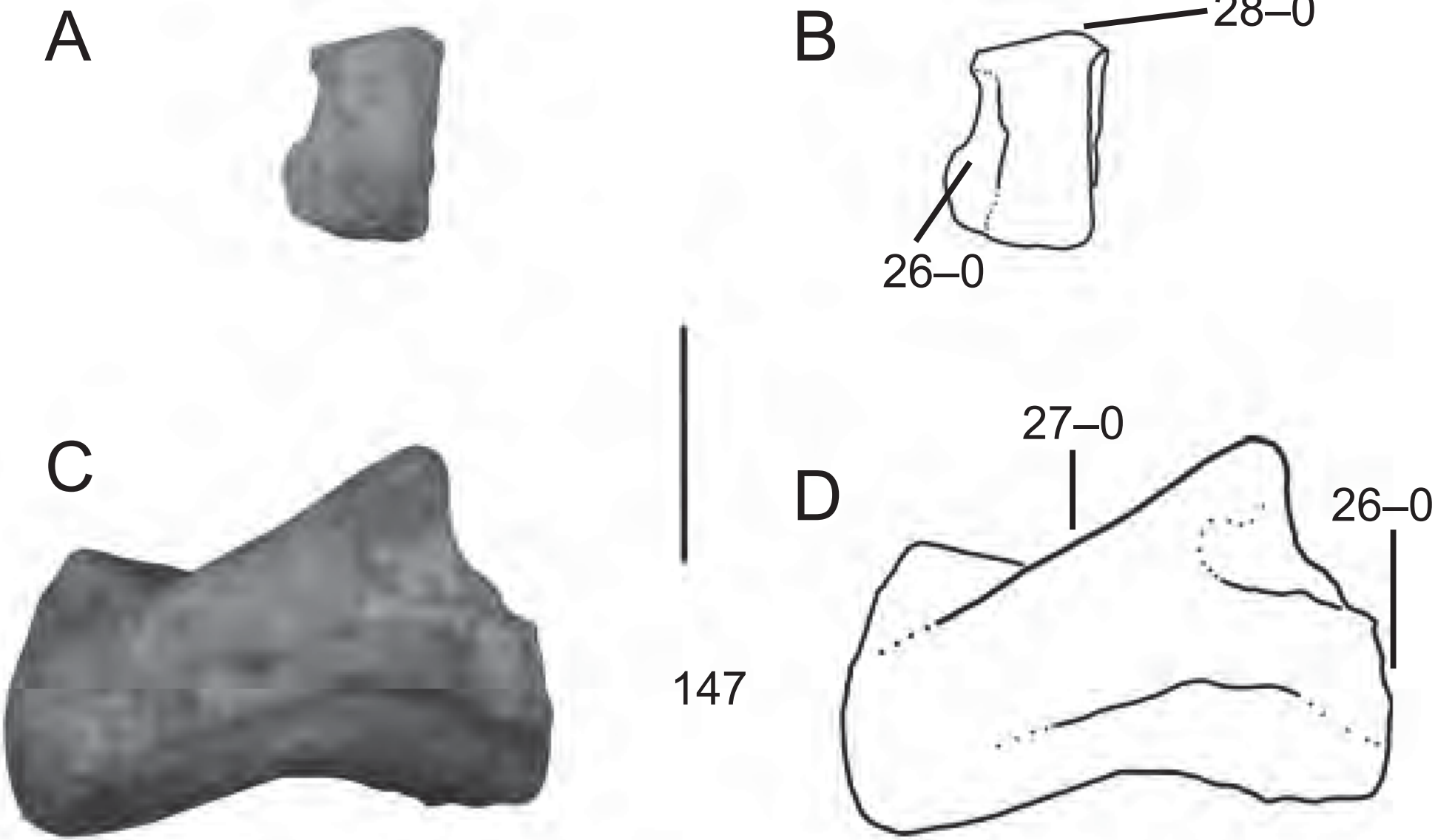
A
B
28–0
26–0
C
147
D
27–0
26–0

Figure 13. A Photograph and **B** line drawing of right tarsal III and metatarsals II and III of *Megapnosaurus rhodesiensis* (QG 1029) possessing mature character states in anterior view. Scale is 1 cm. Abbreviations: **mt2**, metatarsal II; **mt3**, metatarsal III; **t3**, tarsal III.

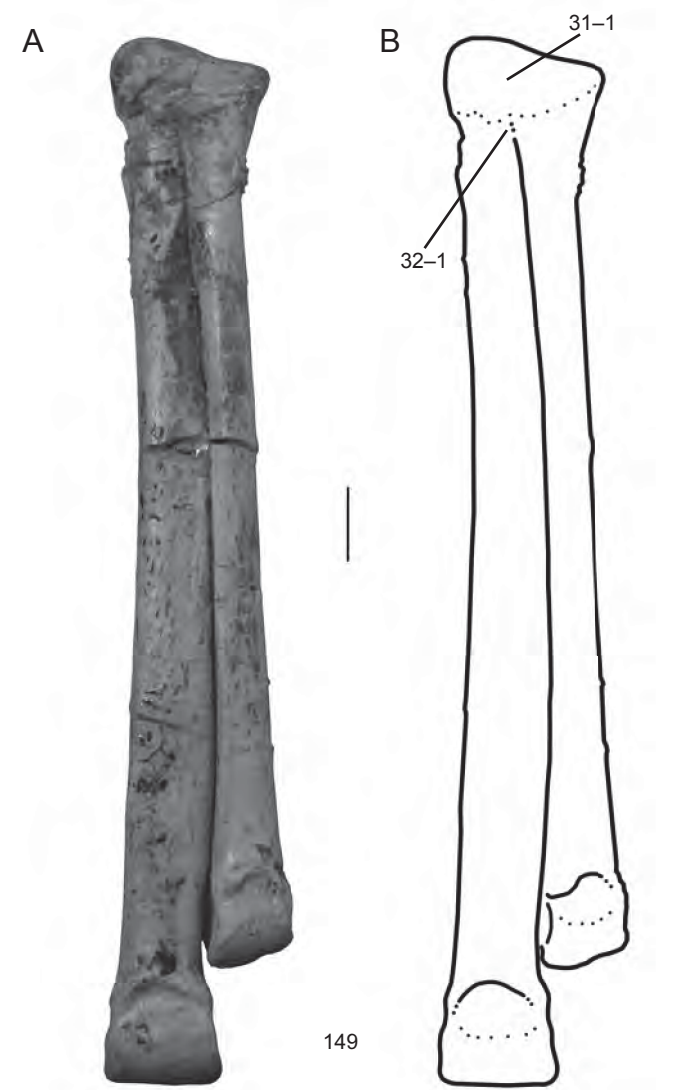

149

Figure 14. Ontogenetic sequence analysis (OSA) reticulating diagram showing all 136 equally parsimonious reconstructed developmental sequences for the full-body dataset of 27 ontogenetic characters of *Coelophysis bauri*. Developmental sequences proceed from the least to most mature semaphoront. Maturity score which represents the number of developmental events undergone by an individual; the x-axis is dimensionless and is only used for visual clarity. The detailed OSA diagram for this analysis, with character state transitions, semaphoront weights, and representative femoral lengths, can be found in the supplemental data.

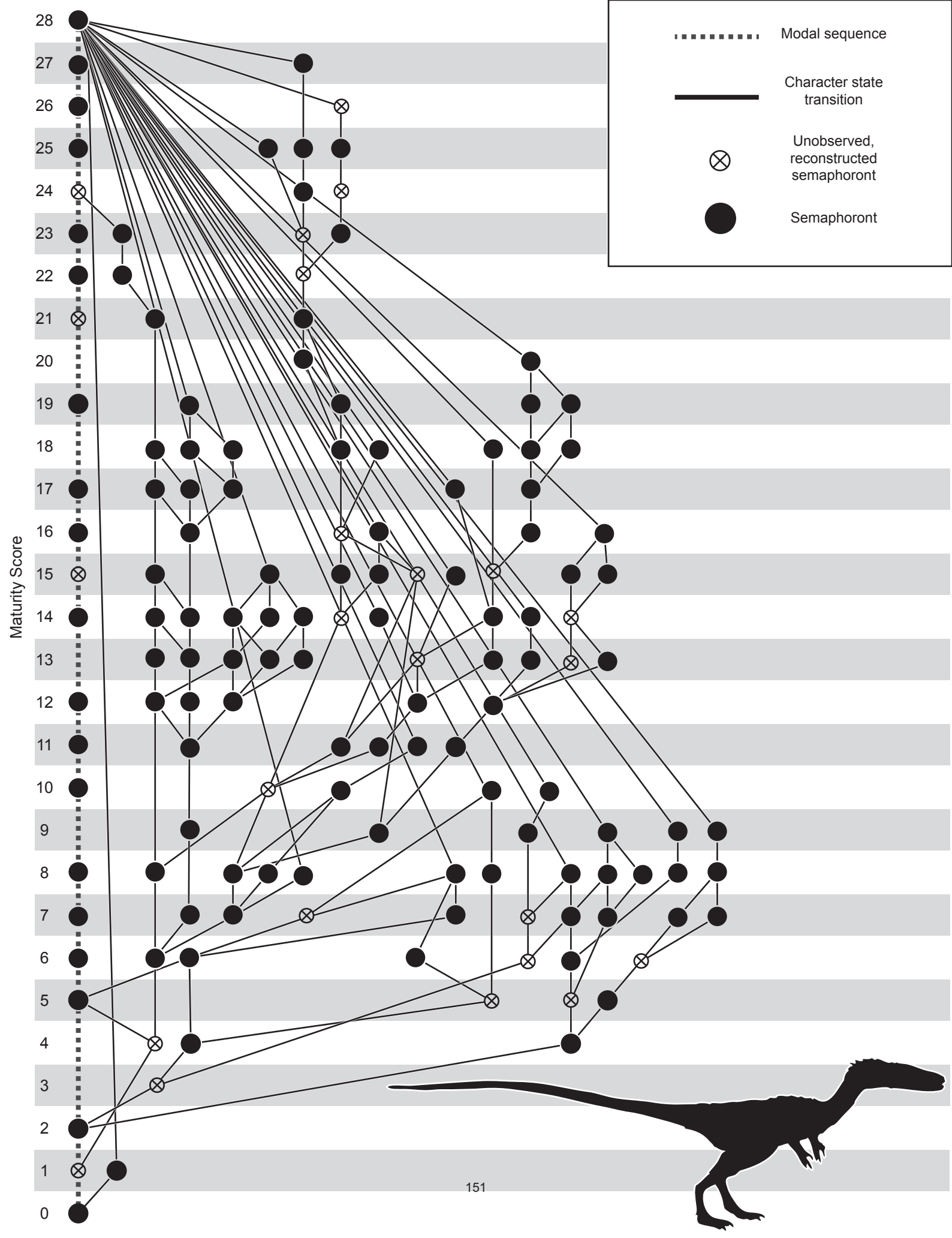
Modal sequence
Character state transition
Unobserved, reconstructed semaphoront
Semaphoront
Maturity Score
28
27
26
25
24
23
22
21
20
19
18
17
16
15
14
13
12
11
10
9
8
7
6
5
4
3
2
1
0

Figure 15. A OSA reticulating diagram showing all 82 equally parsimonious reconstructed developmental sequences for the femoral dataset of 10 ontogenetic characters of *Coelophysis bauri*. **B** OSA reticulating diagram showing all 145 equally parsimonious reconstructed developmental sequences for the femoral dataset of 10 ontogenetic characters of *Megapnosaurus rhodesiensis*. Key follows Fig 14. The detailed OSA diagram for these analyses can be found in the supplemental data.

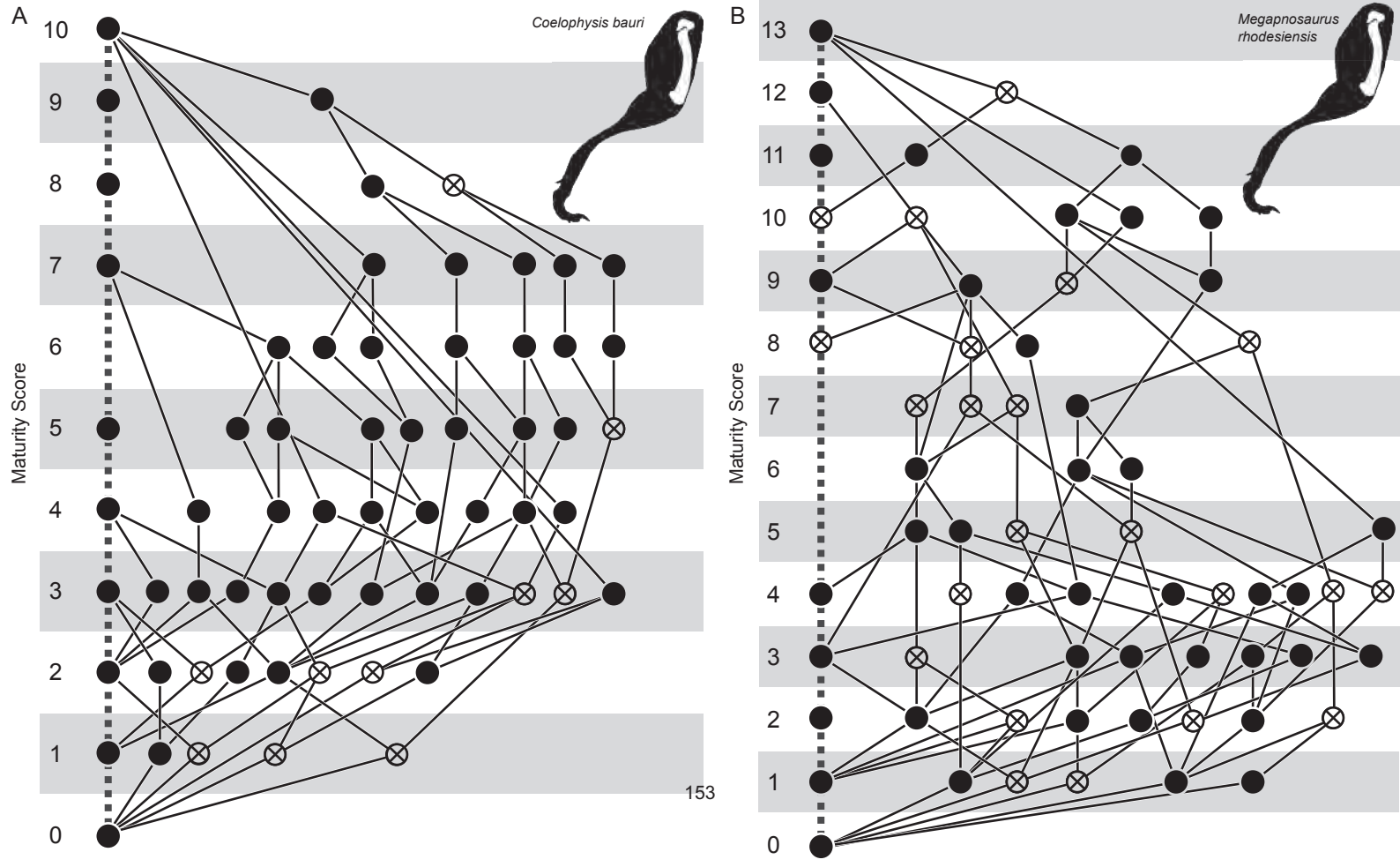
A
Coelophysis bauri
Maturity Score
10
9
8
7
6
5
4
3
2
1
0
153
B
Megapnosaurus rhodesiensis
Maturity Score
13
12
11
10
9
8
7
6
5
4
3
2
1
0

Figure 16. A OSA reticulating diagram showing all 35 equally parsimonious reconstructed developmental sequences for the tibial, tarsal, and pedal dataset of 8 ontogenetic characters of *Coelophysis bauri*. **B** OSA reticulating diagram showing the single parsimonious reconstructed developmental sequence for the tibial dataset of 6 ontogenetic characters of *Megapnosaurus rhodesiensis*. **C** OSA reticulating diagram showing both equally parsimonious reconstructed developmental sequences for the humeral dataset of 4 ontogenetic characters of *Megapnosaurus rhodesiensis*. **D** OSA reticulating diagram showing all 16 equally parsimonious reconstructed developmental sequences for the pelvic dataset of 5 ontogenetic characters of *Coelophysis bauri*. **E** OSA reticulating diagram showing all 3 equally parsimonious reconstructed developmental sequences for the pelvic dataset of 5 ontogenetic characters of *Megapnosaurus rhodesiensis*.

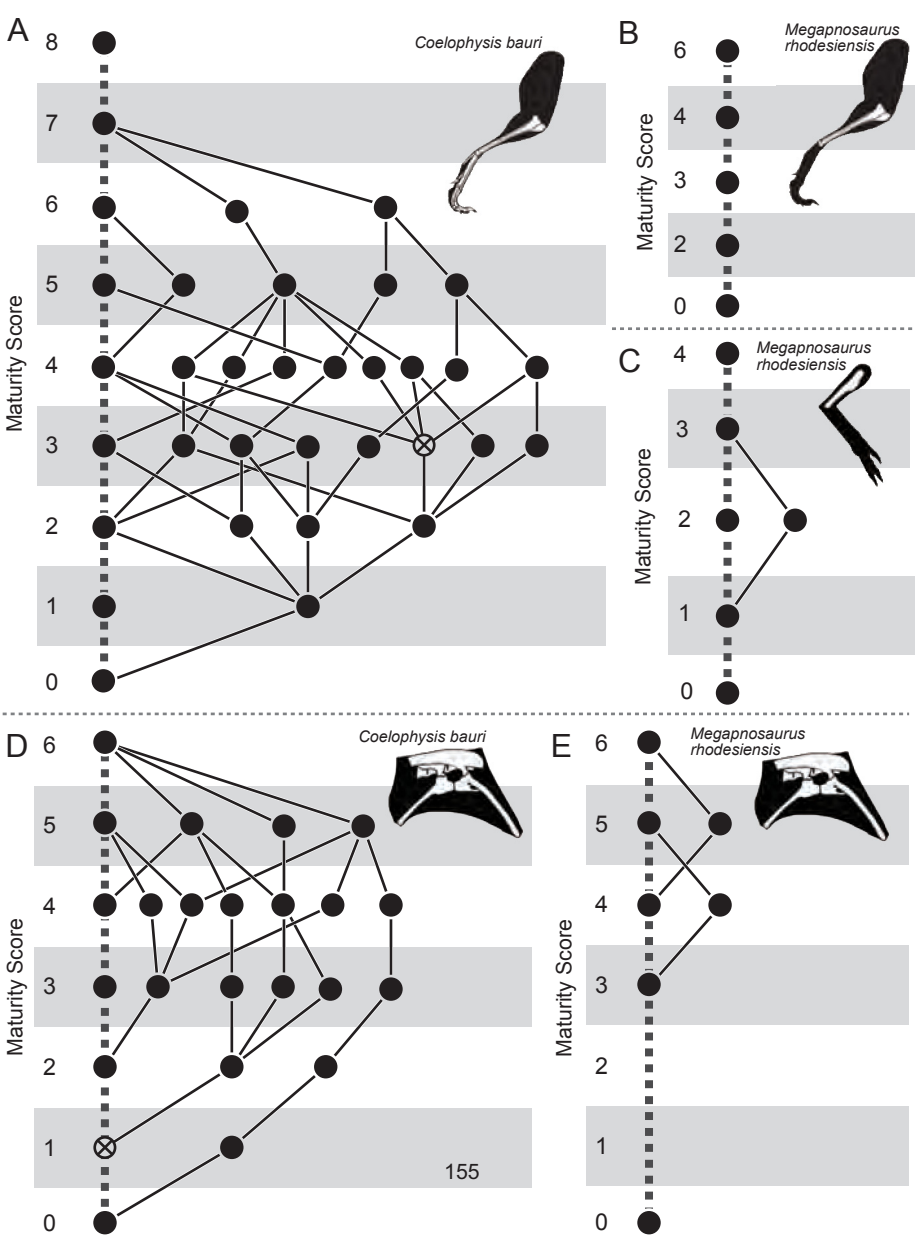
A
Coelophysis bauri
Maturity Score
8
7
6
5
4
3
2
1
0
B
Megapnosaurus rhodesiensis
Maturity Score
6
4
3
2
0
C
Megapnosaurus rhodesiensis
Maturity Score
4
3
2
1
0
D
Coelophysis bauri
Maturity Score
6
5
4
3
2
1
0
155
E
Megapnosaurus rhodesiensis
Maturity Score
6
5
4
3
2
1
0

Figure 17. Comparisons between the modal developmental sequences of the full body dataset and femoral, lower hindlimb (tibia, tarsus, pes), and pelvic datasets. **A** Modal sequence of femoral characters in the full-body OSA (top) and the femoral OSA (bottom). **B** Modal sequence of tibial, tarsal, and pedal characters in the full-body OSA (top) and the tibial, tarsal, and pedal OSA (bottom). **C** Modal sequence of pelvic characters in the full-body OSA (top) and the pelvic OSA (bottom).

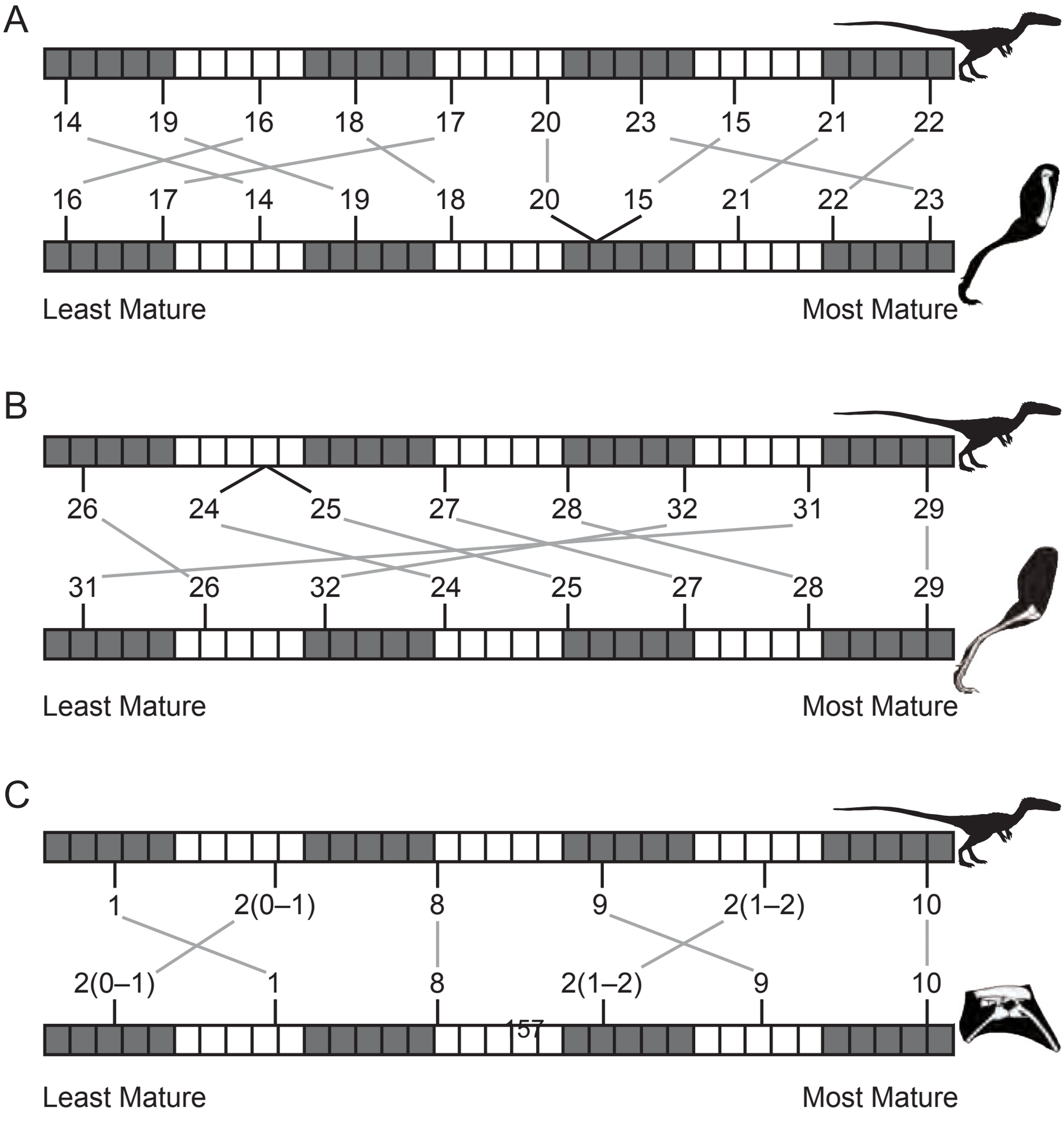
A
14 19 16 18 17 20 23 15 21 22
16 17 14 19 18 20 15 21 22 23
Least Mature
Most Mature
B
26 24 25 27 28 32 31 29
31 26 32 24 25 27 28 29
Least Mature
Most Mature
C
1 2(0–1) 8 9 2(1–2) 10
2(0–1) 1 8 2(1–2) 9 10
Least Mature
Most Mature

Figure 18. A Photograph and **B** line drawing of a relatively large individual of *Coelophysis bauri* (TMP 1984.063.0001) that possesses entirely immature character states in lateral view. Non-target skeletal elements and matrix have been lightened in Photoshop to highlight relevant skeletal elements. Scale bar is 1 cm. Abbreviations: **acet**, acetabulum; **fem**, femur; **il**, ilium; **isch**, ischium; **pub**, pubis; **sac**, sacrum.

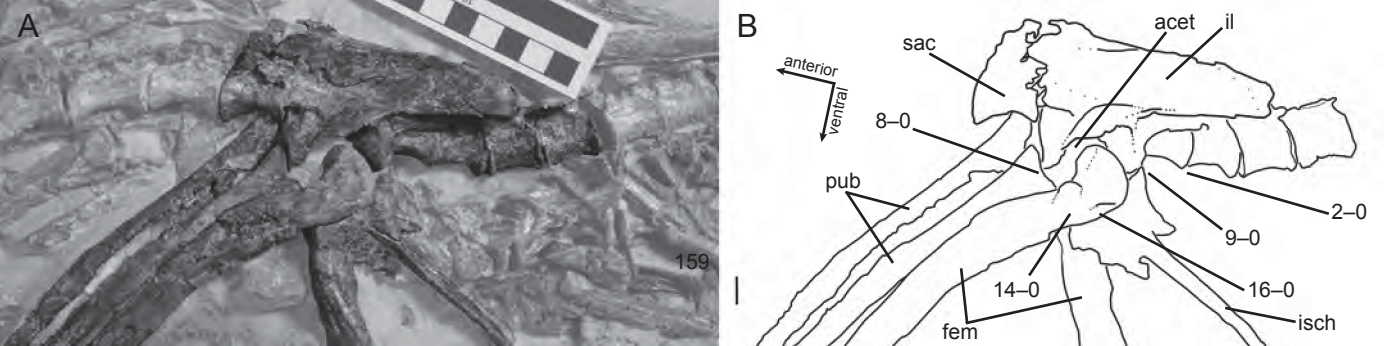
A
159
B
anterior
ventral
sac
acet
il
8–0
pub
2–0
9–0
14–0
16–0
fem
isch

Figure 19. A Photograph and **B** line drawing of a smaller individual of *Coelophysis bauri* (MNA V3318) which possesses many mature character states in left dorsolateral view. Non-target skeletal elements and matrix have been lightened in Photoshop to highlight relevant skeletal elements. Scale bar is 1 cm. Abbreviations: **fem**, femur; **il**, ilium; **isch**, ischium; **pub**, pubis; **sac**, sacrum.

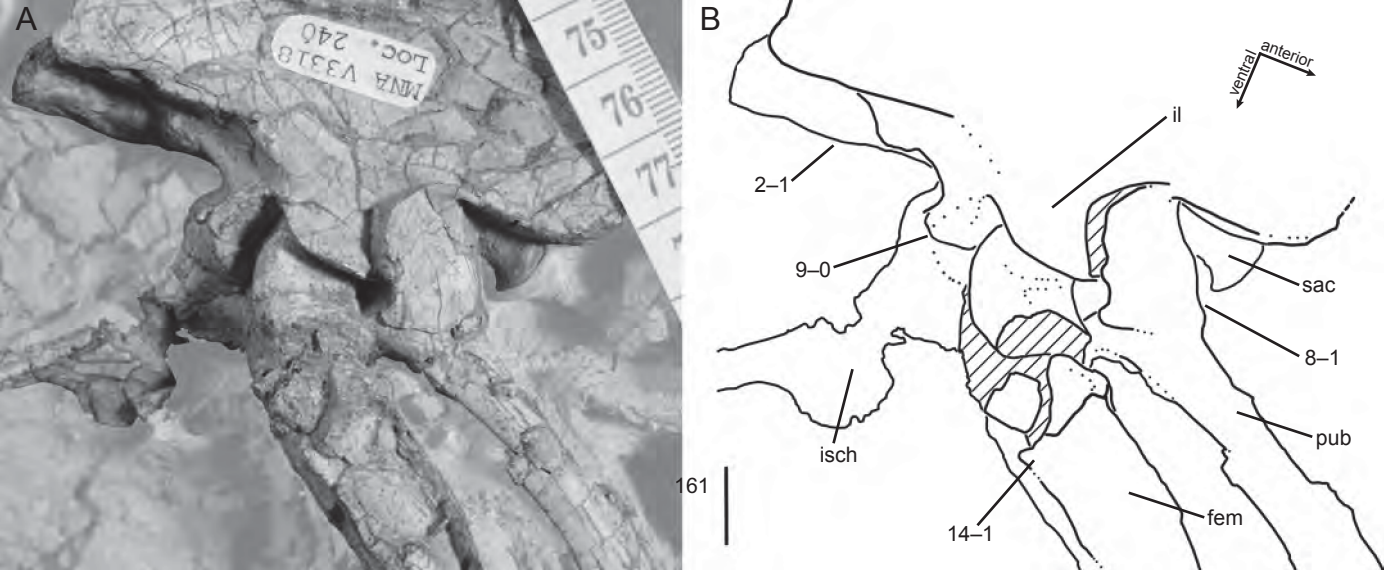
A
MNA V3318
Loc. 240
75
76
77
B
ventral
anterior
il
2–1
9–0
sac
8–1
pub
isch
161
14–1
fem

Figure 20. A Size distribution of individuals of *Coelophysis bauri* by femoral length, shown as frequency of bins (left y-axis) and kernel density (right y-axis). **B** Size distribution of individuals of *Megapnosaurus rhodesiensis* by femoral length, shown as frequency of bins (left y-axis) and kernel density (right y-axis). **C** Comparison between size distribution kernel density of *Coelophysis bauri* and *Megapnosaurus rhodesiensis*.

A

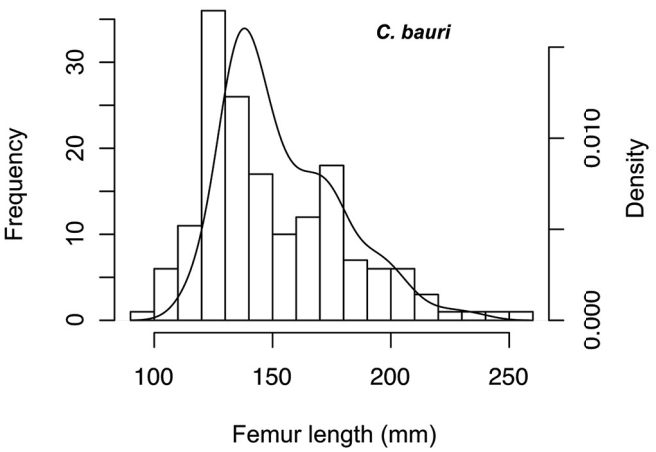
C. bauri
Frequency
0
10
20
30
Density
0.000
0.010
100
150
200
250
Femur length (mm)

B

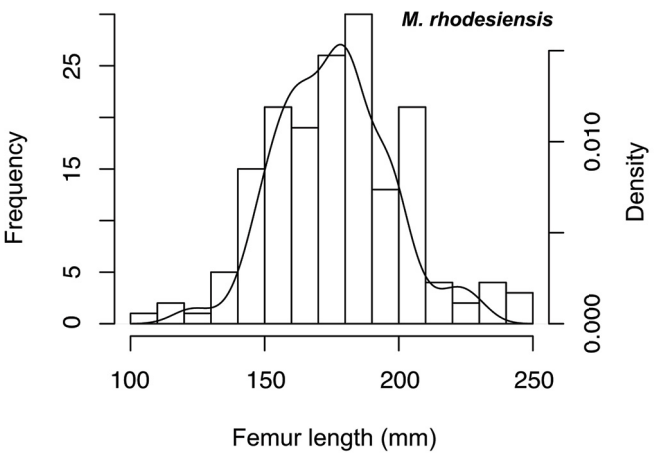
M. rhodesiensis
Frequency
0
5
15
25
Density
0.000
0.010
100
150
200
250
Femur length (mm)

C

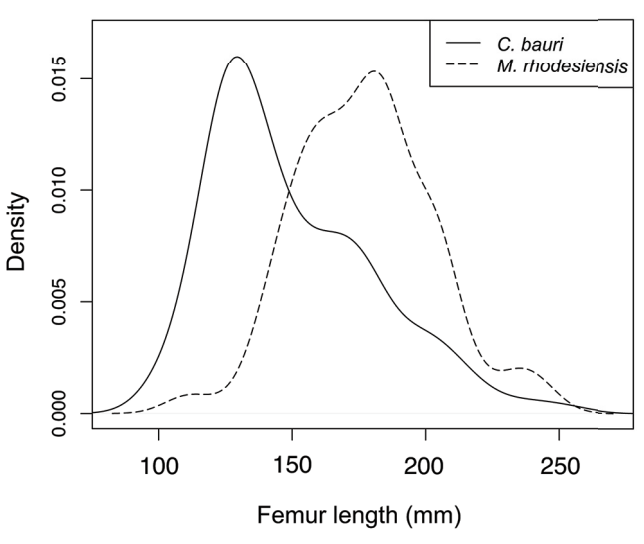
C. bauri
M. rhodesiensis
Density
0.000
0.005
0.010
0.015
100
150
200
250
Femur length (mm)

Figure 21. The range of orders in OSA sequences that each ontogenetic character attains mature state in the full-body OSA of *Coelophysis bauri*. Character 2 is a multistate character, and each state change is treated as a separate character because it is a distinct developmental event. For a single step with multiple state changes, each of those state changes are regarded as having occurred in that step, e.g., two character transitions that occur in step 7 are both regarded as having occurred in step 7, instead of artificially increasing resolution. However, the following developmental step is not sequential (e.g., the step following the two-character step 7 is not regarded as step 8, but step 9, etc.). Manually reconstructed developmental events (see Methods) are excluded.

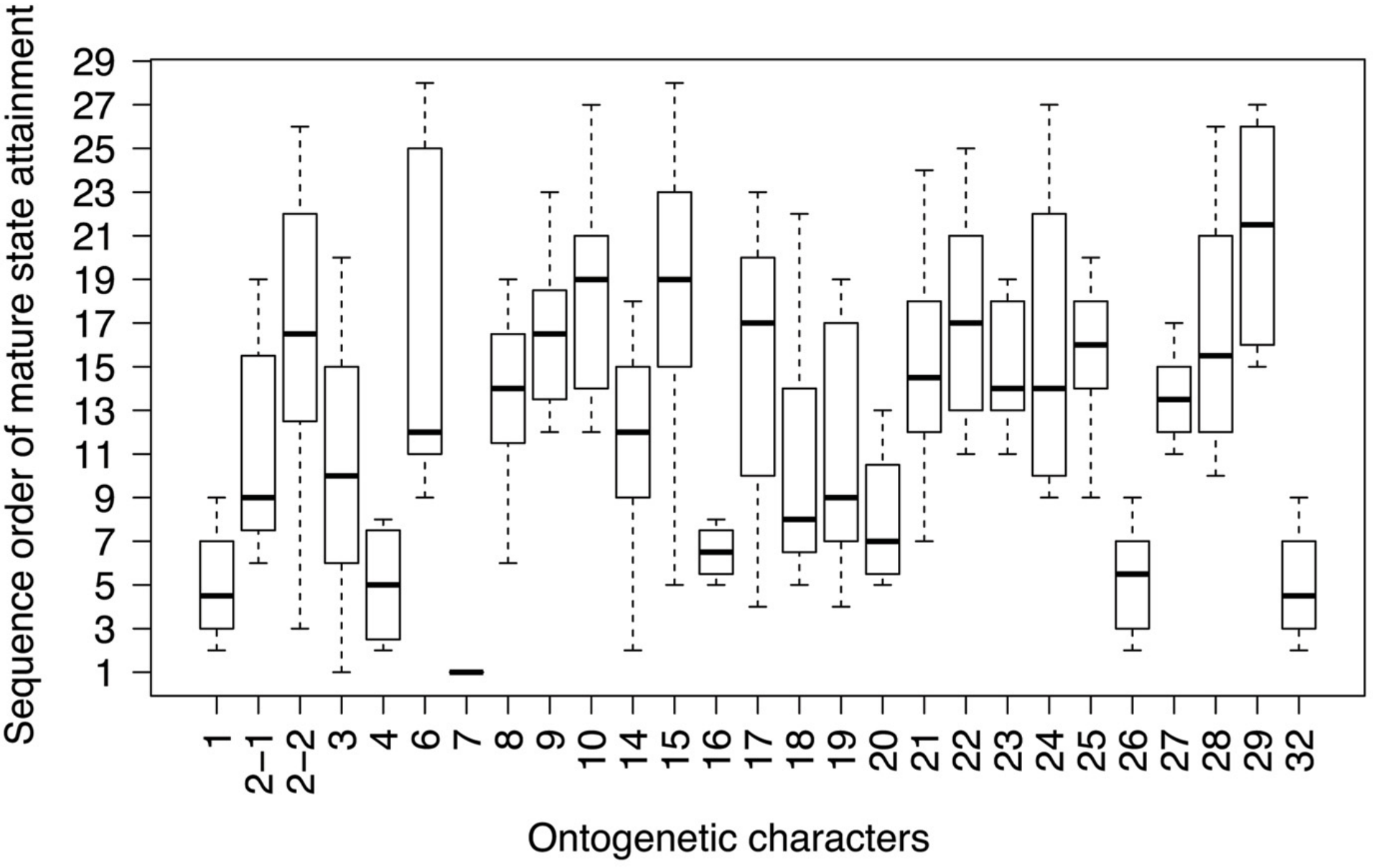
Sequence order of mature state attainment
29
27
25
23
21
19
17
15
13
11
9
7
5
3
1
1
2–1
2–2
3
4
6
7
8
9
10
14
15
16
17
18
19
20
21
22
23
24
25
26
27
28
29
32
Ontogenetic characters

Figure 22. Modal sequence orders of 11 homologous femoral characters from the femoral OSAs of the theropods *Coelophysis bauri* and *Megapnosaurus rhodesiensis*, and of the silesaurid *Asilisaurus kongwe*. Anterior trochanter is abbreviated **at**, and because it is present in all known individuals of *C. bauri* and *M. rhodesiensis*, it is considered to have appeared first in ontogeny in these taxa. All other character numbers follow those of this study. *Asilisaurus kongwe* OSA data taken from Griffin and Nesbitt (2016).

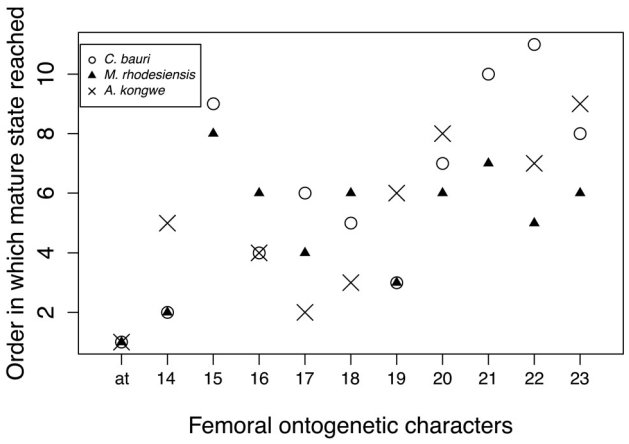
C. bauri
M. rhodesiensis
A. kongwe
Order in which mature state reached
2
4
6
8
10
at
14
15
16
17
18
19
20
21
22
23
Femoral ontogenetic characters

Chapter 3

DOES THE MAXIMUM BODY SIZE OF THEROPODS INCREASE ACROSS THE TRIASSIC–JURASSIC BOUNDARY? INTEGRATING ONTOGENY, PHYLOGENY, AND BODY SIZE

Christopher T. Griffin* and Sterling J. Nesbitt, Virginia Polytechnic Institute and State University.

*corresponding author: ctgriff@vt.edu

Formatted for *Biology Letters*

ABSTRACT

Mass extinctions change the global ecological landscape, and the end-Triassic mass extinction is thought to have precipitated the rise of dinosaur dominance, with dinosaurs filling niches of other large-bodied reptilian lineages that ended. This has also been explicitly hypothesized to occur within theropod dinosaurs, the North American footprint record of which suggests an increase in maximum body size across the Triassic-Jurassic boundary. Without taking ontogenetic stage in account, the maximum size of the rare large Triassic theropods from Europe, North and South America support this as a global trend, with the largest known individuals remaining smaller than the largest Early Jurassic theropods. However, both morphological data and histological examination suggest that known large-bodied Triassic theropods are represented by immature individuals still growing rapidly at time of death, indicating that the maximum body size of Triassic theropods did not significantly increase across the Triassic-Jurassic boundary. The size increase recorded in the sediment of eastern North America is a local, not global trend. Instead of a simple ecological replacement of non-dinosaurian archosaurs by dinosaurs, the rise of theropod dinosaur dominance was an extended process across the end of the Late Triassic.

KEYWORDS: Dinosaur, Theropod, Triassic, extinction, ontogeny, histology.

INTRODUCTION

Dinosaurs originated 230 million years ago as minor ecological players with limited body sizes, diversity, and ecological niches (Langer and Benton, 2006; Brusatte et al., 2010), but became an extremely widespread and ecologically diverse clade, including some of the largest-bodied taxa known, in later terrestrial ecosystems. Although data are

scarce, the rise of dinosaurs is hypothesized to have been an extended and gradual process that occurred throughout the Late Triassic (Irmis 2011). Theropod dinosaurs were present as early as the Carnian (Martinez et al. 2011), but for the entire known Triassic were almost without exception small-bodied (1–2 m in length) carnivores, with large-bodied theropods only becoming common in the Jurassic (Allain et al. 2007). In support, the theropod footprint record of the Late Triassic–Early Jurassic of eastern North America suggests that a sharp increase in theropod body size occured across the Triassic–Jurassic (T–J) boundary, synchronous with a terrestrial mass extinction (Olsen et al. 2002). This supports the hypothesis of ecological replacement of large, carnivorous non-dinosaurian archosauriforms, which were common and geographically widespread during the Triassic but were eliminated by the Late Triassic extinction, by theropods. Although a few partial skeletons of comparatively large theropods are known, they are still within the size range of reported Triassic footprints, supporting this hypothesis (Olsen et al. 2002; Fig. 1). However, based on a number of morphological characters, these specimens have been suggested to represent ontogenetically immature individuals (Carpenter 1997; Rauhut and Hungerbühler 1998), complicating our understanding of the evolution of maximum body size of theropods across the T-J boundary.

In this study, we use osteohistology in conjunction with ontogenetically informative morphological characters to test the hypothesis that the maximum body size of theropods increased across the T-J boundary, and link this to the patterns of post-extinction recovery that resulted in the ecological dominance of dinosaurs.

Institutional Abbreviations: **HMN**, Museum für Naturkunde, Humboldt Universität, Berlin, Germany; **NMMNH**, New Mexico Museum of Natural History and Science,

Albuquerque, New Mexico, USA; **PULR**, Paleontología, Universidad Nacional de La Rioja, La Rioja, Argentina; **UCM**, University of Colorado Museum of Natural History, Boulder, Colorado, USA; **UCMP**, University of California Museum of Paleontology, Berkeley, California, USA.

METHODS

The footprint size of the holotype individual of *Dilophosaurus wetherilli* (UCMP 37302) was estimated by measuring the proximodistal length of the articulated pes (i.e., ~35 cm in length). We used comparative measurements of homologous elements of Triassic Period theropods and *Dilophosaurus* to determine how these taxa compared in body size to *Dilophosaurus*, with limb bone measurements as a proxy for body size. We then estimated the track size of these taxa by proportion, assuming that the proportions between *Dilophosaurus* body size and track size held across these taxa, so that a taxon ~80% the body size of *Dilophosaurus* was estimated to have a track length 80% that of *Dilophosaurus*. Footprint data were taken from Olsen et al. (2002).

We assessed the skeletal maturity of the Triassic theropods *Gojirasaurus quayi* (UCM 47721), *Liliensternus liliensterni* (HMN MB.R.2175; at least two individuals form a syntype), and *Zupaysaurus rougieri* (PULR 076) using morphological characters shown to be ontogenetically informative in the coelophysid theropods *Coelophysis bauri* and *Megapnosaurus rhodesiensis* (Chapter 1; Chapter 2, Fig. 21). Additionally, we used these criteria to assess the skeletal maturity of a partial neotheropod skeleton from the Late Triassic Bull Canyon Formation of New Mexico (NMMNH P-4569; "Bull Canyon neotheropod") and an isolated fibula from the same locality (NMMNH P-4563). We also histologically sampled ribs and a fragmentary long bone of this individual, as well as an

isolated fibula with neotheropod affinity from the same formation (NMMNH P-4563) using standard histological techniques (Supplementary Information). We compared the sizes of these specimens to measurements of the large Early Jurassic neotheropod *Dilophosaurus wetherilli* (UCMP 37302), using measurements either taken in person (*G. quayi*, Bull Canyon neotheropod), or from the literature (*L. liliensterni*, *Z. rougieri*).

RESULTS

Eight ontogenetic characters could be assessed for *Gojirasaurus quayi* (characters 2, 3, 8, 10, 24, 25, 27,29; Chapter 1; Chapter 2), and all possessed the hypothesized immature character state for these characters (Fig. 2D–G; Fig. S1). *Liliensternus liliensterni* was more complete, and of the twenty-six ontogenetic characters (characters 2, 4, 7, 8—11, 13—29, 31, 32; Chapter 1; Chapter 2) that could be evaluated in this specimen, all but one character possessed the immature character state (Fig. S2, S3). In this specimen, one right scapulacoracoid was partially fused; however, another right scapula assigned the same specimen number was unfused to the coracoid, so this character is ambiguously distributed between the individuals making up the *L. liliensterni* syntype. Only six ontogenetic character states can be assessed from the holotype of *Zupaysaurus rougieri*, but three possess immature states (characters 3, 27—29 are immature, and character 26 is mature; Chapter 1; Chapter 2). Although eight ontogenetic characters could be assessed for the Bull Canyon neotheropod individual (Fig. 2A; Fig. S4), five of these (characters 3, 10, 11, 27, 28; Chapter 1; Chapter 2) are clearly the unfused, immature character state. The astragalus and calcaneum (character 26; Chapter 1; Chapter 2) are only partially fused with a clear gap between the two elements, which would be scored as the immature character state following Chapter 2. Two femoral

characters (characters 19 and 21; Chapter 1; Chapter 2) are mature. NMMNH P-4569 possesses two synapomorphies of Neotheropoda: the supra-acetabular crest of the ilium projects ventrally (character 189, Nesbitt et al. 2009; character 198, Martill et al. 2016), and the (partial, because of ontogenetic immaturity) coossification of the astragalus and calcaneum (character 283, Nesbitt et al. 2009; character 304, Martill et al. 2016). NMMNH P-4563 possesses a single ontogenetic character (Fig. S4) in the mature state (character 30; Chapter 1, Chapter 2) which is also a synapomorphy of Neotheropoda (Nesbitt et al. 2009).

The rib histology of the Bull Canyon neotheropod suggests that it was skeletally immature and still growing rapidly when it died (Fig. 2B). There are no lines of arrested growth (LAGs) preserved, so an approximate ontogenetic age cannot be determined for this individual. There is no external fundamental system (EFS), and the bone tissue remains highly vascularized to the subperiosteal surface. The osteohistology of the large (68% the size of *Dilophosaurus*), isolated fibula from the same locality as the Bull Canyon neotheropod (NMMNH P-4563) possesses one LAG, which may indicate the individual had reached at least one year of age. However, this LAG divides two histological regions: the deep region is highly porous and extremely unusual, and may be pathological, whereas the superficial region is more conventional woven bone with longitudinal/reticular vascular style. Therefore, this LAG may be related to some unusual growth style or pathology rather than to the annual growth cycle of this individual. Like the Bull Canyon neotheropod (NMMNH P-4569), the histology of the fibula remains highly vascularized to the subperiosteal surface, with no EFS or indications of slowing growth, suggesting that the individual was rapidly growing at the time of death (Fig. 2C).

DISCUSSION

Although rare, all known large-bodied Triassic theropods are smaller than the largest Early Jurassic theropod, *Dilophosaurus wetherilli*. Therefore, the worldwide body fossil record appears to agree with the theropod footprint record of eastern North America, supporting the hypothesis that a sudden increase in the maximum body size of theropods, occurring across the Triassic-Jurassic transition, is a worldwide trend. However, the morphology of the largest Triassic theropods suggests they are skeletally immature, with almost no ontogenetic characters possessing mature character states, and those few characters that do are characters which appear early in ontogenetic sequence or extremely variable in sequence order (Chapter 2). Additionally, the histology of the Bull Canyon neotheropod and the isolated neotheropod fibula also suggest that these individuals were still growing rapidly at death, and had not reached the more advanced ontogenetic stages in which growth begins to slow before complete cessation of growth. The largest of these Traissic theropods (*Gojirasaurus*) is roughly 79% the size of the largest Early Jurassic theropod, and the smallest (the Bull Canyon neotheropod) is roughly 60% the size of the largest Early Jurassic theropod. Although *D. wetherilli* (UCMP 37302) also possesses immature character states and may be skeletally immature (Welles 1984; Tykoski 2005), because this specimen was only used as a way to estimate the body size of the largest trackmaker in the Newark Supergroup, the maturity of this individual does not effect how we tested Olsen et al.'s (2002) hypothesis. Taken together, with the largest Triassic theropods close in size to the largest Early Jurassic theropods and still growing rapidly, these data suggest that the increase in theropod maximum body size was a local trend, restricted to eastern North America, and worldwide the largest

theropod species were roughly the same size, whether in the Triassic or Early Jurassic. Additionally, the presence of the relatively large-bodied *Herrerasaurus ischigualastensis* in earlier Late Triassic sediments demonstrates that the theropod track record of Eastern North America is not a complete record of global body size of Triassic Period theropods (Fig. 1). Therefore, instead of a simple ecological replacement of large carnivorous pseudosuchian archosaurs by theropods after the former went extinct, our data suggest that this replacement was more gradual, with rare, large-bodied theropods coexisting with their more common pseudosuchian counterparts in the Late Triassic. Then, as the majority of pseudosuchian clades went extinct at the end of the Triassic, large theropods filled the ecological space left vacant by these clades, becoming more abundant in the Early Jurassic, with the rapid size increase in theropod footprints of the Newark Supergroup a reflection of this increase in abundance.

ACKNOWLEDGEMENTS

We thank A. Marsh for *Dilophosaurus* measurements, R. Irmis for photographs of *Liliensternus*, T. Culver of UCM for access to collections, A. Marsh, P. Olsen, R. Irmis, K. Padian, the Virginia Tech Integrative and Organismal Biology group and the VT Paleobiology Research Group for discussion. We also thank M. Stocker, L. Freeman, and M. Colbert for helpful reviews of the manuscript.

REFERENCES

Allain, R., R. Tykoski, N. Aquesbi, N.-E. Jalil, M. Monbaron, D. Russell, and P. Taquet. 2007. An abelisauroid (Dinosauria: Theropoda) from the Early Jurassic of the High Atlas

Mountains, Morocco, and the radiation of ceratosaurs. Journal of Vertebrate Paleontology 27:610–624.

Brusatte, S. L., S. J. Nesbitt, R. B. Irmis, R. J. Butler, M. J. Benton, and M. A. Norell. 2010. The origin and early radiation of dinosaurs. Earth-Science Reviews 101:68–100.

Carpenter, K. 1997. A giant coelopysoid (Ceratosauria) theropod from the Upper Triassic of New Mexico, USA. Neues Jahrbuch für Geologie und Paläontologie 205:189–208.

Irmis, R. B. 2011. Evaluating hypotheses for the early diversification of dinosaurs. Earth and Environmental Science Transactions of the Royal Society of Edinburgh 101:397–426.

Langer, M. C., and M. J. Benton. 2006. Early dinosaurs: a phylogenetic study. Journal of Systematic Palaeontology 4:309–358.

Martill, D. M., S. U. Vidovic, C. Howells, and J. R. Nudds. 2016. The oldest Jurassic dinosaur: A basal neotheropod from the Hettangian of Great Britain. PLoS ONE 11:e0145713. DOI: 10.1371/journal.pone.0145713

Martínez, R. N., P. C. Sereno, O. A. Alcobar, C. E. Colombi, P. R. Renne, I. P. Montañez, and B. S. Currie. 2011. A basal dinosaur from the dawn of the dinosaur era in southwestern Pangaea. Science 331:206–210.

Nesbitt, S. J., N. D. Smith, R. B. Irmis, A. H. Turner, A. Downs, and M. A. Norell. 2009. A complete skeleton of a Late Triassic saurischian and th early evolution of dinosaurs. Science 326:1530–1533.

Olsen, P. E., D. V. Kent, H.-D. Sues, C. Koeberl, H. Huber, A. Montanari, E. C. Rainforwth, S. J. Fowell, M. J. Szajna, and B. W. Hartline. 2002. Ascent of dinosaurs linked to an iridium anomaly at the Triassic-Jurassic boundary. Science 296:1305–1307.

Rauhut, O. W. M. 2003. Interrelationships and evolution of basal theropod dinosaurs. Special

Papers in Palaeontology 69:1–213.

Rauhut, O. W. M., and A. Hungerbühler. 1998. A review of European Triassic theropods. Gaia 15:75–88.

Rogers, R. R., C. C. Swisher, III, P. C. Sereno, A. M. Monetta, C. A. Forster, and R. N. Martínez. 1993. The Ischigualasto tetrapod assemblage (Late Triassic, Argentina) and the 40 Ar/39 Ar dating of dinosaur origins. Science 260:794–797.

FIGURES

Figure 1. Body size of Triassic and Jurassic theropods and *Herrerasaurus* compared with the maximum theropod track size of dated localities in the Newark Supergroup (Olsen et al. 2002), illustrating the apparent increase in maximum theropod body size across the T-J boundary. The y-axes are in parallel: a *Dilophosaurus*-sized theropod would make a track ~35 cm long, a theropod 80% the size of *Dilophosaurus* would make a track ~28 cm long, etc. Data are available in Table S1.

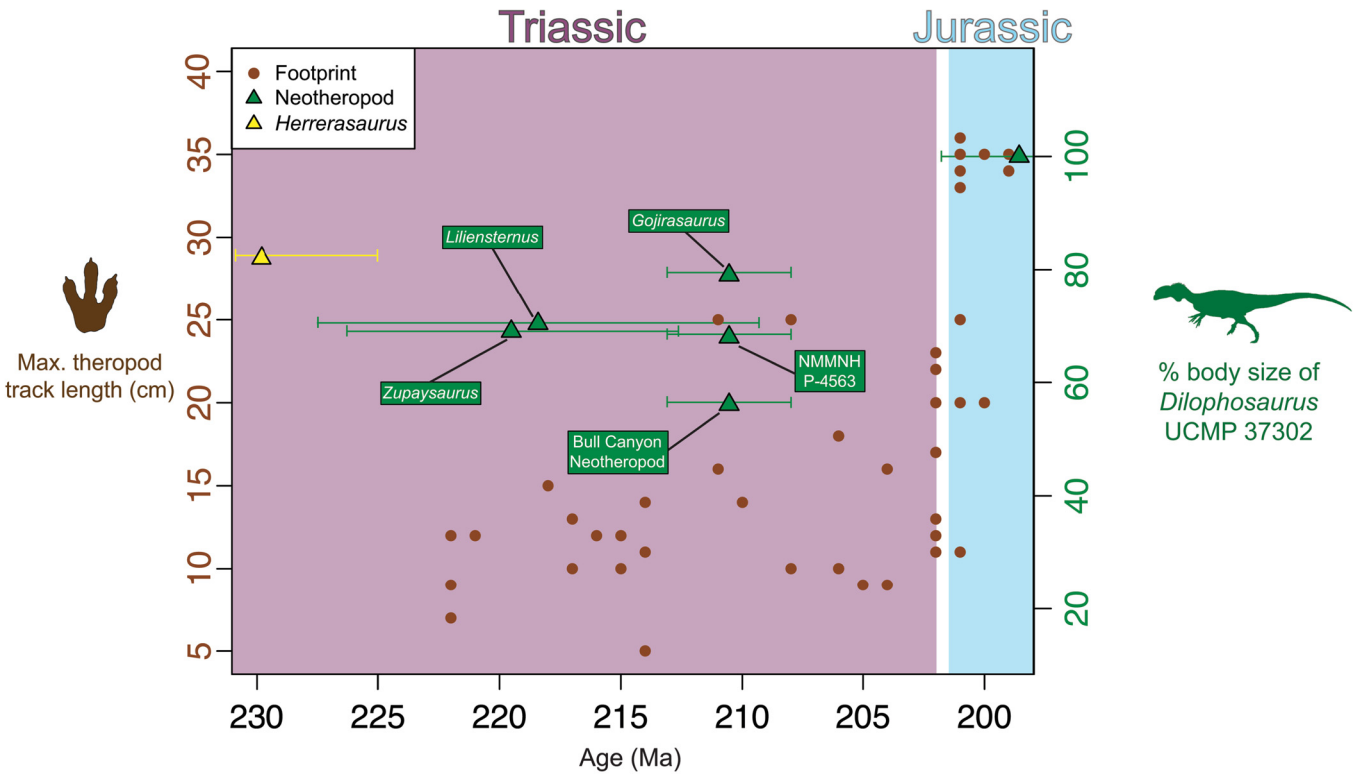
Triassic
Jurassic
Footprint
Neotheropod
Herrerasaurus
Lilliensternus
Gojirasaurus
Zupaysaurus
NMMNH P-4563
Bull Canyon Neotheropod
Max. theropod track length (cm)
% body size of Dilophosaurus UCMP 37302
Age (Ma)
230
225
220
215
210
205
200
5
10
15
20
25
30
35
40
20
40
60
80
100

Figure 2. Multiple lines of evidence support the early ontogenetic stage of known individuals of large-bodied Triassic theropods. **A** Ontogenetic character states of the Triassic theropod *Coelophysis bauri* with the range of order in ontogenetic sequences that these characters transition from the immature to mature state, allowing allowing the ontogenetic stage of the Bull Canyon neotheropod to be estimated based on suites of character states. Red indicates characters which were scored as immature, giving an upper bound on ontogenetic stage; yellow indicates mature characters, giving a lower bound; white boxes are characters that could not be scored. The light red region indicates the ontogenetic stages that are consistent with the character states. For similar data for other taxa, see Fig. S5. **B** Rib histology of the Bull Canyon neotheropod, with subperiosteal surface oriented to the left; scale bar is 500 μm. Inset is detail of subperiosteal surface, scale bar is 200 μm. **C** Fibular histology of NMMNH P-4563, with subperiosteal surface oriented to the right; scale bar is 500 μm. Inset is detail of subperiosteal surface, scale bar is 200 μm. Both B and C are viewed under cross-polarized light with a gypsum wedge. **D** Distal left tibia of *Gojirasaurus*, unfused to astragalus. **E** Distal right scapula of *Gojirasaurus*, unfused to coracoid. **F** Sacral of *Gojirasaurus*, unfused to other sacrals. **G** Right pubis of *Gojirasaurus,* unfused to ilium or ischium. **H** Right ilium of *Liliensternus*, unfused to pubis or ischium. **I** Right femur of *Liliensternus*, lacking most ossified muscle scars. **J** Right humerus of *Liliensternus*, lacking muscle scars. All characters in D–J possess the hypothesized immature state. Scale bars for D–J are 1 cm.

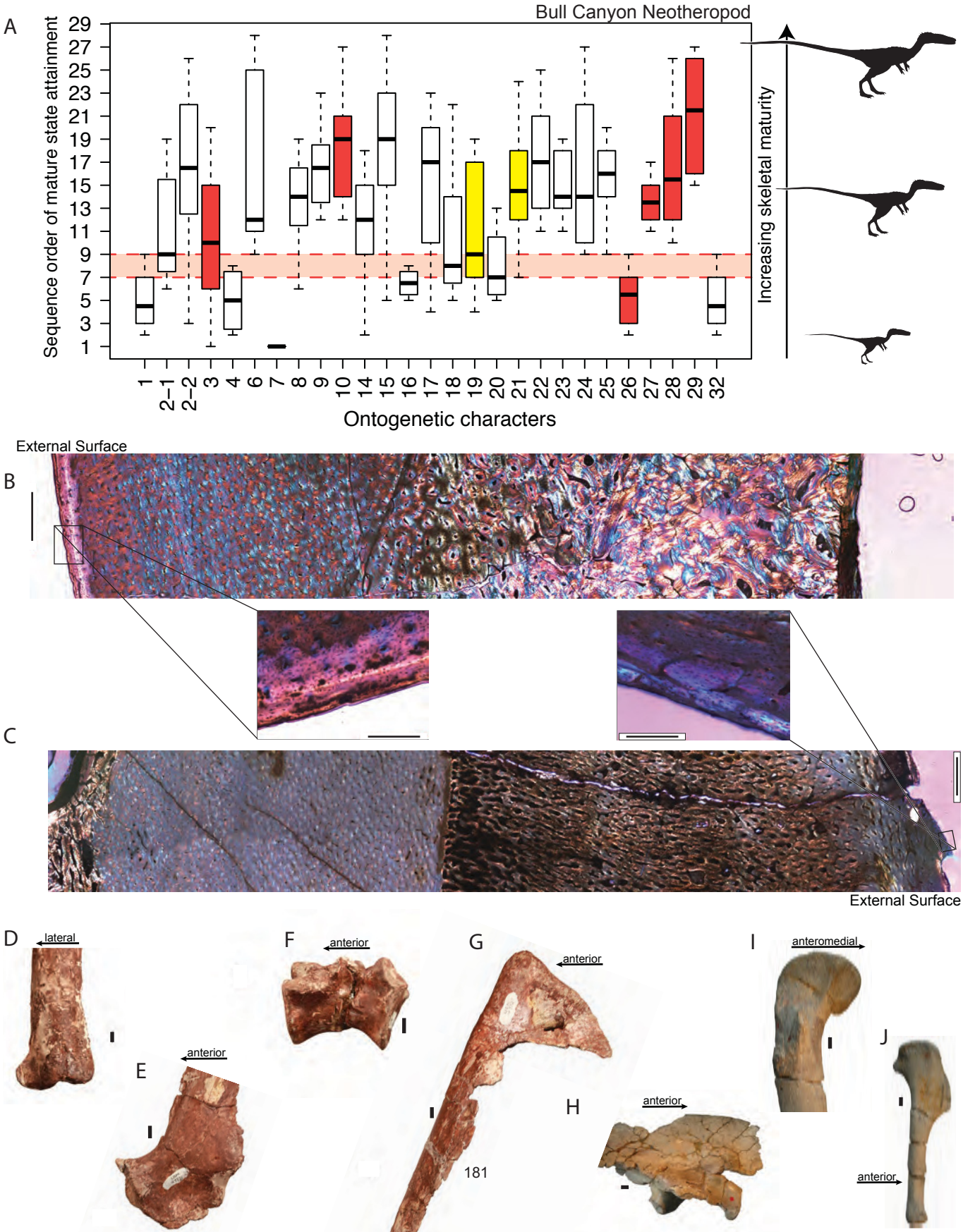
A
Bull Canyon Neotheropod
Sequence order of mature state attainment
29
27
25
23
21
19
17
15
13
11
9
7
5
3
1
1
2–1
2–2
3
4
6
7
8
9
10
14
15
16
17
18
19
20
21
22
23
24
25
26
27
28
29
32
Ontogenetic characters
Increasing skeletal maturity
External Surface
B
C
External Surface
D
lateral
E
anterior
F
anterior
G
anterior
H
anterior
I
anteromedial
J
anterior
181